Multimodality Imaging Guidelines of Patients with Transposition of the Great Arteries: A Report from the American Society of Echocardiography Developed in Collaboration with the Society for Cardiovascular Magnetic Resonance and the Society of Cardiovascular Computed Tomography

Meryl S. Cohen, MD, FASE (Chair), Benjamin W. Eidem, MD, FASE (Co-Chair), Frank Cetta, MD, FASE, Mark A. Fogel, MD, Peter C. Frommelt, MD, FASE, Javier Ganame, MD, PhD, FASE, B. Kelly Han, MD, Thomas R. Kimball, MD, FASE, Rebecca K. Johnson, RDCS, FASE, Luc Mertens, MD, PhD, FASE, Stephen M. Paridon, MD, Andrew J. Powell, MD, FASE, and Leo Lopez, MD, FASE, *Philadelphia, Pennsylvania; Rochester and Minneapolis, Minnesota; Milwaukee, Wisconsin; Hamilton and Toronto, Ontario, Canada; Cincinnati, Ohio; Boston, Massachusetts; and Miami, Florida*

(J Am Soc Echocardiogr 2016;29:571-621.)

Keywords: Congenital heart disease, Transposition of the great arteries, Arterial switch operation, Atrial switch operation, Rastelli operation, Nikaidoh operation

TABLE OF CONTENTS

From The Children's Hospital of Philadelphia, Philadelphia, Pennsylvania (M.S.C., M.A.F., S.M.P.); the Mayo Clinic, Rochester, Minnesota (B.W.E., F.C., R.K.J.); the Medical College of Wisconsin, Milwaukee, Wisconsin (P.C.F.); McMaster University, Hamilton, Ontario, Canada (J.G.); the Minneapolis Heart Institute, Children's Heart Clinic at the Children's Hospitals and Clinics of Minnesota, Minneapolis, Minnesota (B.K.H.); Cincinnati Children's Hospital, Cincinnati, Ohio (T.R.K.); The Hospital for Sick Children, Toronto, Ontario, Canada (L.M.); Boston Children's Hospital, Boston, Massachusetts (A.J.P.); and Nicklaus Children's Hospital, Miami, Florida (L.L.).

All authors reported no actual or potential conflicts of interest in relation to this document.

Reprint requests: American Society of Echocardiography, 2100 Gateway Centre Boulevard, Suite 310, Morrisville, NC 27560 (E-mail: ase@asecho.org).

0894-7317/$36.00

http://dx.doi.org/10.1016/j.echo.2016.04.002

Abbreviations

ASE = American Society of Echocardiography

ASO = Arterial switch operation

AtrSO = Atrial switch operation

AV = Atrioventricular

BAS = Balloon atrial septostomy

CMR = Cardiovascular magnetic resonance

CT = Computed tomography

EF = Ejection fraction

IV = Intravenous

IVC = Inferior vena cava

LGE = Late gadolinium enhancement

LV = Left ventricular

PDA = Patent ductus arteriosus

PET = Positron emission tomography

PH = Pulmonary hypertension

Qp/Qs = Pulmonary-to-systemic flow ratio

RV = Right ventricular

SPECT = Single-photon emission computed tomography

SVC = Superior vena cava

TEE = Transesophageal echocardiography

TGA = Transposition of the great arteries

3D = Three-dimensional

TTE = Transthoracic echocardiography

2D = Two-dimensional

VSD = Ventricular septal defect

EXECUTIVE SUMMARY

Transposition of the great arteries (TGA) is a congenital heart defect with ventriculoarterial discordance in which the aorta is aligned with the right ventricle and the pulmonary artery is aligned with the left ventricle. When atrioventricular (AV) concordance is present, this anatomy results in cyanosis because the systemic and pulmonary circulations are in parallel. The clinical diagnosis and management of patients with TGA has improved dramatically over the past three decades because of the evolution and availability of multiple imaging modalities and strides made in the surgical management of these patients. Despite these technical advances, patients with TGA require long-term surveillance because of ongoing anatomic and hemodynamic abnormalities. The purpose of this report is to present guidelines for multimodality imaging in this cohort of patients.

Goals of Imaging

The goals of imaging in patients with TGA are to provide accurate and reproducible anatomic and hemodynamic information that facilitate medical and surgical planning and to provide surveillance imaging to evaluate potential issues related to the type of surgical operation that has been chosen.

Imaging Modalities

We review each imaging modality used in the diagnosis and follow-up of patients with TGA including the strengths, limitations, and clinical utility. We also define an optimal imaging protocol for each modality. In addition, an integrated multimodality imaging algorithm is defined and discussed.

Echocardiography

Echocardiography remains the main diagnostic imaging modality for TGA because of its widespread availability and portability. Transthoracic echocardiography (TTE) with two-dimensional (2D) and Doppler echocardiography provides comprehensive anatomic and hemodynamic evaluation in the majority of patients with TGA and is usually the only modality required for preoperative evaluation. For postoperative imaging, echocardiography is often used to assess for residual, recurrent or new pathology. Transesophageal echocardiography (TEE) is indicated in patients with poor windows, during intraoperative imaging, and in patients (usually adolescents or adults) who require cardioversion for arrhythmia.

Cardiovascular Magnetic Resonance

Cardiovascular magnetic resonance (CMR) plays a major role in the evaluation of patients with TGA. It is used primarily to image patients after surgical intervention. It provides important information regarding myocardial performance and viability as well as quantitative assessment of valvar function and accurate evaluation of baffles, conduits, and extracardiac structures such as the branch pulmonary arteries and the aortic arch.

Cardiovascular Computed Tomography

Multidetector computed tomography (CT) is typically used in patients with TGA who cannot undergo CMR. Adults with TGA who have had the atrial switch operation (AtrSO) frequently have pacemakers; thus, CT is an alternative imaging modality to provide incremental information to echocardiography.

Nuclear Scintigraphy

The primary use of nuclear imaging in patients with TGA is to assess myocardial viability or to assess blood flow to the branch pulmonary arteries after the arterial switch operation (ASO). Imaging can be performed at rest and during stress (exercise or pharmacologic) to determine if there are myocardial perfusion defects.

Exercise and Stress Imaging

Exercise testing and stress imaging are predominantly used to assess for myocardial perfusion problems in patients with TGA, particularly after the ASO. In patients with concern for coronary ischemia, stress imaging can unmask issues that are not present at rest in this population.

Cardiac Catheterization and Angiography

Diagnostic cardiac catheterization is rarely used in the preoperative evaluation of TGA but is required when balloon atrial septostomy (BAS) is performed to improve mixing and alleviate cyanosis. Some institutions use angiography to diagnose or confirm coronary artery (CA) anatomy before an ASO. Postoperative angiography is performed to assess for CA stenosis after CA reimplantation or during interventions such as branch pulmonary artery balloon dilation and stent placement. In the AtrSO, angiography is used to assess for baffle leaks or narrowing of the systemic or pulmonary venous pathways.

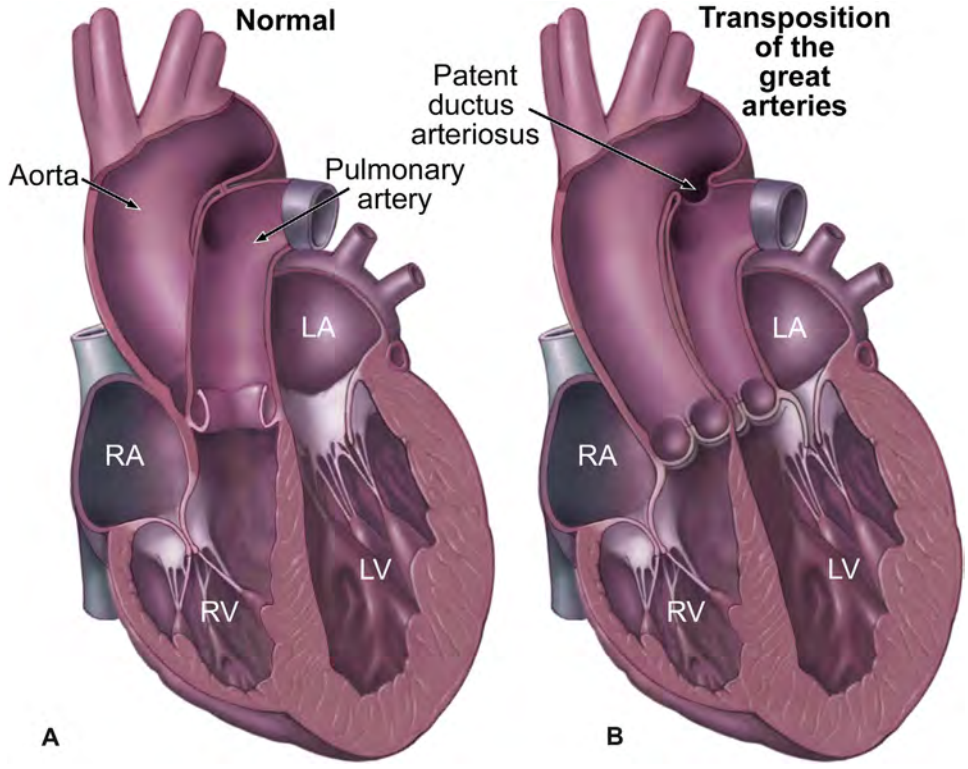

Figure 1 **(A)** A heart with normally related great arteries with the pulmonary artery arising from the right ventricle and the aorta arising from the left ventricle. **(B)** A heart with TGA with the aorta arising from the right ventricle and the pulmonary artery arising from the left ventricle. Note that the great arteries in TGA are parallel to each other rather than in a spiral relationship. *LA*, Left atrium; *LV*, left ventricle; *RA*, right atrium; *RV*, right ventricle.

BACKGROUND

TGA is a conotruncal abnormality defined as discordant ventriculoarterial connections; the aorta arises from the right ventricle and the pulmonary artery arises from the left ventricle. This is in the setting of D-looped ventricles in situs solitus or L-looped ventricles in situs inversus. Cyanosis occurs because the systemic and pulmonary circulations run in parallel rather than in series with deoxygenated blood from the systemic veins returning directly to the aorta and oxygenated blood from the pulmonary veins returning directly to the pulmonary artery (Figure 1). The cyanosis is usually severe, resulting in early neonatal recognition, typically in the first few hours of life. TGA is in distinct contrast to corrected TGA, in which there is AV discordance in addition to ventriculoarterial discordance; this constellation of findings results in a circulation that runs in series rather than in parallel. Because the physiology and surgical strategy for corrected TGA is so different from that for TGA, this lesion will not be further discussed.

TGA occurs in approximately 31.5 in 100,000 live births.[1] It is the 10th most common congenital heart defect and the second most common cyanotic lesion after tetralogy of Fallot.[1] Male individuals are affected more commonly than female individuals in a 2:1 ratio.[2] The etiology of TGA remains unknown, but it likely has a genetic origin.[3] There has been an association with maternal diabetes mellitus.[4] During development of the normal heart, the conotruncus (representing the primitive outflow tracts and semilunar valves) rotates such that the pulmonary artery is aligned with the right ventricle and the aorta is aligned with the left ventricle.[5] In TGA, it is likely that the normal rotation of the conotruncus is inhibited, preventing the normal alignment of the great vessels and resulting in ventriculoarterial discordance.

TGA may occur as an isolated defect or in association with other cardiac anomalies. In the majority of patients with TGA, the aorta is rightward and anterior to the pulmonary artery, but there can be wide variability in the spatial relationships between the great arteries, including the rare relationship of a posterior and/or leftward aorta.[6] Approximately 60% of patients with TGA have an intact ventricular septum, and the other 40% have ventricular septal defects (VSD).[7] At birth, a patent foramen ovale and patent ductus arteriosus (PDA) are usual and allow a variable amount of mixture of oxygenated and deoxygenated blood. If the foramen ovale is closed or very small, cyanosis may be severe enough to require urgent intervention with a BAS, a catheter-directed enlargement of the foramen ovale pioneered by Dr. William Rashkind.[8] VSDs can be simple (perimembranous type or muscular type) or more complex (malalignment type with associated outflow tract obstruction, doubly committed subarterial type, or inlet type). The type of VSD often dictates the surgical option required to address the anomaly.

Before the 1950's, TGA was a fatal disease resulting in death in 89% of patients by 1 year of age.[9] Early death resulted from severe cyanosis. If there was an adequate atrial communication and/or VSD, mortality was delayed to later in childhood as a result of pulmonary vascular disease. In the early 1950's, surgical correction of TGA was attempted with an early form of the ASO. The outcomes were quite poor, primarily because of an inability to successfully transfer the CAs from the aorta to the "neo"-aorta. In that same decade, different strategies to palliate TGA were developed, eventually leading to the AtrSO. Variations of this procedure were pioneered and reported by Drs. Mustard and Senning (Video 1; available at www.onlinejase.com).[10,11] The AtrSO, in which the superior vena cava (SVC) and inferior vena cava (IVC) are baffled to

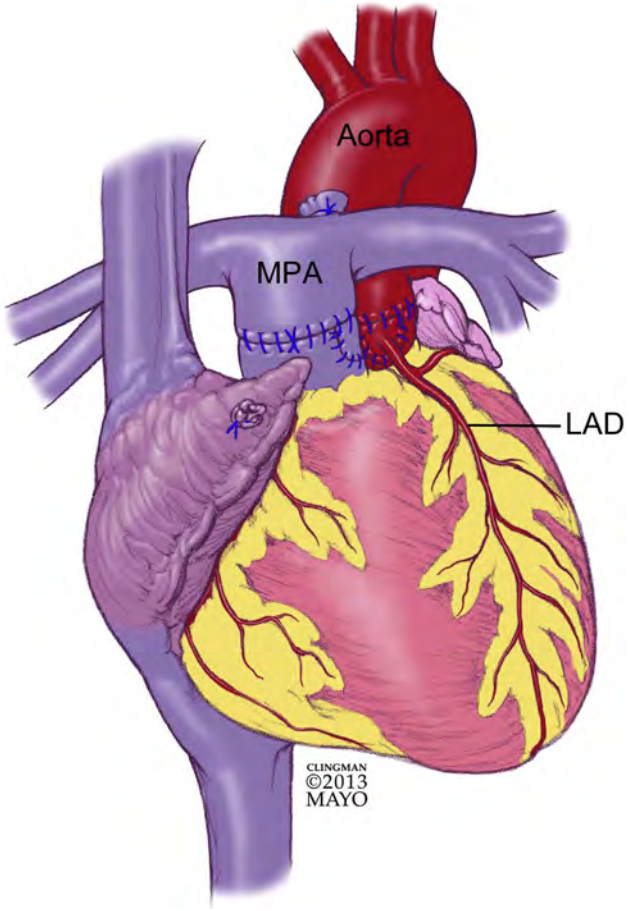

Figure 2 This figure depicts the ASO with the LeCompte maneuver. Note the main pulmonary artery (MPA) and branch pulmonary arteries are located anterior to the aorta. The location of the left anterior descending CA (LAD) after translocation to the neoaorta is also displayed. Used with permission of Mayo Foundation for Medical Education and Research, all rights reserved.

the mitral valve and the pulmonary veins are baffled to the tricuspid valve, was the first operative procedure for TGA that resulted in acceptable operative and midterm survival.[11-13] Although the AtrSO achieved widespread success from the mid-1960's through the early-1980's, the search continued for a more "physiologic" procedure because of the known long-term complications such as right ventricular (RV) dysfunction and significant tricuspid regurgitation (in a ventricle potentially unsuited for a lifetime as the systemic pumping chamber), arrhythmias, and a small but important prevalence of obstruction of the systemic and/or pulmonary venous pathways.[14-17]

In 1975, Jatene *et al.*[18] performed the first successful ASO. Although not a true anatomical "correction," this landmark operation effectively achieved circulation in series with the morphologic left ventricle acting as the systemic pumping chamber. During the ASO, the great arteries are transected and "switched" to the other semilunar valve, and the CAs are translocated to the "neoaorta" (Video 2; available at www.onlinejase.com). The LeCompte maneuver[19] is also performed during the operation to avoid distortion of the branch pulmonary arteries in the process of switching the great vessels. The LeCompte maneuver relocates the aorta posterior to the pulmonary artery such that both branch pulmonary arteries drape anteriorly to the aorta (Figure 2, Video 2; available at www.onlinejase.com). Although the ASO is a more "physiologic" procedure compared to the AtrSO, it is by no means a "corrective repair," as it requires multiple suture lines as well as mobilization and reimplantation of the CAs.

In the setting of posterior malalignment VSD and left ventricular (LV) (subpulmonary) outflow tract obstruction alternative surgical strategies are required for repair because a successful ASO requires a relatively normal pulmonary valve. Most patients with posterior

Table 1 Structural and functional abnormalities encountered in TGA

Preoperative TGA
Atrial communication (for adequate mixing)
VSD (in 40%)
LV outflow tract obstruction
Pulmonary valve (stenosis)
RV outflow tract obstruction
Aortic valve (stenosis)
Aortic arch (coarctation, interruption)
Ductus arteriosus
CA variations
After ASO
Early
PH
Ventricular dysfunction
CA kinking or stenosis
Residual VSD (if one present)
Supravalvar pulmonary stenosis
Supravalvar aortic stenosis
Neoaortic or neopulmonary valve regurgitation
Branch pulmonary artery stenosis
Aortopulmonary collateral vessels
Late
PH
Ventricular dilation and dysfunction
CA stenosis/occlusion
Supravalvar pulmonary stenosis
Neoaortic root dilation
Neoaortic valve regurgitation
Branch pulmonary artery stenosis
Subaortic obstruction
After AtrSO
Systemic venous baffle obstruction
Pulmonary venous baffle obstruction
Atrial baffle leak
Tricuspid regurgitation
RV dysfunction
Sinus node dysfunction/atrial arrhythmias
After Rastelli/Nikaidoh operation
Residual VSD
Ventricular dilation and dysfunction
Subaortic obstruction
Conduit obstruction
Conduit regurgitation
CA stenosis/kinking (if reimplanted)

Table 2 Comparison of imaging modalities

Characteristic	Echocardiography	CMR	CT angiography	Nuclear scintigraphy
Availability	++++	++	++	+
Portability	++++	–	–	–
Radiation exposure	–	–	+++	++++
Safety with pacers	++++	+	+++	+++
CA anatomy	++	+++	+++	–
Aortopulmonary collateral vessels	+	++++	++	–
Supravalvar aortic stenosis (ASO)	++++	++++	++++	–
Supravalvar pulmonary stenosis (ASO)	++++	++++	++++	–
Branch PA stenosis (ASO)	++	++++	++++	–
Neoaortic root dilation (ASO)	++++	++++	++++	–
Neoaortic regurgitation (severity) (ASO)	++	++++	–	–
CA stenosis (ASO)	+	+++	++++	++
Myocardial ischemia (ASO)	+	+++	–	++++
Systemic venous baffle obstruction (AtrSO)	++	+++	+++	–
Pulmonary venous baffle obstruction (AtrSO)	++	+++	+++	–
Baffle leak (AtrSO)	++	++	–	+
RV dysfunction (AtrSO)	++	++++	+++	–
Residual VSD (Rastelli/Nikaidoh)	++++	+++	+	–
Subaortic obstruction (Rastelli/Nikaidoh)	++++	++++	+++	–
Conduit obstruction (Rastelli/Nikaidoh)	+++	+++	+++	–
Conduit regurgitation (Rastelli/Nikaidoh)	++	++++	–	–

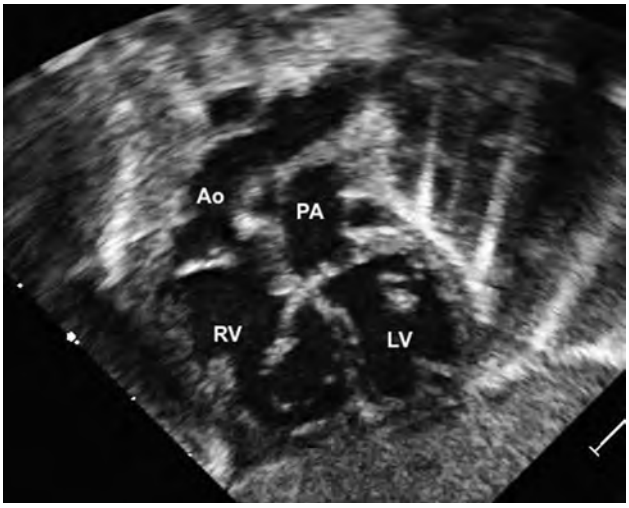

Figure 3 Two-dimensional subxiphoid left anterior oblique view demonstrates the relationship of the great arteries in TGA. The aorta (Ao) is seen arising from the right ventricle and the pulmonary artery is seen arising from the left ventricle. The aorta is seen arching over the pulmonary artery. *LV*, Left ventricle; *PA*, pulmonary artery; *RV*, right ventricle.

malalignment VSDs have hypoplastic pulmonary valves with thickened leaflets and subpulmonary narrowing. Thus, the typical operation performed in this setting is the Rastelli procedure (Video 3; available at www.onlinejase.com).[20] The pathway from the baffle becomes the neo–left ventricle, with the VSD acting as the subaortic region. Alternatively, the Nikaidoh operation may be performed.[21] This is a more complex procedure also known as aortic translocation. It is performed to avoid late obstruction of the baffled LV outflow tract that can occur after the Rastelli operation. The Nikaidoh procedure involves division of the small posterior pulmonary annulus and mobilization of the aortic root, which is moved to the open pulmonary annulus, thus bringing it closer to the left ventricle. The CAs are often translocated to avoid kinking, and the VSD is closed with a patch. A pathway from the right ventricle to the pulmonary arteries is then created.

For TGA in the setting of anterior malalignment VSD with RV (subaortic) outflow tract obstruction, an ASO is performed along with a combination of augmentation of the RV outflow tract (similar to tetralogy of Fallot)[22] and VSD closure. The aortic arch is also repaired if obstructed or interrupted. Because most of the consequences of this complex repair fall under other categories, it will not be further discussed as an individual lesion.

Diagnostic information in patients with TGA can be obtained using a variety of diagnostic tools in the preoperative and postoperative period. The choice of when to perform echocardiography, CMR, cardiovascular CT, nuclear scintigraphy, x-ray angiography, or a combination of these diagnostic procedures is dictated by the clinical question and institution-related issues. The aim of this document is to describe the role of each diagnostic modality in the care of patients with TGA before and after surgical repair and to provide guidelines for a multimodality approach that takes into account these concerns. For each imaging modality, a general overview is provided along with a discussion of its strengths and limitations. Guidelines are presented for the use of the each modality in patients with TGA.

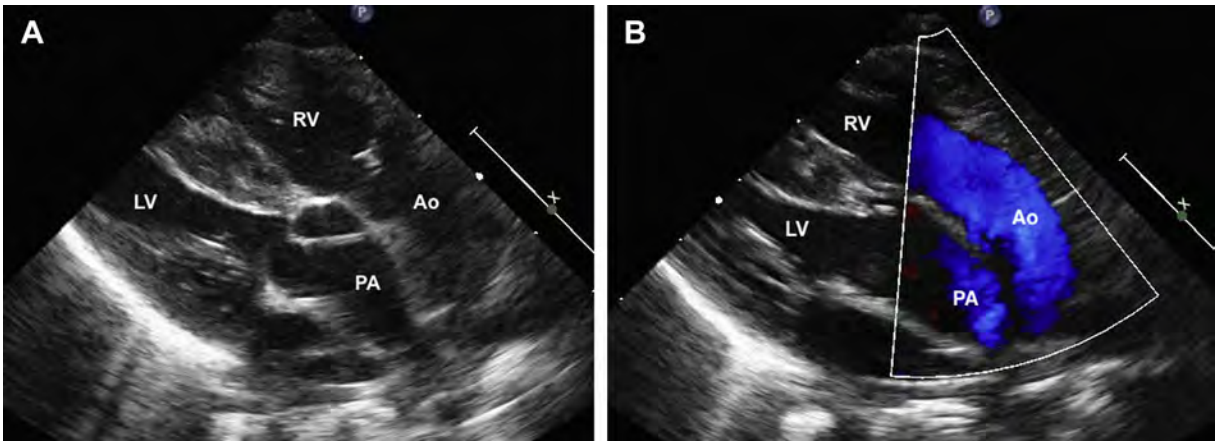

Figure 4 **(A)** Parasternal long-axis view of a patient with TGA and intact ventricular septum demonstrates the parallel relationship of the great arteries. **(B)** The same view with color flow demonstrates unobstructed flow to both great arteries. *Ao*, Aorta; *LV*, left ventricle; *PA*, pulmonary artery; *RV*, right ventricle.

GENERAL CONSIDERATIONS

In patients with TGA, the diagnostic evaluation of the preoperative and postoperative patient has different goals. Various structural and functional abnormalities must be considered (Table 1). The preoperative patient is cyanotic, and initial imaging is usually performed to assess for adequate mixing of the pulmonary and systemic circulations. This is primarily achieved with TTE. Occasionally, a complete echocardiographic study must be delayed until a BAS is performed. For postoperative imaging, understanding each patient's prior medical and surgical history is essential because there are several management strategies for patients with TGA. Evaluation of the previous operative reports is critical to that end. If medical records are not available, the patient's age can offer a clue to the type of surgical procedure performed. The AtrSO was performed from the 1950's through the early 1980's and is now rarely performed in patients who have late clinical presentation (at weeks to months of age). The majority of patients born after the early 1980's have primarily had the ASO or a variation of this procedure. Those patients with posterior malalignment VSD have generally had Rastelli or Nikaidoh operations. Patients with TGA are now surviving into adulthood. Imaging is an important component of the long-term follow-up of these patients, and this guideline will provide cardiology practitioners with a strategy to determine the best modalities to use in various clinical situations.

GOALS OF IMAGING

In a patient with TGA, each of the abnormalities listed in Table 1 can be evaluated using a combination of imaging modalities. The advantages of each modality are listed in Table 2.

ECHOCARDIOGRAPHY

Overview of Modality

Two-dimensional and Doppler echocardiography provide the ability to evaluate the majority of anatomic and hemodynamic abnormalities in patients with TGA.[23] TTE identifies anatomic detail, including levels of shunting, the relationship of the great vessels to each other, qualitative assessment of ventricular function, and the presence and significance of additional congenital heart abnormalities. In most patients, the CA anatomy can also be identified using a combination of 2D and color flow Doppler. Doppler echocardiography is particularly important in this population for noninvasive hemodynamic assessment of the atrial communication and the PDA, severity of outflow tract obstruction, AV and semilunar valve function, and assessment of the VSD (if present). TEE is typically used to assess the adequacy of intraoperative repair[24]; it can also be used to guide interventional procedures such as closure of baffle leaks or stenting of venous baffle limbs after the AtrSO. TEE is also useful to evaluate valve anatomy when TTE does not provide adequate images. More recently, myocardial deformation imaging is emerging as a tool to evaluate regional wall motion abnormalities in this population, particularly in those who have undergone the ASO and may have CA stenosis or ischemia.

Strengths and Limitations

Echocardiography has been used as the primary diagnostic imaging modality in patients with TGA since the 1980's. It is widely available, relatively inexpensive, portable, and, importantly, quite safe. Ultrasound does not generally cause harm to human tissue. Moreover, practitioners are well trained to use this modality.

There are important limitations of echocardiography in patients with TGA. In the preoperative evaluation, the resolution is such that accurate diagnosis of CA anatomy is sometimes not possible. In older patients, the acoustic windows often become challenging; in some cases, other modalities are required to answer anatomic and physiologic questions. Particular data such as end-diastolic pressure and pulmonary vascular resistance cannot be accurately measured by echocardiography. Moreover, accurate quantitative information on right heart size and function, quantitative assessment of valvar regurgitation, accurate identification of CA ischemia, and optimal visualization of extracardiac structures are better delineated using other modalities.

Preoperative Assessment of TGA with Echocardiography

The preoperative transthoracic echocardiographic evaluation of a patient with TGA must obtain every piece of information necessary to ensure that the surgical strategy chosen is appropriate. Hence,

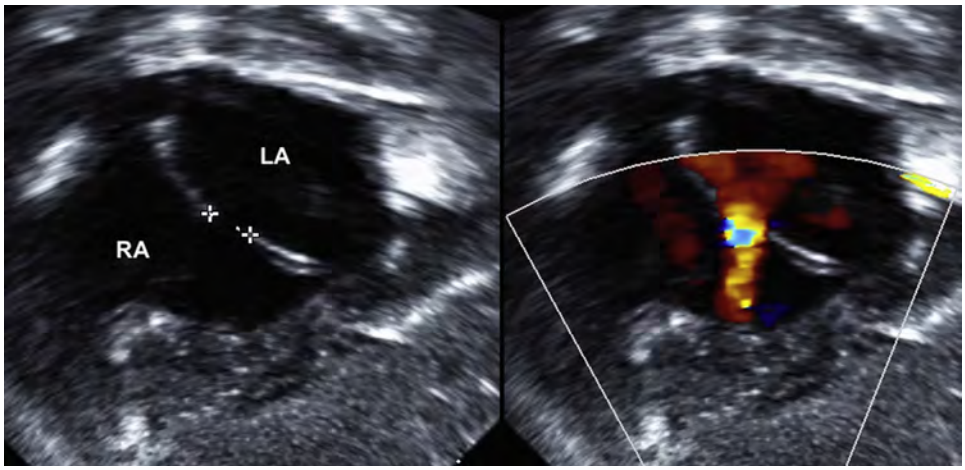

Figure 5 Subxiphoid left anterior oblique view in color-compare mode highlights the atrial communication in an infant with TGA with intact ventricular septum. In this case, the atrial communication was considered adequate for mixing and a BAS was not required. *LA*, Left atrium; *RA*, right atrium.

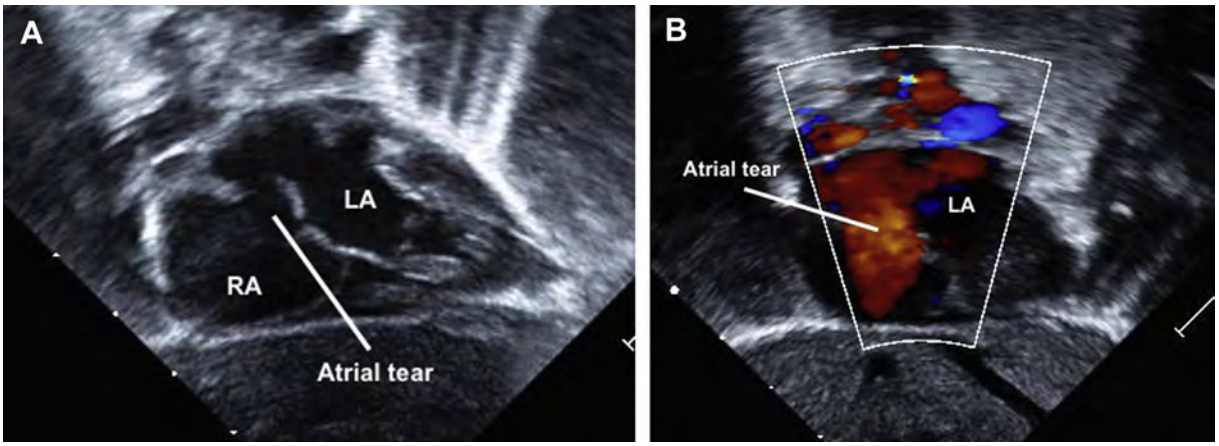

Figure 6 **(A)** Subxiphoid frontal (long-axis) view demonstrates an adequate atrial communication created after BAS. The portion of the septum primum that is torn with the balloon is seen flapping into the left atrium (LA). **(B)** The same view with color flow demonstrates significant atrial level shunting after BAS. *RA*, Right atrium.

echocardiography must be performed carefully and systematically. The majority of infants with TGA do not require another modality for diagnostic purposes. The segmental approach to anatomic diagnosis provides the best framework in which to obtain a comprehensive assessment of the cardiac malformation and its associated lesions. A strict protocol is necessary when evaluating neonates with congenital heart disease, and most centers follow the protocol for a pediatric echocardiogram established by the American Society of Echocardiography (ASE) Pediatric and Congenital Heart Disease Council in 2006.[23]

Anatomic Assessment of TGA. The diagnosis of TGA can be made with the first sweep in the subxiphoid frontal (long-axis) view. This view shows that the first visible great artery originates from the left ventricle and bifurcates into a right and left branch, identifying it as the pulmonary artery. Sweeping further anteriorly reveals the origin of the aorta from the RV (Figure 3, Video 4; available at www.onlinejase.com). The great arteries typically arise in parallel in TGA in contrast to the normal heart where the great arteries spiral around each other. If the protocol begins with a parasternal long-axis sweep, the initial image shows that the proximal great arteries take a parallel course as they originate from the two ventricles (Figures 4A and 4B, Video 5; available at www.onlinejase.com).

Interrogation of the atrial communication is one of the most important components of the initial assessment of a patient with TGA. After birth, there is a normal increase in pulmonary blood flow, which results in increased pulmonary venous return to the left atrium. An atrial communication results in effective left-to-right shunting at the atrial level, providing oxygenated blood to the systemic circulation.[25] In those patients with a small atrial communication, the increase in left atrial pressure may partially or completely close the flap valve of the foramen ovale, hindering the passage of oxygenated blood into the right atrium and resulting in marked cyanosis. Assessment of the adequacy of the atrial communication is achieved by clinical knowledge of the systemic oxygen saturation as well as echocardiographic measurement of the size of the atrial communication and the mean pressure gradient across the interatrial septum (Figure 5). If the defect is deemed too small by these criteria, BAS will be necessary to enlarge the atrial communication (Video 6; available at www.onlinejase.com). TTE or TEE can be used to guide catheter-directed

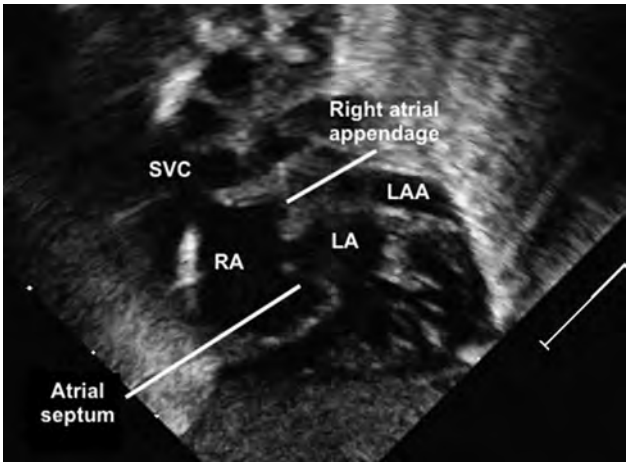

Figure 7 Subxiphoid frontal (long-axis) view demonstrates leftward juxtaposition of the atrial appendages. The atrial septum is seen perpendicular to the diaphragm (it should be parallel when the atrial septum is in the normal position). The right atrial appendage is visualized as it crosses over toward the left atrium (LA). The left atrial appendage (LAA) (in its normal position) sits just inferior to the right atrial appendage. *RA*, Right atrium.

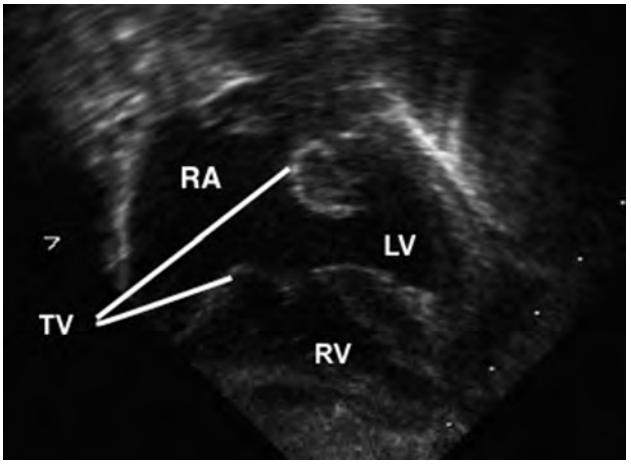

Figure 8 Subxiphoid left anterior oblique view of a straddling tricuspid valve through an inlet (AV canal) type VSD in a patient with TGA. The great arteries are not seen in this view. *LV*, Left ventricle; *RA*, right atrium; *RV*, right ventricle; *TV*, tricuspid valve.

Table 3 Nomenclature of the types of VSDs seen in TGA

Anderson term	Van Praagh/ Weinberg term	STS term	ISNPCHD term
Perimembranous	Membranous/ conoventricular	Type 2	Central
Perimembranous with malalignment	Conoventricular with malalignment, malalignment		Outlet with malalignment
Doubly committed subarterial	Conal septal, conal septal hypoplasia	Type 1	Outlet
Perimembranous inlet	AV canal type	Type 3	Inlet
Muscular	Muscular	Type 4	Trabecular

ISNPCHD, International Society of Nomenclature of Paediatric and Congenital Heart Disease; *STS*, Society of Thoracic Surgeons.

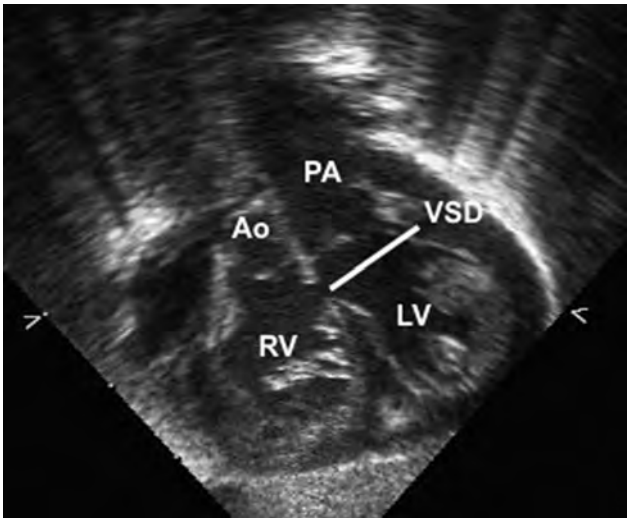

Figure 9 Subxiphoid left anterior oblique view demonstrates a VSD (doubly committed subarterial, conal septal) that sits just under both great arteries. Note the semilunar valves are at the same level and the tissue in between the two outflow tracts is quite small and fibrous rather than muscular. *Ao*, Aorta; *LV*, left ventricle; *PA*, pulmonary artery; *RV*, right ventricle.

BAS either at the patient's bedside or in the cardiac catheterization laboratory. The resulting atrial communication after BAS can be readily recognized (Figures 6A and 6B, Video 7; available at www.onlinejase.com). If the atrial communication is deemed adequate by echocardiography but the patient is markedly cyanotic, other etiologies such as high pulmonary vascular resistance or pulmonary vein stenosis must be considered.

Once the diagnosis of TGA is confirmed with the first transthoracic echocardiographic images and the atrial communication is deemed adequate (or the patient has undergone BAS), the segmental approach can be used to evaluate for all possible associated lesions. In the clinically stable patient, evaluation of the systemic and pulmonary veins represents the first part of this endeavor. A persistent left SVC occurs in approximately 4% of patients with TGA.[26] Its presence can have significant impact during surgical intervention, particularly at the time of cardiopulmonary bypass cannulation. Partial or total anomalous pulmonary venous return can also occur and must be excluded in the evaluation because this anomaly would likely be repaired at the same time as the primary surgical repair for TGA.[27]

On further imaging of the atria, the atrial appendages should be identified. Leftward juxtaposition of the atrial appendages occurs in approximately 2% of patients with TGA.[26] Conversely, >50% of patients with juxtaposition of the atrial appendages have TGA.[26,28] Because of its unusual appearance, leftward juxtaposition sometimes mimics a moderate or large atrial communication. In leftward juxtaposition of the atrial appendages, a subxiphoid frontal (long-axis) sweep shows the atrial septum in a perpendicular orientation to the diaphragm (Figure 7, Video 8; available at www.onlinejase.com) (in the normal heart, the atrial septum is parallel to the diaphragm in this view). As the probe sweeps anteriorly, the ostium of the right atrial appendage will become apparent, and the appendage itself is seen passing behind

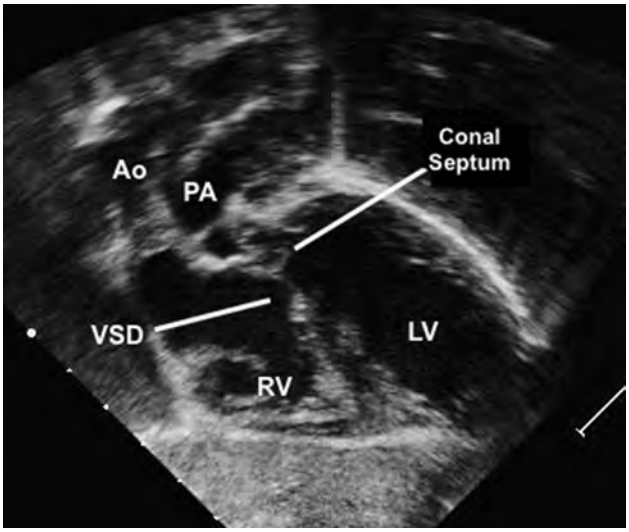

Figure 10 Subxiphoid left anterior oblique view in a patient with TGA and posterior malalignment type VSD demonstrates the conal septum deviated into the left ventricular outflow tract, just under the pulmonary valve. This conal septal deviation causes subpulmonary obstruction. *Ao*, aorta; *LV*, left ventricle; *PA*, pulmonary artery; *RV*, right ventricle.

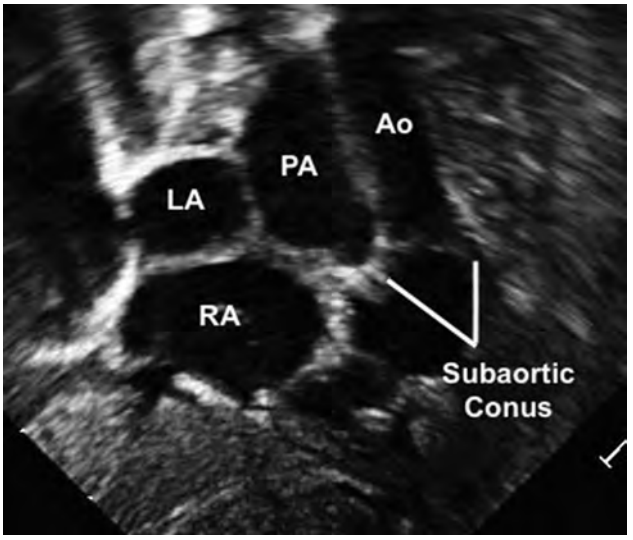

Figure 12 Subxiphoid right anterior oblique view in a patient with TGA demonstrates subaortic conus (ring of muscle under the aortic valve). Not seen in this image is the fact that there is no subpulmonary conus (the pulmonary valve is in fibrous continuity with the mitral valve). *Ao*, Aorta; *LA*, left atrium; *PA*, pulmonary artery; *RA*, right atrium.

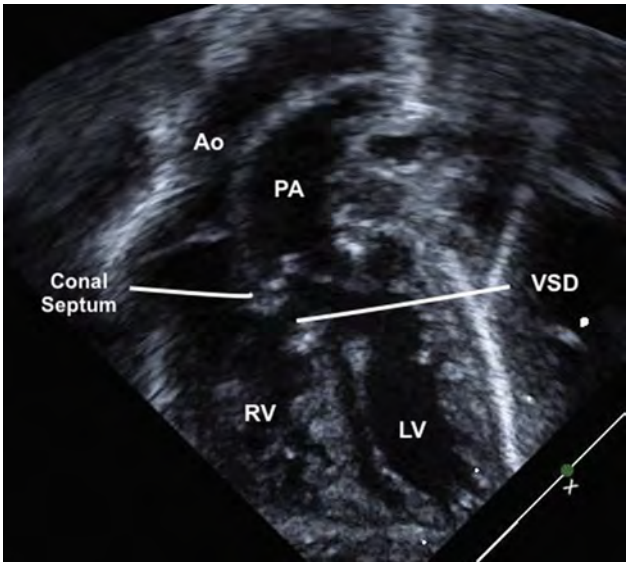

Figure 11 Apical five-chamber view of a patient with TGA and anterior malalignment type VSD demonstrates the conal septum deviated toward the right ventricle (RV) and the VSD sitting under the pulmonary valve. Not seen in this image is the fact that this patient also has transverse arch hypoplasia. *Ao*, Aorta; *LV*, left ventricle; *PA*, pulmonary artery.

the pulmonary artery. This structure can also be seen posterior the pulmonary artery in apical four-chamber and parasternal long-axis views.

Abnormalities of the AV valves may also occur in association with TGA, and these include a common AV valve in a complete AV canal defect, AV valve hypoplasia and/or stenosis, cleft mitral valve, and straddling and/or overriding AV valves.[29,30] Abnormalities of the tricuspid valve, including abnormal attachments to the conal septum or to the crest of the ventricular muscular septum, occur frequently in patients with TGA in association with a VSD.[29] All views can be used to identify these AV valve abnormalities. Subxiphoid and apical four-chamber views are particularly useful to determine if an AV valve is straddling. In addition to anatomic abnormalities, AV valves may be regurgitant, possibly related to ventricular dysfunction or ischemia from severe cyanosis.

A common associated lesion in patients with TGA is a VSD, occurring in approximately 40% of these patients.[2,31,32] As in normally related great arteries, VSDs in TGA can be divided into five different anatomic categories (Table 3). VSDs may be variable in size and may be multiple. A VSD in association with TGA significantly increases the complexity of the disease and may dictate the surgical strategy. The echocardiographic study must evaluate the entire ventricular septum, delineate all the margins of the VSD(s), and exclude other associations with TGA and VSD such as outflow tract obstruction, aortic coarctation, straddling AV valves, and prolapsing semilunar valves. Accurate assessment of the size of the defect is important to determine whether it needs to be closed during the primary surgical intervention. Small VSDs may be hemodynamically insignificant or may close spontaneously. With inlet (AV canal type) VSDs, imaging must include assessment for a straddling tricuspid valve (Figure 8). Doubly committed subarterial (conal septal) defects have fibrous continuity between the aortic and pulmonary valves (Figure 9). Thus, closure of these defects may result in distortion of semilunar valve leaflets and valve regurgitation. Conoventricular (malalignment) defects are associated with outflow tract obstruction. Posterior malalignment of the conal septum results in LV (subpulmonary) outflow tract obstruction (Figure 10). With anterior malalignment of the conal septum, the RV (subaortic) outflow tract is narrow, and distal arch obstruction is common (Figure 11). Muscular defects, if large, may be challenging to close because of their location in the ventricular septum. Subxiphoid, apical, and parasternal views provide complimentary imaging that helps define the location and size of VSDs. Identifying multiple VSDs can be challenging when the pressure is equal between the ventricles. Ventricular

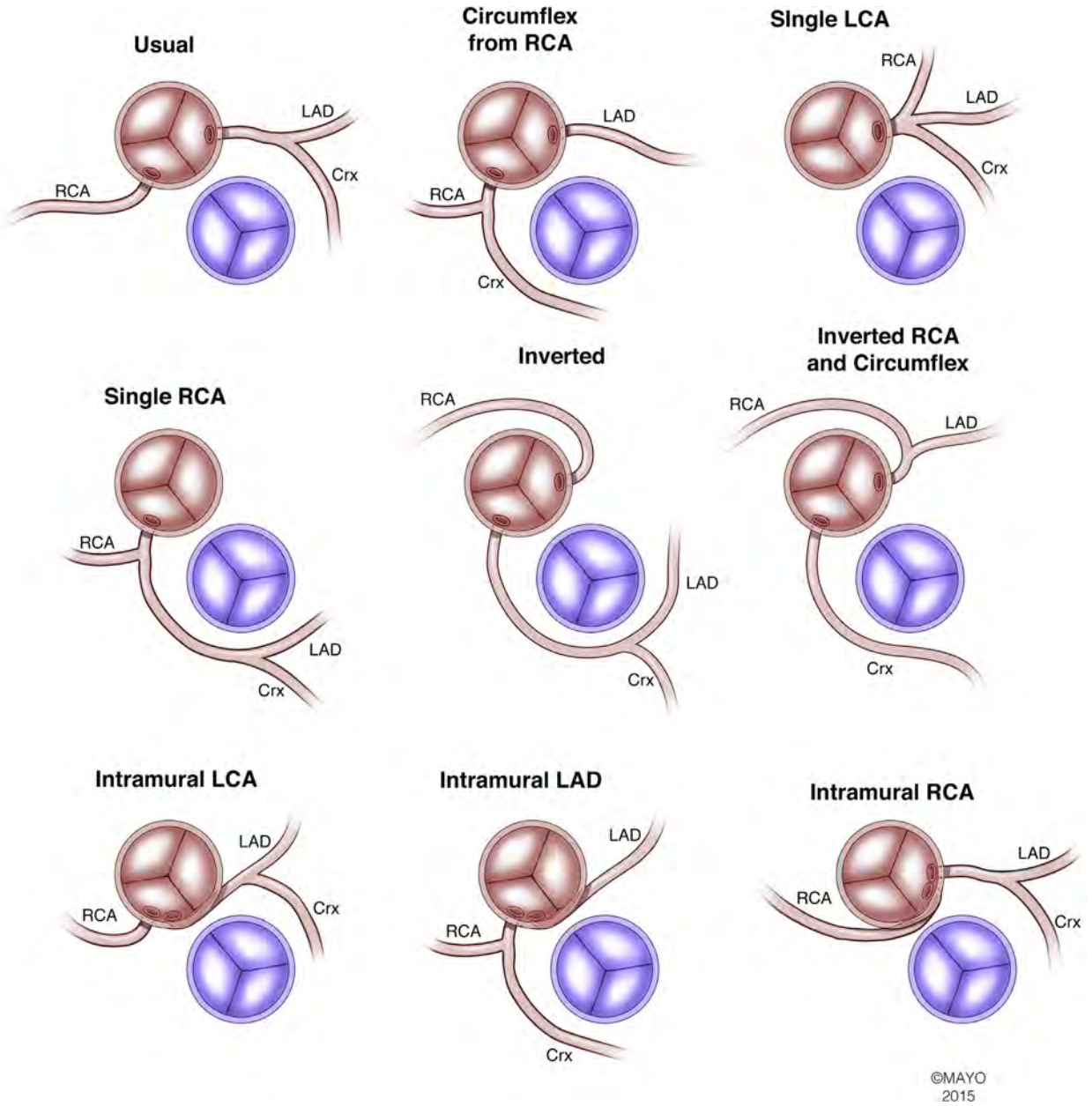

Figure 13 Variations of CA anatomy in patients with TGA. The aortic valve is in red and the pulmonic valve is in blue. *Crx*, Circumflex CA; *LAD*, left anterior descending CA; *LCA*, left CA; *RCA*, right CA. Used with permission of Mayo Foundation for Medical Education and Research, all rights reserved.

hypoplasia may also occur in the setting of TGA with VSD, particularly when AV valve straddling or outflow tract obstruction is seen.[33]

Conus is defined as the ring of muscle that sits entirely under a great vessel. Conus can be present under one, both, or neither great artery. In the normal heart, subpulmonary conus is present (muscular separation between the tricuspid and pulmonary valves), and there is no subaortic conus (mitral-to-aortic fibrous continuity). The most common conal morphology in patients with TGA is persistence of the subaortic conus with regression of the subpulmonary conus (Figure 12); this conal anatomy is seen in 88% to 96% of patients with TGA.[34,35] Bilateral conus is seen in 3% to 7%; bilaterally absent conus or only subpulmonary conus with absent subaortic conus are both rare in TGA.

LV outflow tract obstruction occurs in almost 10% of patients with TGA and VSD and can have significant implications in terms of the surgical approach.[32] The mechanisms for obstruction include ventricular septal hypertrophy, aneurysmal membranous septum billowing into the subpulmonary region, a subvalvar fibromuscular ridge, abnormal attachments of the mitral valve apparatus to the ventricular septum, posterior malalignment of the conal septum, and pulmonary valvar stenosis.[36] Occasionally, dynamic subpulmonary stenosis occurs in TGA and intact ventricular septum with bowing of the ventricular septum into the LV outflow tract secondary to RV hypertension, a condition which usually resolves after the ASO. In contrast, anterior malalignment of the conal septum into the RV outflow tract occurs less frequently and is associated with multiple levels of aortic outflow

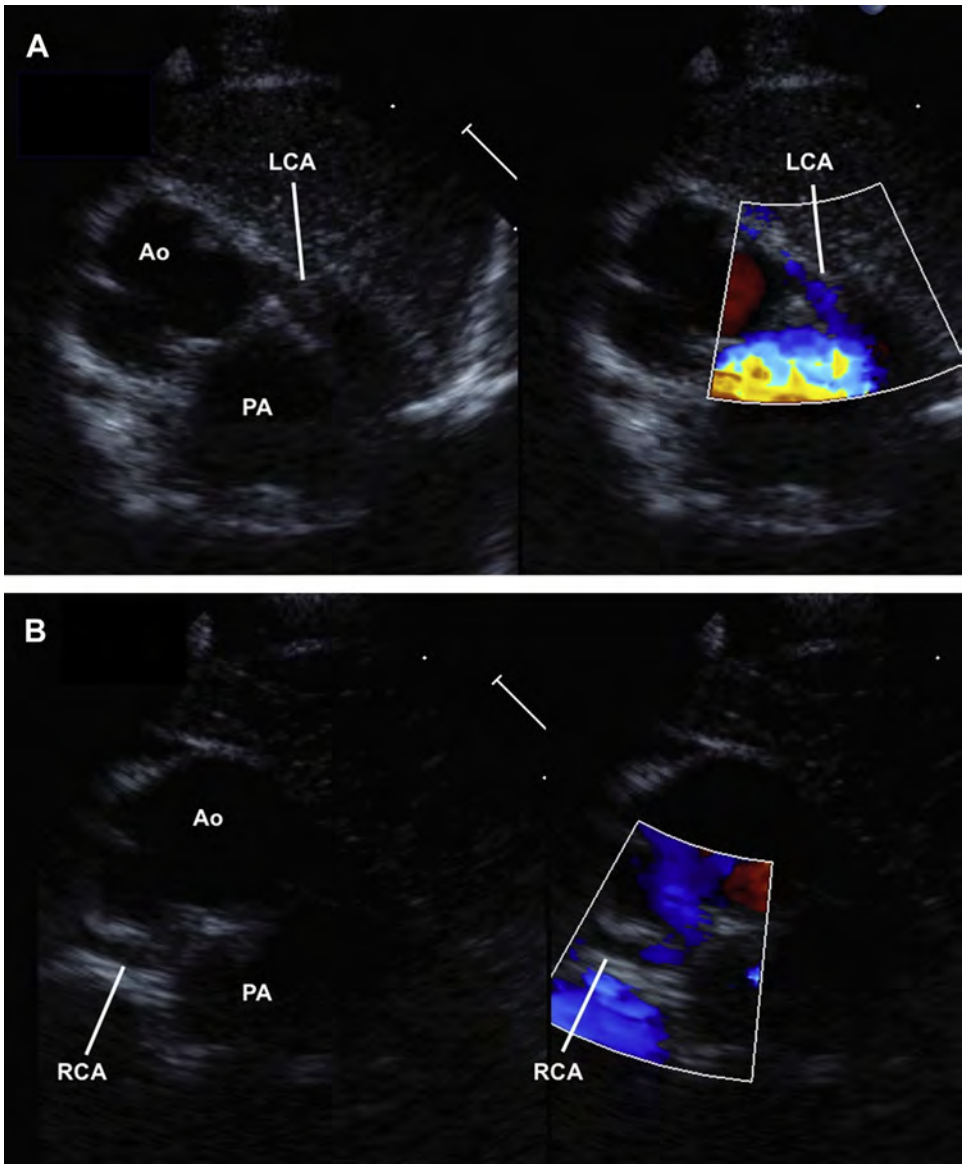

Figure 14 High parasternal view in color-compare mode in a patient with TGA demonstrates **(A)** the usual pattern of the left CA (LCA) arising from the left-facing sinus to the pulmonary artery and **(B)** the right CA (RCA) arising from the right-facing sinus to the pulmonary artery. *Ao*, Aorta; *PA*, pulmonary artery.

tract obstruction, including subvalvar and valvar aortic stenosis as well as aortic coarctation or aortic arch interruption. Subxiphoid, apical, and parasternal views all provide comprehensive images of the RV and LV outflow tracts to aid in determining the mechanism for obstruction, and suprasternal views are especially useful in assessing aortic arch abnormalities.

In TGA, the CAs are never in the normal position because the aorta is transposed and is usually anterior to the pulmonary artery. With the introduction of the ASO (which includes CA translocation to the neoaorta), assessment of CA anatomy has become a fundamental component of the echocardiographic evaluation of neonates with TGA. Recognition of CA anatomy is important because some variations of CA anatomy may be difficult to "switch" or are associated with later CA events.[37-39] Despite the anatomic variations, it is currently accepted that all CA patterns can be surgically translocated. The presence of an intramural CA, where a segment of the proximal CA runs within the wall of the aorta, appears to carry the highest risk for events and has been consistently associated with poor early outcome in multiple surgical series.[37-39] The intramural segment makes surgical CA transfer more complex and increases the risk for CA stenosis.[39,40] The presence of a single CA ostium has also been described as a higher risk for early mortality.[38]

The CA ostia are almost always located in one or both of the two aortic sinuses facing the pulmonary artery. The most common CA variations seen in TGA are displayed in Figure 13. The "usual" CA pattern in TGA involves the origin of the left main CA (which gives rise to the anterior descending and circumflex CAs) from the leftward and/or anterior facing aortic sinus and origin of the right CA from the rightward and/or posterior facing aortic sinus; this arrangement occurs in 65% of all patients (Figures 14A and 14B).[7] Common CA variants include circumflex CA from the right CA (13%), single right CA with the left main CA coursing behind the pulmonary artery (7%),

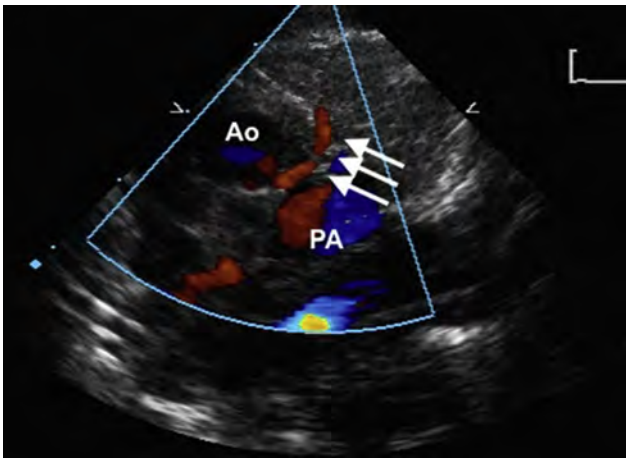

Figure 15 High parasternal view using color Doppler demonstrates an intramural left CA arising from the right-facing sinus, which takes a course between the aorta (Ao) and the pulmonary artery (PA) *(white arrows)*. Transferring this CA to the neoaorta could result in distortion of the vessel.

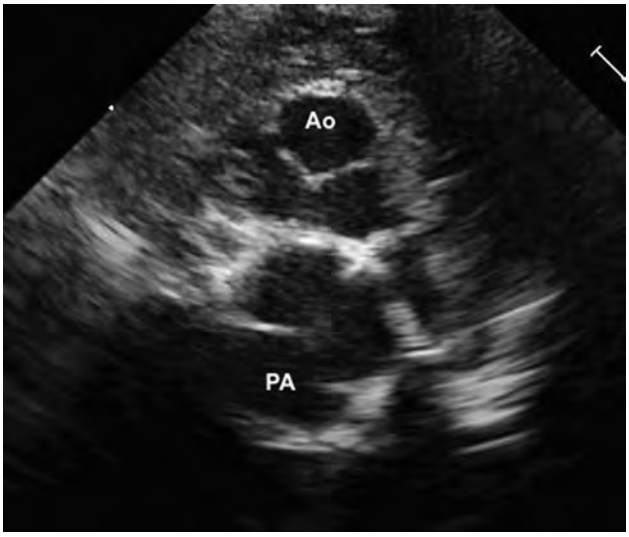

Figure 16 High parasternal view of the aortic and pulmonary valves. Usually the commissures align between the vessels but in this case they are offset. *Ao*, Aorta; *PA*, pulmonary artery.

and origin of the right CA and anterior descending CA from the leftward and/or anterior facing sinus and origin of the circumflex CA from the rightward and/or posterior facing sinus (inverted right CA and circumflex; 6%). More rare variants include a single right CA with the left main CA taking an intramural course between the great arteries (3%), inverted CAs with origin of the left main CA from the rightward and/or posterior facing sinus and origin of the right CA from the leftward and/or anterior facing sinus (3%), single left CA with the right CA coursing in front of the aorta (2%), and single left CA with the right CA taking an intramural course between the great arteries (1%). Parasternal short-axis views provide the best evaluation of the CA anatomy, particularly in demonstrating the origins of the CA ostia and assessing for an intramural CA, which courses between the two great arteries (Figure 15). This view is also useful in the evaluation of commissural alignment between the aortic and pulmonary valves, because this information can become important when planning the translocation of the CA "buttons" to the pulmonary (neoaortic) root (Figure 16). The parasternal long-axis view is occasionally better at displaying the bifurcation of the left main CA into the anterior descending and circumflex CAs. In all of the variants other than the "usual" arrangement and those with an intramural CA, one of the CA branches will travel behind the pulmonary artery and/or in front of the aorta (Figures 13 and 17, Video 9; available at www.onlinejase.com). These variants are frequently first recognized in subxiphoid and apical sweeps.

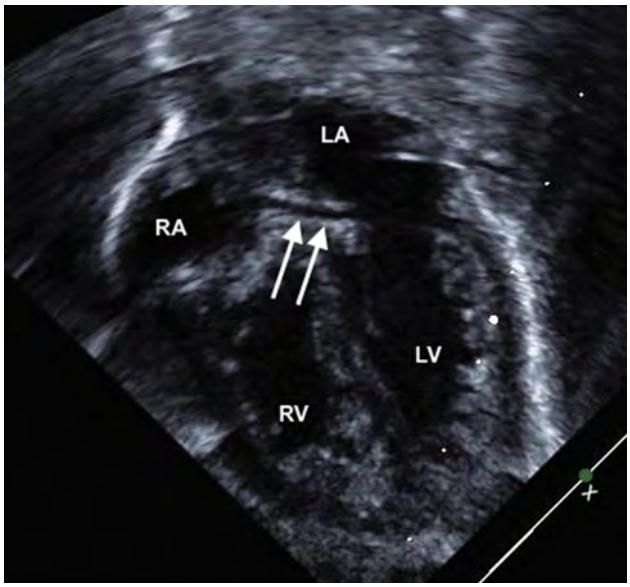

Figure 17 Apical four-chamber view demonstrates a CA coursing just posterior to the pulmonary artery *(white arrows)* suggesting that the circumflex artery arises from the right-facing coronary sinus. *LA*, Left atrium; *LV*, left ventricle; *RA*, right atrium; *RV*, right ventricle.

Abnormalities of the branch pulmonary arteries or the aortic arch can occur in the setting of LV or RV outflow tract obstruction, respectively. These structures are best evaluated in high parasternal, right parasternal border, and suprasternal views. Other than the atrial communication, the PDA is an important contributor to the mixing of blood between the parallel circulations of the systemic and pulmonary vascular beds. The PDA is best evaluated in the high left parasternal view[23] or the suprasternal sagittal (long-axis) view because of the parallel relationship of the aorta and pulmonary artery (Figure 18). Finally, aortopulmonary collateral vessels can be seen in TGA. Although echocardiography is not the best modality for their detection, collateral vessels can sometimes be seen arising from the descending aorta in multiple views, including subxiphoid and suprasternal.

Patient Preparation. Generally, preoperative imaging of infants with TGA occurs in the first few hours to days of life. Most infants with this diagnosis are already hospitalized from birth and are housed in a neonatal or cardiac intensive care unit. Occasionally, the diagnosis will not be recognized and an infant may be in a well-baby nursery or even be evaluated as an outpatient. Because imaging is performed in early infancy, sedation is generally not required, as the neonate can be calmed with feeding or with other noninvasive interventions.

Scanning Protocol. ASE guidelines exist for the routine pediatric transthoracic echocardiographic examination.[23] Preoperative

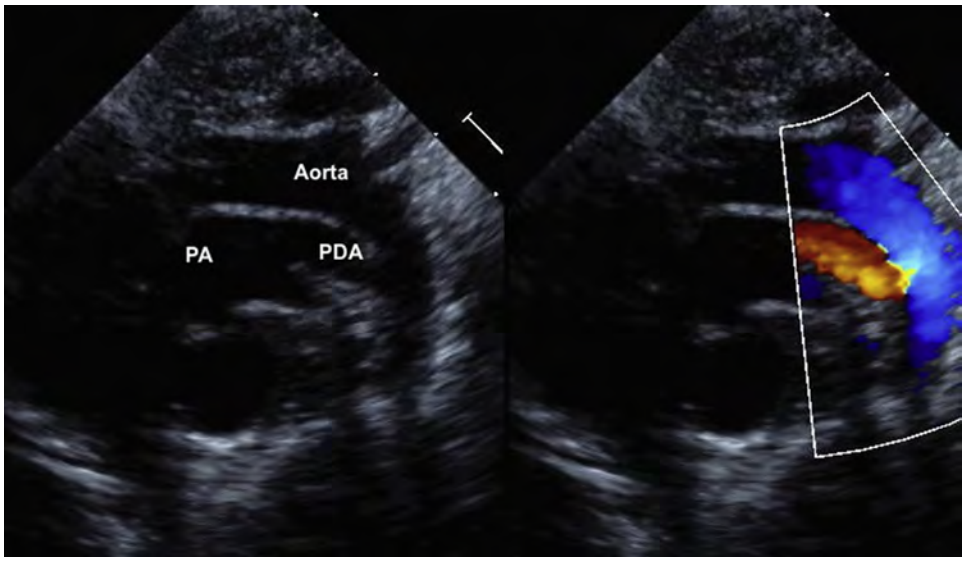

Figure 18 Suprasternal sagittal view in color-compare mode in a patient with TGA shows the parallel relationship of the aorta, the pulmonary artery (PA), and the PDA. The PDA is shunting from the aorta to the PA.

Table 4 Standard protocol for preoperative TTE in patient with TGA

View	Structure	Comments
Subxiphoid		
Frontal (long-axis)	Atrial septum, atria, pulmonary veins, relationship of pulmonary artery and aorta, identify presence and location of VSD	Assess atrial level shunt, assess for juxtaposition of the atrial appendages, identify dilated coronary sinus
Sagittal (short-axis)	Systemic and pulmonary veins, atrial septum, AV valve morphology, presence and location of VSD, outflow tracts, relationship of pulmonary artery and aorta	Assess for AV valve abnormalities, type of VSD, type and severity of outflow tract obstruction
Apical		
Four-chamber	Coronary sinus, AV valve function, ventricular size and function, CA anomalies	Assess for straddling AV valves, ventricular hypoplasia, can diagnose circumflex artery from the RCA
Five-chamber	Outflow tracts, semilunar valve function	Abnormal attachments of AV valve to the conal septum, doubly committed subarterial VSD
Parasternal		
Long-axis	Relationship of great arteries to the ventricles	Assess for conal septal malalignment and outflow tract obstruction
Short-axis	Size and location of semilunar valves, size and location of VSD (if present), position of ventricular septum, ventricular performance	High parasternal short-axis highlights the CA anatomy
Suprasternal		
Frontal (short-axis)	Relationship of pulmonary artery and aorta, size of branch pulmonary arteries, arch sidedness	Assess for left SVC or partial anomalous pulmonary venous drainage
Sagittal (long-axis)	Arch anatomy and PDA	Assess for arch obstruction and size and direction of flow of PDA

RCA, Right CA.

echocardiographic evaluation is outlined in detail in Table 4. Pertinent findings are highlighted below.

In the subxiphoid frontal (long-axis) view, the atrial septum is well delineated to determine if an atrial communication is present and adequate for mixing. When sweeping in a posterior-to-anterior direction, the relationship of the aorta and the pulmonary artery is seen (in TGA, typically the aorta is anterior and to the right of the pulmonary artery). Occasionally, a CA branch is seen coursing behind the pulmonary artery during this sweep, suggesting that the CA anatomy is not the "usual" arrangement (Video 7; available at www.onlinejase.com).

The subxiphoid sagittal (short-axis) sweep highlights the systemic and pulmonary venous connections, the atrial septum, and the AV valve morphology. The ventricular septum is well

delineated in this view: a perimembranous VSD will be seen behind the septal leaflet of the tricuspid valve, a muscular VSD will be seen within a completely muscular rim anywhere in the muscular septum, a doubly committed subarterial (conal septal) VSD will be seen just below both semilunar valves with absence or deficiency of the conal septum, and an inlet (AV canal type) VSD will be seen in the area of the AV valves. The RV and LV outflow tracts are also well evaluated in this view, particularly in terms of posterior or anterior deviation of the conal septum as well as dynamic subpulmonary obstruction (when the ventricular septum is intact). The relationship of the aorta and the pulmonary artery (anterior/posterior or side by side) can be confirmed in this sweep after initially using the frontal (long-axis) view.

The apical four-chamber view provides information regarding the relative sizes of the AV valves, the presence of AV valve stenosis and/or regurgitation, straddling or override of the AV valves, and the presence of a mid-muscular VSD or an apical muscular VSD. Anterior angulation provides information regarding the LV and RV outflow tracts and semilunar valves. This is another view where a CA may be seen coursing posterior to the pulmonary artery, suggesting that the CA anatomy is not "usual" (Figure 17).

For TGA, the parasternal long-axis view displays the fibrous continuity between the mitral and pulmonary valves in the majority of patients (without a subpulmonary conus). The parallel orientation of the proximal great arteries is confirmed in this sweep (Figures 4A and 4B, Video 5; available at www.onlinejase.com). Parasternal short-axis view displays the relative locations and sizes of the semilunar valves as well as the presence of commissural alignment (Figure 16). The sweep in this view is excellent at displaying the location and size of VSDs if present, the relative size and function of the ventricles, and the relative position of the ventricular septum. CA anatomy is best evaluated in this view, and every effort should be made to follow the CA branches as far distally from the aorta as possible and to exclude an intramural CA.

The suprasternal short-axis sweep helps determine the aortic arch sidedness as well as the branching pattern. In addition, absence of an innominate vein in this sweep should increase the suspicion for a persistent left SVC. A suprasternal long-axis sweep provides information regarding the PDA and helps exclude aortic coarctation or aortic arch interruption (Figure 18).

Reporting Elements and Measurements

- Systemic and pulmonary venous connections
- Size of foramen ovale/atrial septal defect
- Juxtaposition of the atrial appendages, if present
- Tricuspid and mitral valve anatomy, size, and function
- RV and LV size and function
- VSD type, size, number, and direction of flow, if present
- Type and severity of obstruction of RV and LV outflow tracts, if present
- Size, morphology and function of the aortic and pulmonary valves
- Type and severity of aortic arch obstruction, if present
- Patency of ductus arteriosus, size, direction of flow, and restriction of flow, if present
- CA anatomy
- Size of branch pulmonary arteries and severity of obstruction, if present
- Arch sidedness and branching and assessment for obstruction/interruption

Recommendations. TTE is the primary diagnostic imaging modality in the preoperative assessment of TGA. A complete study will usually identify all anatomic structures and the important features of the defect. For TGA, TTE can also be used to guide BAS at the bedside in the intensive care unit. Rarely, additional modalities are required to confirm the diagnosis of TGA before surgery. In particular, if there is concern about the CA anatomy, then cardiac CT or angiography can be used.

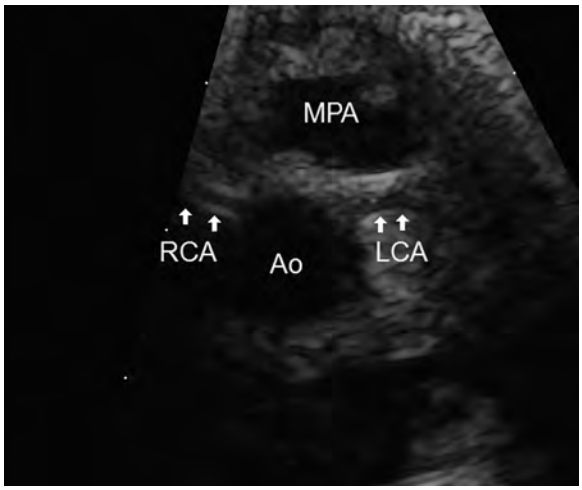

Figure 19 High parasternal view of the CAs in an infant with TGA after the ASO. The proximal course of the right CA (RCA) from the anterior right sinus and the left CA (LCA) form the anterior left sinus of the neoaortic (Ao) root are visualized. The main pulmonary artery (MPA) is seen anterior to the neoaortic root.

Postoperative Assessment of TGA with Echocardiography

Early and late residual lesions may occur after surgery for TGA, and the majority of these complications can be diagnosed by noninvasive methods.

Early Sequelae after ASO. Mortality risk for the ASO has decreased significantly since the procedure was initially described in 1975.[18] Current reviews suggest that the surgical mortality is now <5%,[37,41-46] but there are anatomic subtypes that have higher perioperative mortality. These include certain CA patterns, multiple VSDs, aortic arch anomalies, and inlet (AV canal) type VSD and straddling AV valve. Early sequelae that complicate postoperative recovery as well as clinical status during later infancy and early childhood include CA stenosis, pulmonary hypertension (PH), supravalvar and branch pulmonary artery stenosis, LV outflow tract obstruction, supravalvar aortic stenosis, and neoaortic valve regurgitation. Each of these complications will be discussed in more detail.

CA Stenosis. CA stenosis secondary to occlusion or kinking as part of the CA translocation procedure is the most common cause of early mortality after ASO.[37-39,41,42,45,47] During the ASO, difficulty separating from cardiopulmonary bypass heralds a problem with CA reimplantation. TEE after the procedure may be helpful in assessing for regional wall motion abnormalities and in some cases for evaluating CA flow. Lowering the scale and narrowing the color sector can enhance imaging of CA blood flow. Some institutions have had success with intraoperative CA imaging and color Doppler interrogation to help determine adequacy of the CA transfer.[48] A left main CA velocity-time integral > 0.14 and a left main CA peak systolic velocity > 0.6 cm/sec have been associated with need for surgical revision of the CA.

In the immediate postoperative period, CA stenosis or occlusion should be considered in any infant with identified low cardiac output syndrome with echocardiographic evidence of significant LV

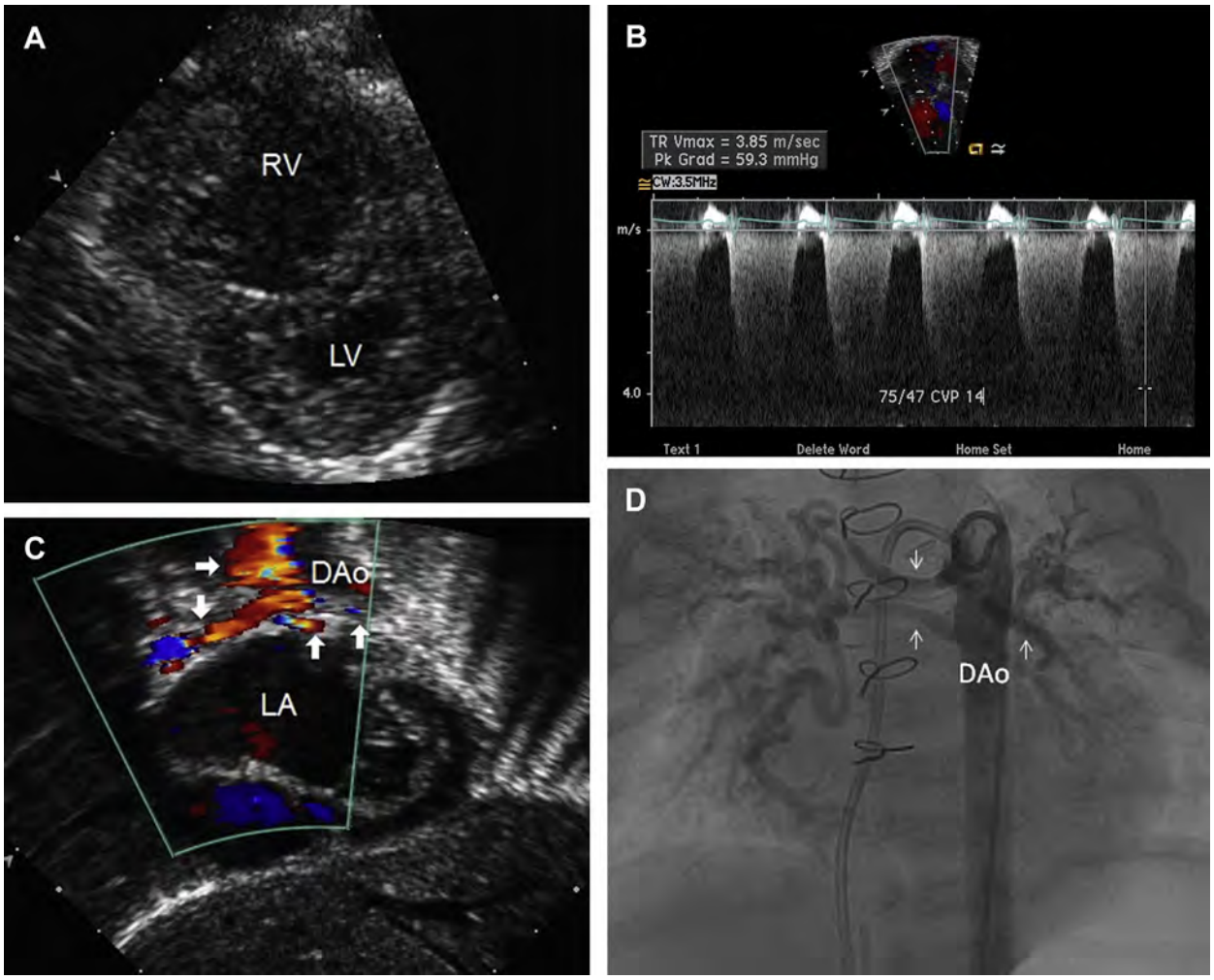

Figure 20 Imaging that identified significant pulmonary artery hypertension secondary to aortopulmonary collateral vessels in an infant with TGA after the ASO. **(A)** Initial suspicion of PH was raised by abnormal systolic septal bowing into the left ventricle (LV) from a parasternal short-axis window, consistent with increased RV pressure. **(B)** RV hypertension was confirmed by a tricuspid regurgitant (TR) jet predicting a peak RV–right atrial gradient (Pk Grad) of 59 mm Hg with a measured central venous pressure (CVP) of 14 mm Hg and systemic blood pressure of 75/47 mm Hg. No branch pulmonary artery stenosis was found to explain the RV hypertension. **(C)** In subxiphoid view, multiple color flow signals *(arrows)* superior to the left atrium (LA) and arising from the descending thoracic aorta (DAo) were identified, consistent with aortopulmonary collateral vessels. **(D)** Descending aortic (DAo) angiography confirmed the presence of multiple large aortopulmonary collateral vessels *(white arrows)*, and these were successfully coil-occluded with subsequent rapid resolution of the PH.

dysfunction, especially when regional wall motion abnormalities are seen (Video 10; available at www.onlinejase.com). On postoperative TTE, the neo-CA ostia can frequently be imaged with the implanted CA ostia and proximal course of the CAs generally seen arising from the anterior left and right sinuses of the neoaortic root (Figure 19). Color flow mapping can also be used to assess patency of the CA, providing qualitative documentation of antegrade flow. If postoperative access to the chest wall or scarring limits parasternal imaging, TEE can also be used to assess the CA origins and flow patterns in the early postoperative period. Of note, the presence of global LV dysfunction early after surgery is not uncommon, especially in the older infant with intact ventricular septum. This dysfunction typically improves over the first few days after surgery in patients who do not have CA injury.

PH. Accelerated development of PH in infants with TGA has been well described and is associated with more complicated postoperative recovery and higher mortality.[49] This risk appears to be greatest in those with large VSDs.[50] Early ASO appears to significantly diminish but not abolish this risk.[51,52] Another less well recognized cause of persistent PH in an infant after ASO is the presence of abnormal aortopulmonary collateral circulation.[53] These collateral vessels can also result in a large left-to-right shunt, complicating early recovery. Septal position in the parasternal short-axis view can give a clue to elevated RV pressure (Figure 20A). Spectral Doppler assessment of RV pressures using the tricuspid regurgitation jet or residual VSD jet can provide an accurate estimate of the presence and severity of PH (Figure 20B). Color flow mapping can identify multiple flow signals around the descending thoracic aorta suggestive of abnormal aortopulmonary collateral formation (Figures 20C and 20D).

Supravalvar and Branch Pulmonary Artery Stenosis. Supravalvar pulmonary stenosis is the most common short-term complication after an ASO, with an incidence of 5% to 30%.[42,47,54,55] This can be related to diffuse main pulmonary artery hypoplasia, discrete obstruction secondary to development of suture line narrowing at

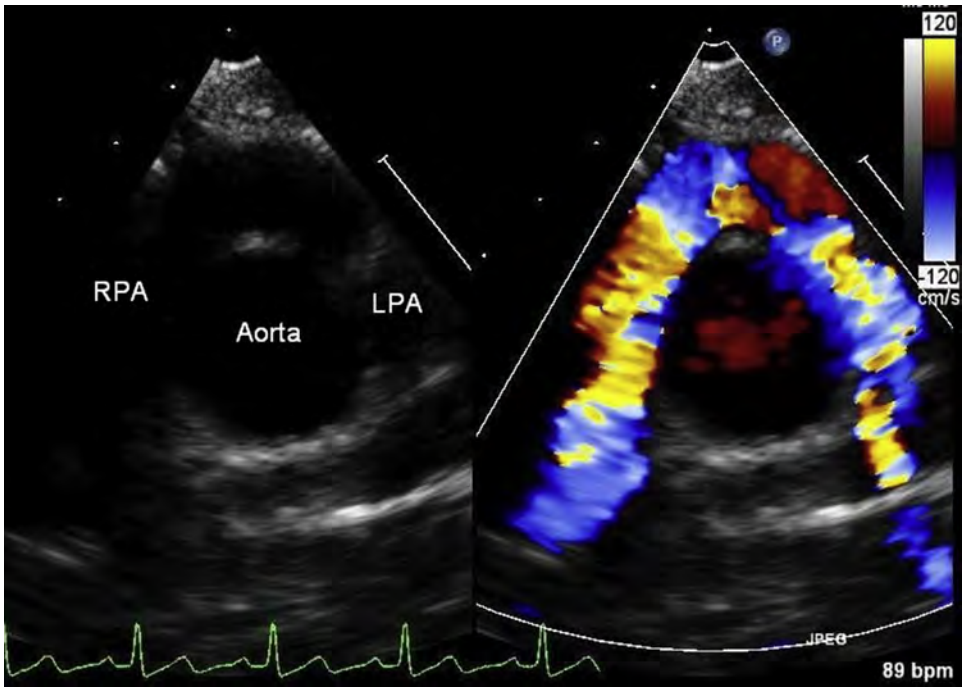

Figure 21 High parasternal view in color-compare mode demonstrates the anterior relationship of the branch pulmonary arteries to the aorta after the LeCompte maneuver. *LPA*, Left pulmonary artery; *RPA*, right pulmonary artery.

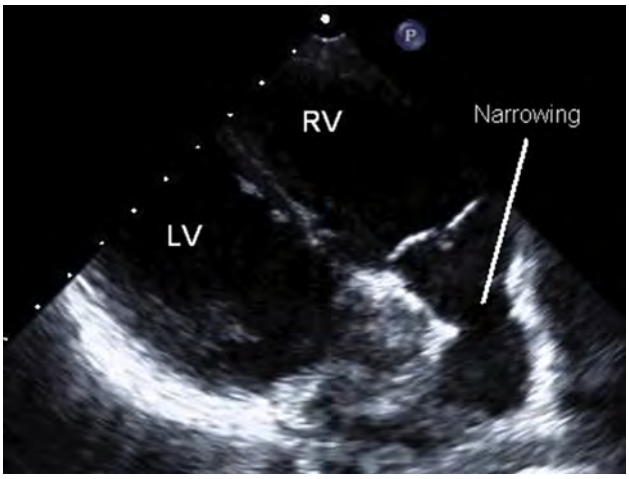

Figure 22 Parasternal long-axis view demonstrates narrowing of the supravalvar region above the neopulmonary valve after the ASO. *LV*, Left ventricle; *RV*, right ventricle.

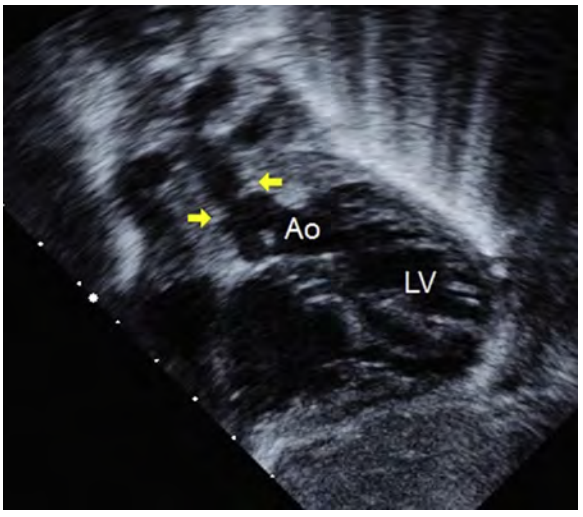

Figure 23 Subxiphoid left anterior oblique view of supravalvar aortic stenosis in an infant with TGA after the ASO. The LV and neoaortic (Ao) outflow tract is visualized. Discrete linear supravalvar obstruction is seen in the neoaorta *(yellow arrows)* related to narrowing at the neoaortic suture line.

the arterial anastomosis, and/or branch pulmonary artery stenosis. The neopulmonary artery often appears mildly narrowed compared with the neoaortic outflow tract (Video 11; available at www.onlinejase.com). Branch pulmonary artery stenosis more commonly involves the left pulmonary artery as it stretches across the ascending aorta after the LeCompte maneuver. This is particularly true when the great arteries are in a more side-by-side position (Video 11; available at www.onlinejase.com). Pulmonary outflow abnormalities frequently occur in series, with multiple levels of obstruction that involve both the supravalvar area and branch pulmonary arteries. Doppler interrogation of the severity at each level can be challenging with multiple levels of obstruction.

The position of the branch pulmonary arteries is unique after the LeCompte procedure with the vessels straddling anterior to the ascending aorta. This is best seen in a high parasternal view (Figure 21).[23] Assessment of the neopulmonary valve and supravalvar area can be imaged from apical, parasternal, and subxiphoid windows (Figure 22). The best Doppler alignment should be used for accurate estimates of pressure gradients through this area. Neopulmonary valve regurgitation is readily identified by color Doppler, but significant regurgitation is rarely a complication without anatomic abnormalities of the neopulmonary (native aortic) valve.

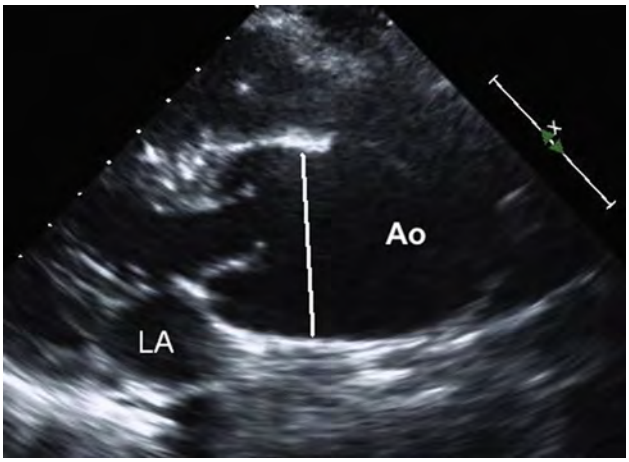

Figure 24 Parasternal long-axis view of a dilated neoaortic root in an adolescent patient after the ASO. Note the lack of the normal ST junction and the relatively normal size of the valve annulus in comparison with the root. The neoaortic root is measured inner edge to inner edge as per typical pediatric method. *Ao*, Aorta; *LA*, left atrium.

Supravalvar Aortic Stenosis and Neoaortic Valve Regurgitation. Similar to the RV outflow tract, the supravalvar aortic region may be obstructed after the ASO, most commonly because of suture line narrowing (Figure 23). If significant, this narrowing can affect neoaortic valve function. Neoaortic valve regurgitation early after ASO is common and generally trivial to mild in severity; more significant regurgitation is usually only seen in patients with a congenitally abnormal neoaortic (native pulmonary) valve or when the ASO is a second-stage repair after a previously placed pulmonary artery band with resultant valvar distortion.[56,57]

Evaluation of the supravalvar aortic region is best performed using the subxiphoid left anterior oblique view (45° clockwise of frontal view) and the apical five-chamber view. Often, the suture line is visible using these views (Figure 23); color flow mapping provides qualitative assessment of the severity of obstruction, and spectral Doppler allows accurate determination of the pressure gradient across this region. Color flow mapping in these views also determines the severity of neoaortic valve regurgitation.

Late Sequelae after ASO. Transection of the great arteries with translocation and reanastomosis, along with translocation of the CAs, has potential consequences that require long-term transthoracic echocardiographic evaluation. These include RV outflow tract obstruction and branch pulmonary artery stenosis, complications of the neoaortic root and valve, subaortic obstruction, and late complications of the CAs.

Supravalvar and Branch Pulmonary Artery Stenosis. The most common long-term complication of the ASO is residual or recurrent RV outflow tract obstruction.[58] Obstruction can occur at any level but most commonly at the suture line of the pulmonary arterial anastomosis (Figure 22). The echocardiographic views have been described in the section on early sequelae after ASO. The orientation of the pulmonary arteries after the LeCompte maneuver increases the risk for residual or recurrent branch pulmonary artery stenosis (Figure 21). Peak Doppler velocities < 2 m/s across the branch pulmonary arteries are within normal limits after the ASO. Higher velocities may require intervention. An estimate of RV pressure by the tricuspid regurgitation jet helps determine the severity of the obstruction. Transcatheter or surgical reintervention may be required.

Neoaortic Root Dilation and Neoaortic Valve Regurgitation. Progressive neoaortic root dilation is a commonly identified late finding after ASO, although significant morbidity is rare.[59,60] Risk factors for neoaortic root dilation have been identified, including previous pulmonary artery band and presence of a VSD. In the pediatric population, the diameter of the neoaortic root is measured from the parasternal long-axis view during systole, inner edge to inner edge (Figure 24). Importantly, *Z* scores of the neoaortic root are used to follow patients over time to determine whether the root is dilating out of proportion to somatic growth.

Neoaortic valve regurgitation has also been observed in this population, though severe regurgitation appears to be rare. Thus far, only 1% to 2% of patients after the ASO have had evidence of hemodynamically important neoaortic valve regurgitation.[56] Surgical intervention for neoaortic valve regurgitation is unusual (1.4%), accounting for only 12% of all reoperations after ASO.[57] The apical three- and five-chamber views and the parasternal long- and short-axis views best demonstrate neoaortic valve regurgitation (Video 12; available at www.onlinejase.com). Spectral Doppler aortic flow patterns and color flow mapping of the regurgitant vena contracta can provide semiquantitative assessment of the degree and progression of neoaortic valve regurgitation. Holodiastolic reversal of flow in the abdominal aorta also suggests severe regurgitation. Severity of LV dilatation and dysfunction are important factors in the decision to operate on the neoaortic valve for severe regurgitation.

Late CA Stenosis and Ischemia. Although discussed in detail in the section on early sequelae of ASO, patients with ASO can rarely present with late findings of CA stenosis or occlusion.[39,61] Patients may be asymptomatic, and the findings on TTE are usually subtle. Regional wall motion abnormalities or progressive ventricular dilation and dysfunction may be clues to CA stenosis or occlusion. In older patients with suspected CA stenosis, other modalities are required for accurate assessment. Stress echocardiography can be used as a screening tool to evaluate for regional wall motion abnormalities. Deformation imaging is a newer tool to assess regional ventricular performance, but its use in this population has been limited thus far. Important ventricular ectopy late after ASO is unusual and should prompt investigation for CA ischemia.

Patient Preparation. Postoperative imaging of a young child (<3 years of age) who has undergone an ASO will often require sedation to obtain adequate images. The medical record and surgical report should be reviewed before imaging to determine if a VSD was closed and if the LeCompte maneuver was performed. Because most patients who have had the ASO are still young, TEE is rarely required as a diagnostic modality unless there are unusual circumstances.

Scanning Protocol. Imaging protocol after ASO is detailed in Table 5. Subxiphoid views demonstrate whether the atrial communication has been closed and can be used to visualize both outflow tracts (Video 11; available at www.onlinejase.com). These views can also determine if there is a residual VSD (if one was present preoperatively). Color flow mapping assessment gives qualitative assessment of outflow tract obstruction and also demonstrates whether there is neopulmonary and/or neoaortic valve regurgitation. In the subxiphoid frontal (long-axis) view, an anterior sweep will often show the branch pulmonary arteries as they drape over

Table 5 Standard protocol for postoperative transthoracic echocardiographic evaluation after ASO (early or late after repair)

View	Structure	Comments
Subxiphoid		
Frontal (long-axis)	Atrial septum, ventricular septum and outflow tracts	Assessment for residual atrial septal defect and residual VSD, determine if there is residual outflow tract obstruction
Sagittal (short-axis)	RV outflow tract; in anterior sweep, ventricular septum, descending aorta	Assessment for pulmonary outflow tract obstruction, for residual VSD, for retrograde flow in the descending aorta
Apical		
Four-chamber	AV valve function, ventricular size and function, assessment for regional wall motion abnormalities	Regional wall motion abnormalities suggest CA stenosis or occlusion
Five-chamber	LV outflow tract	Assessment for supravalvar aortic stenosis and neoaortic regurgitation
Parasternal		
Long-axis	Neoaortic outflow, neopulmonary outflow, residual VSD if present	Assessment for neoaortic root dilation and valve regurgitation, neopulmonary stenosis and/or valve regurgitation
Short-axis	Ventricular function, septal position, residual VSD if present	Assessment for regional wall motion abnormality and PH
High parasternal plane	Branch pulmonary arteries	Assessment for stenosis
Suprasternal		
Sagittal (long-axis)	Aortic arch	Assessment for residual arch obstruction or residual PDA

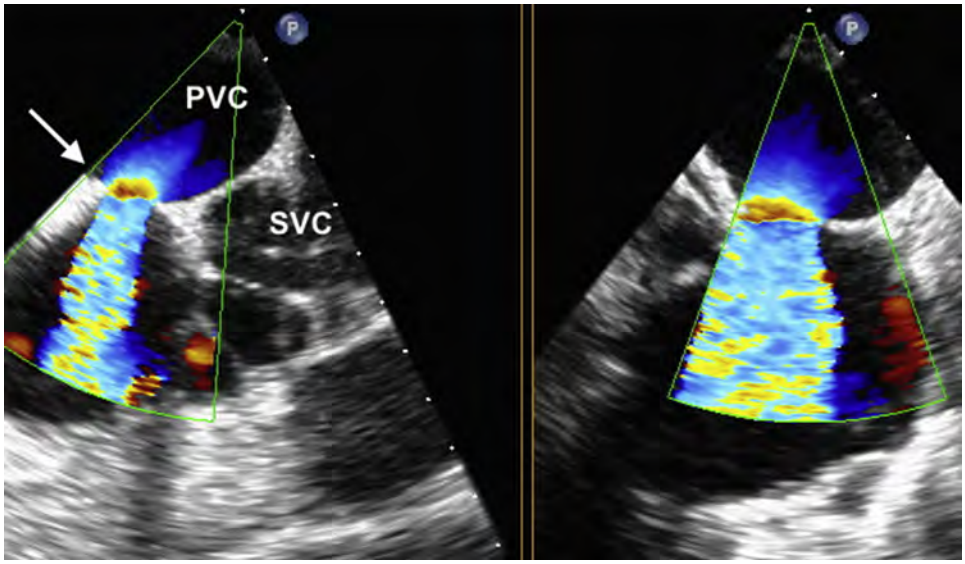

Figure 25 TEE in a biplane view (at 80° and 26°) using color Doppler in an adult patient who has had an AtrSO demonstrating acceleration of flow in the pulmonary venous channel *(white arrow)* (PVC). Note the relationship of the systemic venous channel (SVC) (with a pacing wire seen in the channel) to the pulmonary venous channel, which wraps around it.

the aorta. The subxiphoid sagittal (short-axis) view can also be used to assess for retrograde flow in the descending aorta (which suggests severe neoaortic regurgitation) or a dampened signal (which suggests residual coarctation of the aorta).

The apical four-chamber view demonstrates ventricular performance and assesses AV valve regurgitation. An apical three- or five-chamber view can confirm supravalvar aortic stenosis or LV outflow tract obstruction. It can also be used to determine the severity of neoaortic valve regurgitation (Video 12; available at www.onlinejase.com).

The parasternal long-axis view accurately measures neoaortic root size to assess for progressive dilation (Figure 24). It also can be used to help determine the severity of neoaortic valve regurgitation. With anterior angulation, the RV outflow tract can be interrogated for obstruction and neopulmonary valve regurgitation. Imaging in the parasternal short-axis plane can be used to assess for regional wall

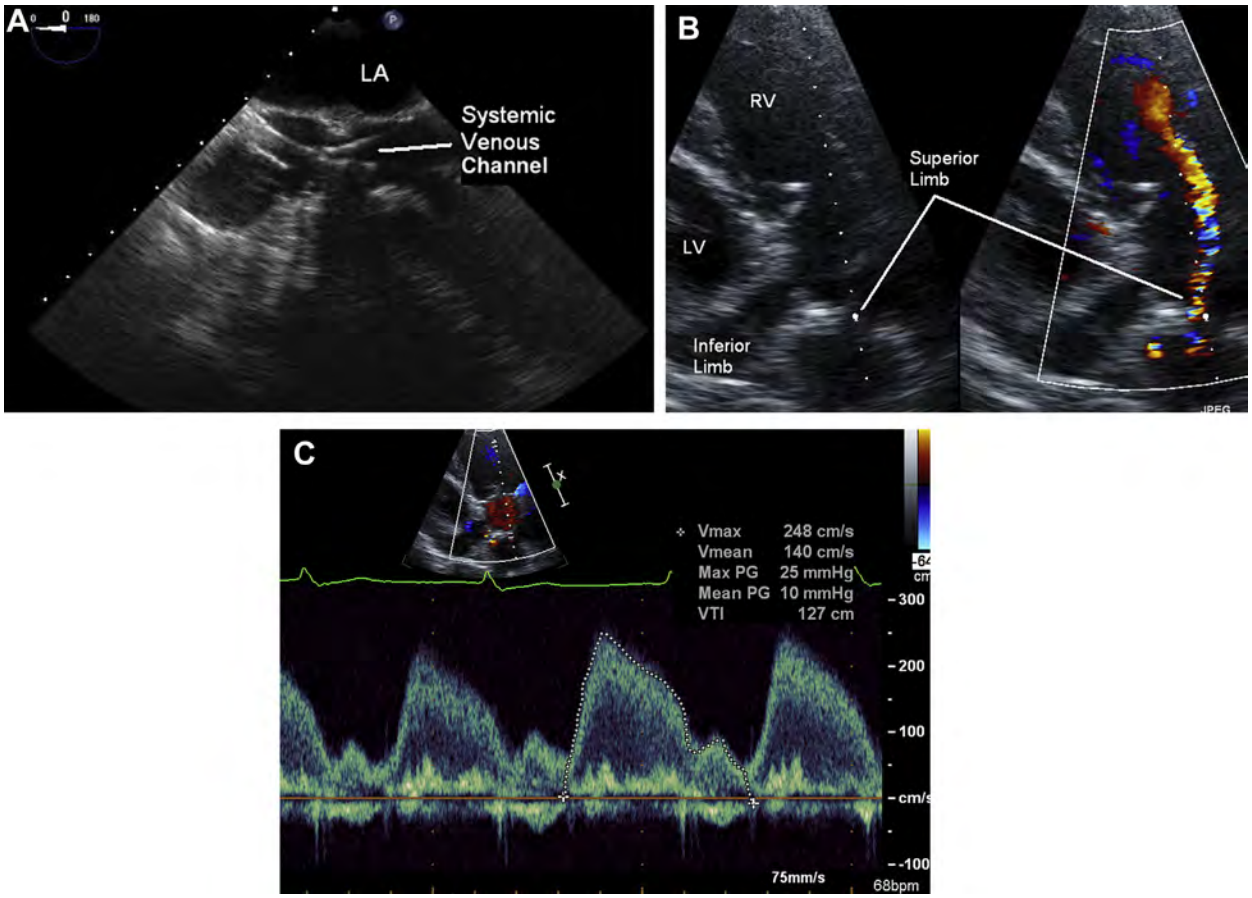

Figure 26 **(A)** TEE in four-chamber view high in esophagus (at 0°) demonstrates the superior limb of the systemic venous channel with two pacing wires seen within the channel. **(B)** Transthoracic image in off-axis parasternal view using color-compare demonstrates significant narrowing of the superior limb of the systemic venous channel. The inferior limb is seen as well. **(C)** Spectral Doppler of the superior limb of the systemic venous channel demonstrates that the flow does not return to baseline and there is a mean gradient of 10 mm Hg. *LV*, Left ventricle; *RV*, right ventricle.

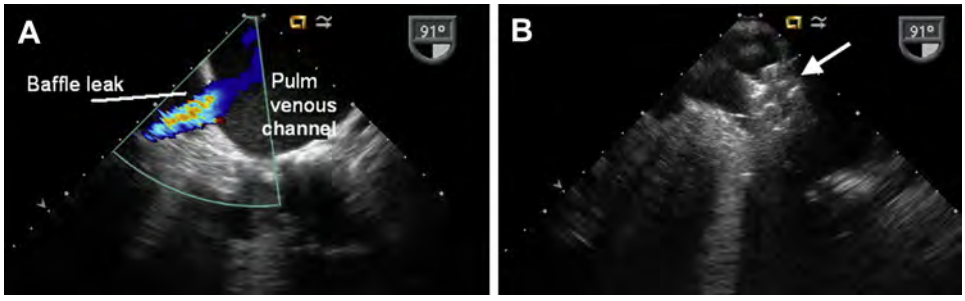

Figure 27 **(A)** TEE in bicaval view (90°) demonstrates a baffle leak in the pulmonary venous channel (a left-to-right shunt). This baffle leak is close to the inferior limb of the systemic venous channel. **(B)** After a catheter-directed intervention, an occluder device is seen closing the baffle leak *(white arrow)*.

motion abnormalities. Residual VSDs can usually be interrogated in this view as well.

The high parasternal plane is used to assess the branch pulmonary arteries. The pulmonary arteries are highlighted as they drape over the ascending aorta (Figure 21). Lack of visualization of a branch pulmonary artery should raise concern about significant stenosis of that vessel. The suprasternal imaging plane is another view that can be used to evaluate the branch pulmonary arteries. It is also used to assess residual or recurrent coarctation of the aorta.

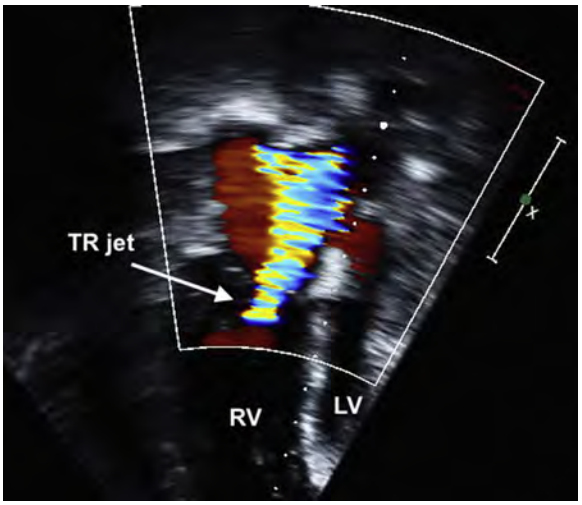

print & web 4C/FPO

Figure 28 Apical four-chamber view in a patient who has had a Senning operation demonstrates significant tricuspid regurgitation (TR) (systemic AV valve regurgitation). Note the dilated right ventricle (RV) and the pancaked left ventricle (LV).

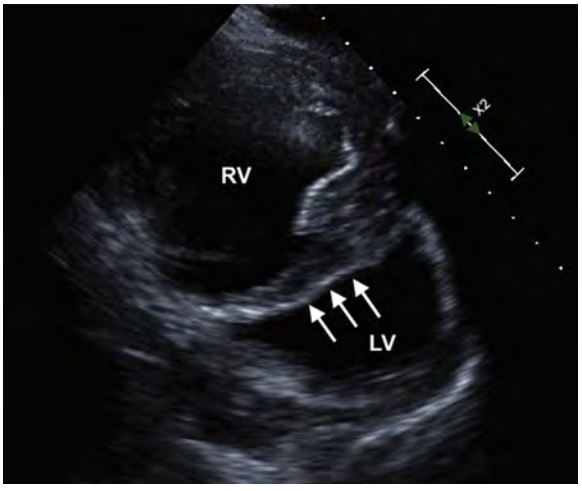

print & web 4C/FPO

Figure 29 Parasternal short-axis view shows the dilated right ventricle (RV) with bowing of the ventricular septum *(white arrows)* into the pancaked left ventricle (LV), as is typical after an AtrSO.

Reporting Elements and Measurements

- Residual atrial communication, size, and direction of flow
- Assessment of severity of tricuspid regurgitation and measurement of tricuspid regurgitation jet to estimate RV pressure, if present
- Assessment of RV size and function
- Assessment of LV size and function with specific attention to regional wall motion abnormalities, possibly including deformation imaging
- Evaluation of size and location of residual VSD, if present, and measurement of the LV-to-RV pressure gradient to estimate RV pressure
- Evaluation of RV outflow tract with specific attention to supravalvar narrowing at the suture site
- Evaluation of the LV outflow tract with specific attention to supravalvar narrowing at the suture site
- Evaluation of neopulmonary valve function
- Evaluation of neoaortic valve function with specific attention to neoaortic root dilation
- Assessment of the branch pulmonary arteries
- Assessment of size and flow of the CAs
- Assessment for residual arch obstruction if coarctation of the aorta was present
- Presence of aortopulmonary collateral vessels

Evaluation after AtrSO. The AtrSO is very rarely used for TGA in the current era, as it has been almost completely replaced by the ASO. There are rare circumstances in which it is still indicated. When TGA presents late (weeks to months of age), LV pressure has fallen to pulmonary artery levels, resulting in an LV that is unprepared to serve as the systemic pumping chamber. Although some institutions perform a pulmonary artery banding procedure to prepare the left ventricle for the ASO, others choose to perform an AtrSO in this patient population. The AtrSO is also occasionally used when the CA anatomy is deemed too high risk for an ASO. Although that the AtrSO is used infrequently today, there remains a large cohort of adult patients who have undergone this procedure who require cardiac surveillance.

The AtrSO entails complex baffling within the atria to redirect blood flow to the opposite AV valve. The Senning procedure, first described in 1958, uses autologous tissue to construct these atrial baffles, whereas the Mustard procedure (initially described several years later), uses prosthetic material to achieve the same goal.[10,11] These differences are subtle and not easily recognized by noninvasive or invasive imaging. In these procedures, systemic venous return is baffled to the mitral valve. The SVC baffle and IVC baffle act as "limbs" and meet together as the blood flow is directed into the mitral valve (Video 1; available at www.onlinejase.com). The pulmonary veins drain around the systemic venous baffle to the tricuspid valve (Videos 13 and 14; available at www.onlinejase.com). Often a patch is required to enlarge the pulmonary venous channel to prevent pulmonary venous obstruction. The AtrSO "corrects" the parallel circulations to circulations in series.

Potential complications after the AtrSO may occur with either the Senning or Mustard procedure. These include stenosis of the systemic and/or pulmonary venous pathways, atrial baffle leak (a physiologic atrial septal defect), important tricuspid (systemic AV valve) regurgitation, and systemic RV dysfunction. Moreover, many patients require pacemakers because of sinus node dysfunction and atrial arrhythmias. The AtrSO can be performed in patients with a VSD as well but outcome is worse for this population.[16] Because most patients with AtrSO are now well into adulthood, TTE may be inadequate to visualize regions of concern. TEE is used more frequently in this population than in those who have undergone ASO.

Baffle Obstruction and Residual Communications. Pulmonary venous baffle obstruction can be an important early or late complication after the AtrSO, with resultant PH and pulmonary interstitial edema. Pulmonary venous obstruction should be suspected when the mitral regurgitation jet velocity begins to increase and the left ventricle begins to hypertrophy. It can be detected by TTE, with the obstruction generally occurring at the distal egress of the pulmonary venous channel as it empties into the right atrium. Occasionally, TEE is required to delineate the region of concern (Figure 25). The mean pressure gradient across the obstruction can be used to estimate the severity of the obstruction.

Systemic venous baffle obstruction occurs in up to 30% of patients and is more common after the Mustard procedure.[62,63] The superior limb of the baffle tends to be smaller than the inferior limb because septum secundum can partially block the pathway. Baffle obstruction can also occur in association with transvenous pacing wires placed in the superior limb of the baffle (Figures 26A–26C).[64] The risk for inferior limb obstruction is significantly lower because the IVC is generally a larger vessel.

Baffle leaks are also a potential complication after AtrSO, resulting in a physiologic left-to-right shunt from the pulmonary venous

Table 6 Standard protocol for postoperative echocardiographic evaluation after the AtrSO (transthoracic and transesophageal imaging)

View	Structure	Comments
Transthoracic imaging		
Subxiphoid	IVC limb of systemic venous baffle, pulmonary venous baffle	Assessment for baffle obstruction or leak
Apical	AV valve, ventricular function, systemic and pulmonary venous baffles	Assessment for baffle obstruction or leak, evaluation for PH (mitral regurgitation jet)
Parasternal		
Long-axis	SVC limb of systemic venous baffle, ventricular function, outflow tracts	Assessment for outflow tract obstruction and semilunar valve function
Short-axis	Pulmonary venous baffle, ventricular function, outflow tracts	
Suprasternal		
Frontal (short-axis)	Proximal SVC, branch pulmonary arteries	
Sagittal (long-axis)	Aortic arch	
Transesophageal imaging		
Midesophageal four-chamber (0°)	Pulmonary venous baffle, AV valves, ventricular function	Assessment for baffle obstruction or leak, evaluation for PH (MR jet)
Midesophageal bicaval (90°)	Systemic venous baffle, outflow tract	Assessment for baffle obstruction or leak, assessment of outflow tract obstruction and semilunar valve function
Transgastric	IVC limb of systemic venous baffle, ventricular function	

MR, Mitral regurgitation.

(morphologic right) atrium to the systemic venous (morphologic left) atrium (Figure 27A). The baffle leak is generally well identified by color flow mapping interrogation of the baffles and should be suspected when there is progressive dilatation of the left atrial and LV chambers. In some cases, the transthoracic echocardiographic window is not adequate to rule out a baffle leak. Injection of agitated saline can help identify the leak when imaging or color assessment is inconclusive. In addition, TEE can be used when transthoracic echocardiographic acoustic windows are poor. Baffle leaks can be successfully closed by occluder devices (Figure 27B).

Tricuspid Regurgitation. Tricuspid regurgitation can become a problem in patients after the AtrSO because it acts physiologically like mitral regurgitation. Importantly, it can cause RV dilation and dysfunction and is a cause of significant morbidity in this population (Figure 28).

RV Dysfunction. The right ventricle is at risk for failure in a significant proportion of the AtrSO population. Although poorly understood, it is thought that the RV develops dysfunction because its anatomy is not intended to handle systemic pressure over a lifetime. After the AtrSO, the right ventricle is often quite hypertrophied and appears dilated, though this is often because the ventricular septum bows into the left ventricle (Figure 29, Videos 15A and 15B; available at www.onlinejase.com). Ventricular function will be further discussed in a later section.

Patient Preparation. Postoperative imaging of patients with AtrSO is often challenged by poor windows. As with the other surgical procedures, the medical record and surgical report should be reviewed before imaging. The imager cannot tell the difference between the Mustard and the Senning procedure, but it is important to know which has been performed, because risk for systemic venous baffle obstruction is more common after the Mustard procedure, and risk for pulmonary venous baffle obstruction is more common after the Senning procedure.

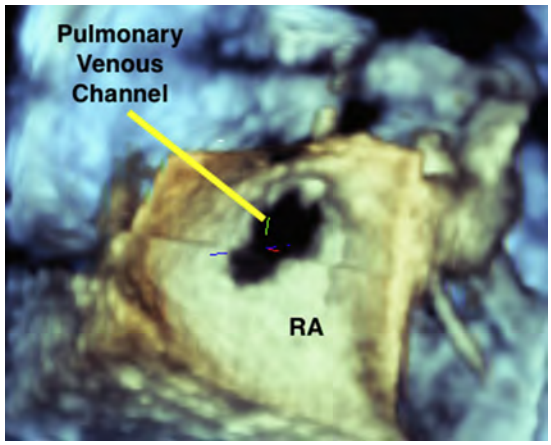

Figure 30 Three-dimensional image looking into the pulmonary venous channel from the right atrium in a patient after the AtrSO. This is the pathway that all of the pulmonary venous flow must traverse to get to the tricuspid valve. *RA*, Right atrium.

Scanning Protocol (TTE). The standard protocol for TTE is detailed in Table 6. TTE allows evaluation of the venous pathways in patients with good acoustic windows. Transthoracic echocardiographic subxiphoid imaging is difficult in the adult because of the distance of the probe from the heart. However, it should be attempted because it is one of the best views to assess the inferior limb of the systemic

Table 7 Standard protocol for postoperative transthoracic echocardiographic evaluation after the Rastelli or Nikaidoh operation

View	Structure	Comments
Subxiphoid		
Left anterior oblique (45° from frontal)	LV outflow tract, ventricular septum	Assess for subaortic obstruction, residual VSD
Sagittal (short-axis)	RV outflow tract	Assess for conduit dysfunction and conduit regurgitation
Apical		
Four-chamber	AV valve, ventricular function	Assess RV pressure estimate (tricuspid regurgitation jet)
Five-chamber	LV outflow tract	Assess for subaortic obstruction
Parasternal		
Long-axis	LV outflow tract, RV outflow tract	Assess for LV outflow tract obstruction, conduit dysfunction and conduit regurgitation
Short-axis	RV outflow tract, branch pulmonary arteries	Assess for conduit dysfunction and conduit regurgitation and branch pulmonary artery stenosis

venous baffle. When the IVC is significantly dilated, obstruction in this limb should be suspected. Often 2D imaging is inadequate, but color flow mapping and spectral Doppler will demonstrate a turbulent jet as the baffle makes its way to the mitral valve (Figures 26B and 26C). The pulmonary venous baffle may be visualized as it is directed toward the diaphragm, and it can be interrogated with color and spectral Doppler in this view as well.

The apical four-chamber view highlights the pulmonary venous baffle (Video 14; available at www.onlinejase.com). When sweeping from posterior to anterior, the imager can sometimes assess the systemic venous baffle as it wraps around the pulmonary venous baffle. Obstruction in the superior limb can be assessed using color and spectral Doppler in this view and an estimate of the mean pressure gradient can be obtained. This view is also ideal to evaluate for dilation and dysfunction of both ventricles. Contrast injection with agitated saline can be used if a baffle leak is suspected.

Imaging from parasternal windows can also be helpful in the assessment of the venous baffles. Specifically the superior limb can be seen crossing the plane of the atrial septum to the mitral valve from the parasternal long-axis sweep. Pulmonary venous baffle assessment is best performed in the parasternal short-axis sweep. The relative size and function of the ventricles can be performed in the parasternal short-axis sweep. The outflow tracts are well seen to assess for obstruction or semilunar valve regurgitation.

The suprasternal window best shows the SVC proximal to the baffle as well as the innominate vein. The pulmonary veins can have Doppler assessment in the "crab" view, and the aortic arch can be interrogated.

Scanning Protocol (TEE). The standard protocol for TEE is detailed in Table 6. TEE may be more sensitive to detect baffle leaks, and baffle obstruction and should be considered when transthoracic windows are poor. TEE is also helpful to guide catheter-based treatment of pathway obstruction such as balloon dilation, stent placement, or device closure of baffle leaks (Figures 27A and 27B, Video 13; available at www.onlinejase.com). Three-dimensional (3D) imaging of the baffles may help the define severity of obstruction as well (Figure 30).

The midesophageal four-chamber view (0°) highlights the pulmonary venous baffle with the probe tilted counterclockwise to the left side. In the same plane directed toward the right, the entrance of the right pulmonary veins into the atrium can be seen. The midesophageal bicaval view (90°) demonstrates both limbs of the systemic venous baffle as they wrap around the pulmonary venous baffle (Video 13; available at www.onlinejase.com). When rotating to the left, the baffle can be seen as it enters the mitral valve. Often a pacemaker lead (if present) can be seen in the superior limb. Assessment of the outflow tracts can be performed in this view as well; sometimes the angle of the probe needs to be adjusted to provide a view of the entire this region. Transgastric imaging highlights the IVC. As the probe is withdrawn into the esophagus, the inferior limb of the baffle can be followed as it makes its way to the mitral valve. This view can also be used to assess ventricular function and the outflow tracts.

Reporting Elements and Measurements

- Assessment of the systemic venous baffle (channel) with particular attention to the superior and inferior limbs
- Assessment of the pulmonary venous baffle (channel)
- Assessment of tricuspid valve (systemic AV valve) function
- Assessment of mitral valve (pulmonary AV valve) function with estimation of LV systolic pressure
- Assessment of RV (systemic ventricle) size and function
- Assessment of LV size and function
- Evaluation of size and location of residual VSD, if present
- Evaluation of aortic and pulmonary valve function

Evaluation after the Rastelli or Nikaidoh Procedure. Surgery for TGA with VSD and associated significant LV outflow tract obstruction usually involves some variation of the Rastelli procedure or the Nikaidoh procedure.[65] The Nikaidoh procedure differs from the Rastelli procedure in that the conal septum is divided and the pulmonary valve is resected. The aortic root is translocated posteriorly and anastomosed to the pulmonary annulus. The VSD is then closed to the new location of the aorta. Placement of a conduit from the right ventricle to the pulmonary artery is then performed for the right side. CA translocation sometimes must be performed depending on the anatomy and location of the CA ostia. The benefit of the Nikaidoh procedure is that it potentially avoids the development of subaortic obstruction.

Early sequelae after these operations are generally related to obstruction in the intraventricular baffle secondary to a restrictive VSD or narrowed baffle tunnel to the aortic root. A residual VSD is also common because of the complex baffle positioning. The conduit from the right ventricle to the pulmonary artery has limited longevity in infants and young children because of lack of growth and progressive conduit stenosis and/or insufficiency. In some cases, the LeCompte maneuver is performed in association with the Nikaidoh procedure depending on the relationship of the conduit to the aorta. Thus, branch pulmonary artery stenosis may occur in these cases. TTE is generally the modality of

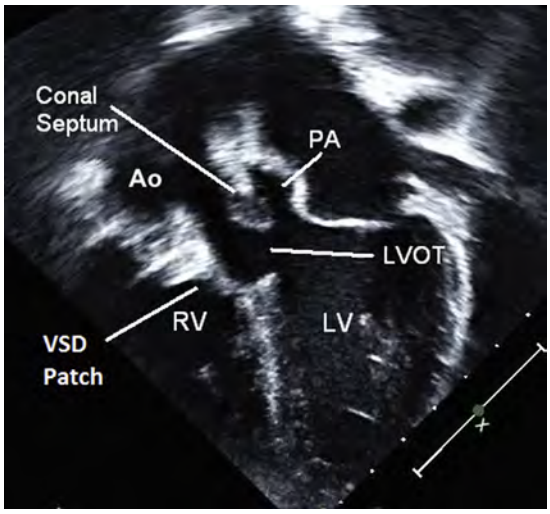

Figure 31 Apical five-chamber view of a patient after the Rastelli procedure demonstrates the pathway from the left ventricle (LV) to the aorta (Ao) after baffling with a VSD patch. Note the conal septum, which is deviated posteriorly and the hypoplastic pulmonary artery (PA) stump (the PA is tied off during the procedure). *LVOT*, LV outflow tract; *RV*, right ventricle.

choice for surveillance of patients who have undergone the Rastelli or Nikaidoh procedure. Rarely, TEE is required for this assessment.

Residual VSD. A residual VSD is a relatively common postoperative complication of the Rastelli and Nikaidoh procedures. Usually, these defects are small peripatch communications that do not impact outcome. Occasionally, an intramural defect will occur[66,67] because the VSD patch is attached to trabeculations rather than the RV free wall itself (Video 16; available at www.onlinejase.com). Intramural defects can enlarge over time and are associated with postoperative morbidity and mortality[67]; thus, recognition of these types of VSDs is important. If a residual VSD is present, interrogation of the pressure gradient across the defect can give an estimate of RV pressure and helps determine the significance of the residual defect.

Subaortic Obstruction. During both procedures, the VSD becomes the opening of the LV outflow tract. In some cases, the VSD requires enlargement to achieve unobstructed flow from the left ventricle to the aorta. Narrowing of this pathway may occur early or late after surgery. Mechanisms of LV outflow tract obstruction include muscular hypertrophy (when subaortic conus is present), narrowing of the VSD, abnormal AV chordal attachments, and/or fibrous tissue formation. Subaortic obstruction is more likely in the Rastelli procedure than the Nikaidoh procedure (which was developed to avoid this complication). Doppler interrogation helps determine the severity and location of the residual obstruction.

Conduit Dysfunction. Conduits are typically made of pulmonary or aortic homograft material, but prosthetic materials can be used as well. They have a life expectancy of 3 to 10 years depending on the size of the patient, the position of the conduit, and the development of calcification. Many conduits include a valve that degrades over time, resulting in clinically important pulmonary regurgitation or stenosis. The long-term consequences of significant conduit regurgitation are out of the scope of this guideline and are discussed in more detail in the guideline document on tetralogy of Fallot.[22]

Conduit replacement during childhood is frequently unavoidable especially when the first operation is performed in the neonatal period. Obstruction may occur anywhere along the conduit, or the conduit may become diffusely small as the patient grows. Accurate measures of conduit stenosis are difficult using Doppler echocardiography because the modified Bernoulli equation has significant limitations when a long, narrow tube is in place. Thus, RV pressure estimates using the velocity of the tricuspid regurgitation jet (if present) or ventricular septal position may help determine the clinical significance of RV hypertension. Conduit regurgitation is often severe and, in some cases, RV dilation and dysfunction may occur.

CA Stenosis. If CA reimplantation is performed (for the Nikaidoh procedure only), the same issues may occur as in patients who have had the ASO (see that section for further details).

Patient Preparation. In the case of the Rastelli or Nikaidoh procedure, review of the operative note is essential because there are subtle differences in the way these procedures are performed. For either, it is important to know what method was used to provide blood flow from the right ventricle to the pulmonary artery (conduit or another method). It also should be noted if a LeCompte maneuver is performed. Moreover, it is important to know if a CA reimplantation procedure was performed to identify possible CA stenosis. For very young children (generally <3 years of age), sedation may be required to perform a complete postoperative study.

Scanning Protocol. For the Rastelli and Nikaidoh operations, a standard echocardiography protocol is detailed in Table 7. Intraoperative TEE is usually performed to assess for residual VSDs, LV outflow tract obstruction, function of the conduit from the right ventricle to the pulmonary artery, and ventricular performance.

Subxiphoid views will demonstrate a residual VSD. The left anterior oblique view (45° clockwise of frontal view) is ideal to assess the LV outflow tract for subaortic obstruction (Videos 17 and 18; available at www.onlinejase.com). For residual intramural VSDs, the sweep must continue anteriorly to detect these defects (Video 16; available at www.onlinejase.com). A subxiphoid sagittal (short-axis) view demonstrates the RV outflow tract and the proximal portion of the conduit from the right ventricle to the pulmonary artery.

The apical four-chamber view can be used to assess the ventricles for hypertrophy and dilation. If tricuspid regurgitation is present, the RV pressure can be estimated from this view; this is generally a more accurate method than the gradient across the conduit. The apical five-chamber view and the parasternal view best display the LV outflow tract for both procedures (Figure 31). If the angle of interrogation is insufficient to assess the Doppler gradient, the mitral valve regurgitation jet can be used to estimate LV pressure with simultaneous measurement of the systolic blood pressure; the difference between these measures gives an estimate of the peak systolic pressure gradient across the subaortic region.

LV outflow tract obstruction is less likely to occur with the Nikaidoh operation than with the Rastelli operation, but the LV outflow tract still requires diligent assessment and follow-up (Video 19; available at www.onlinejase.com). In addition, regional assessment of ventricular performance should be performed (similar to the ASO) because the CAs are often translocated during this procedure.

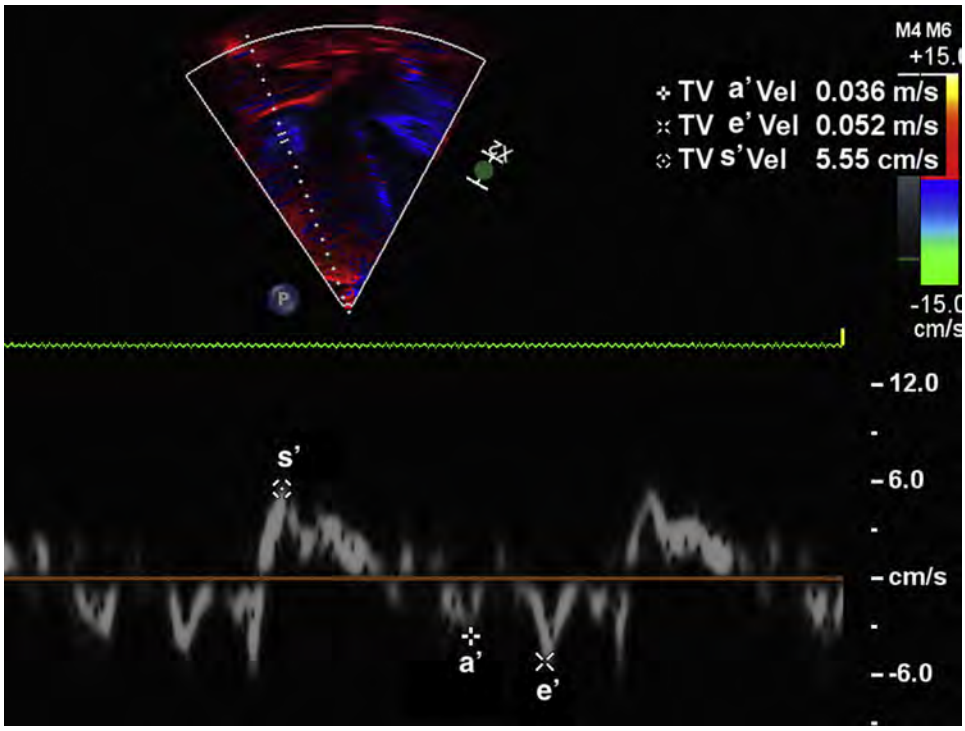

Figure 32 Doppler tissue image of the RV free wall in a patient after the AtrSO demonstrates significantly diminished s′ velocity (5.5 cm/sec) and e′-to-a′ reversal suggestive of both systolic and diastolic dysfunction.

Reporting Elements and Measurements

- Assessment for residual VSD, location, size, and pressure gradient
- Assessment for recurrent subaortic obstruction
- Evaluation of the right ventricle–to–pulmonary artery conduit or other pathway
- Estimate of RV pressure from tricuspid regurgitation jet, if present
- Assessment of AV valve function
- Global and regional assessment of LV function
- Global and regional assessment of RV function
- Assessment of branch pulmonary arteries

Recommendations. Echocardiography is the primary modality used in the postoperative patient with TGA. For young children, TTE can typically detect all the important complications of the ASO, AtrSO, and Rastelli and Nikaidoh procedures. It should also be the first modality used to evaluate adolescent and adult patients because it is noninvasive, nonradiating, ubiquitous, and portable. If there is concern about a particular issue that is not well delineated on TTE or important structures cannot be identified, TEE may be required. This is particularly true in patients who have had the AtrSO because the systemic and pulmonary venous baffles can be difficult to interrogate by TTE, and this subset of patients are older than those who have had the other surgical procedures.

Assessment of Ventricular Function after the ASO and AtrSO

Assessment of Ventricular Function after the ASO. Assessment of ventricular function is an important component of the clinical evaluation after the ASO. Early LV dysfunction is common and is mainly related to myocardial stunning immediately after surgery. Decreased myocardial function is mainly responsible for the low cardiac output syndrome that can be present during the first hours to days after the operation. Importantly, myocardial stunning generally causes global LV dysfunction. The presence of regional myocardial dysfunction immediately after surgery heralds CA ischemia. This may require further, more invasive investigation or even surgical revision of the CA transfer. Late ventricular dysfunction is mainly related to irreversible global ischemic damage that occurred in the perioperative phase or because of late CA stenosis or occlusion. The presence of LV outflow tract obstruction and aortic regurgitation can negatively affect LV function as well.

For the assessment of LV function after the ASO, echocardiography is the routine first-line imaging modality. Standard echocardiographic techniques for the assessment of LV function, as recommended by the ASE guidelines on chamber quantification and function can be used.[68,69] This includes measurement of LV dimensions, shortening fraction, ejection fraction (EF), and assessment of regional myocardial function. LV dimensions can be measured using M-mode or 2D images obtained from the parasternal long- or short-axis view at the level just below the mitral valve leaflets. In pediatric patients, these measurements should include *Z* scores. Mild LV dilation after the ASO has been described and has been associated with the presence of neoaortic regurgitation.[70,71] Systolic function is evaluated by measuring EF using the biplane Simpson method or the 5/6 area-length method. M-mode evaluation of EF or shortening fraction should be used with caution in this patient group, especially in the early postoperative period, because septal dyskinesia can be present resulting in underestimation of function. If LV dysfunction is suspected, regional myocardial assessment can be helpful to rule out CA ischemia. This is based primarily on visual assessment of regional wall motion in all LV segments using the different standard LV echocardiographic views (short-axis at different levels, apical two-, three-, and four-chamber views). In experienced hands, this has been proved to be a sensitive

Table 8 Types of information available from CMR and CTA

Anatomic survey
Postsurgical assessment
Relationship of cardiac structures to sternum before reintervention
Systemic venous and pulmonary venous baffle assessment after the AtrSO
RV outflow tract and branch pulmonary arteries after LeCompte, Rastelli, Nikaidoh
LV to aortic pathway after Rastelli, Nikaidoh
Neoaortic root and valve function after ASO
CA imaging
Reimplanted CAs after the ASO/Nikaidoh
Right CA compression after Rastelli/Nikaidoh
Anomalous CAs in patients who have had the AtrSO
Functional imaging
Assessment of systemic RV systolic function after the AtrSO
Assessment of biventricular systolic function and resting wall motion after ASO
Stress imaging
Adenosine and dobutamine CMR: perfusion and wall motion at rest and with stress for inducible ischemia
CT perfusion or FFR by CT has not been studied in CHD
Valvular regurgitation
CMR: flow imaging and stroke volume differences (estimates multiple levels of regurgitation)
CT: regurgitant fraction can be estimated from stroke volume differences when shunting or polyvalvar regurgitation is not present; reproducibility depends on accurate tracing of the ventricles and requires significant training; findings cannot be verified by flow analysis as they can by CMR
CMR viability
LGE

CHD, Congenital heart disease; *FFR*, fractional flow reserve.

method, but more quantitative techniques can be considered to evaluate regional myocardial function including speckle-tracking echocardiography.[72] If abnormalities in regional myocardial function are detected, further imaging of the CAs may be required. Echocardiographic visualization of CA flow, including CA flow velocity measurements can be useful as a screening technique,[48] but angiography remains the gold standard for diagnosis of CA stenosis or occlusion. Cardiac CT and CMR have also been used for this assessment.[73] In all patients, evaluation of diastolic function using the recommended techniques is suggested.[74] This includes assessing pulsed Doppler patterns of mitral inflow and pulmonary venous flow as well as pulsed tissue Doppler traces from the lateral mitral and medial septal annulus. Diastolic dysfunction is uncommon after the ASO but can be an early marker for the presence of myocardial ischemia.

Assessment of RV function should be an integral part of the echocardiographic assessment after ASO. RV function can be affected by problems involving the right CA, by pulmonary artery stenosis after the LeCompte maneuver, and by the rare presence of persistent PH. Recent data using tissue Doppler, strain imaging, and tricuspid annular plane systolic excursion have demonstrated that although the left ventricle recovers well within 1 year after the ASO, residual RV functional abnormalities may persist.[75] The right ventricle is structurally normal, so the standard recommended techniques may be used[76]; these include measurement of RV dimensions, tricuspid annular plane systolic excursion, fractional area change, and tissue Doppler measurements. When there is evidence of RV dysfunction, additional imaging might be required to identify the etiology. This might include CMR (to measure RV volumes and EF and to image the pulmonary artery branches and proximal CAs) or angiography (to evaluate the CAs, pulmonary artery branches, and measure pulmonary artery pressures).

Assessment of Ventricular Function after the AtrSO. After the AtrSO, the right ventricle becomes the systemic ventricle. During long-term follow-up, it has been shown that progressive RV dilation, RV dysfunction, and tricuspid regurgitation develop in a significant proportion of these patients.[63,77] Thus, assessment of RV function and tricuspid regurgitation is essential in the clinical follow-up of this patient group. In most centers, this is based on routine echocardiographic follow-up with the use of CMR in selected patients suspected of having RV dysfunction.

Often, echocardiographic assessment is based on subjective visual evaluation, but recent recommendations suggest the use of quantitative parameters including tricuspid annular plane systolic excursion, fractional area change, and tissue Doppler velocities (Figure 32). It should be noted, however, that these measurements are all influenced by the presence of tricuspid regurgitation. Progressive tricuspid regurgitation may result in increased tricuspid annular motion and also increased fractional area change, which may falsely suggest good function. Thus these measurements should always be interpreted taking the degree of tricuspid regurgitation into account. Khattab *et al.* showed weak but significant correlation between RV fractional area change and RVEF as measured by cardiac magnetic resonance imaging. A reduction of fractional area change <33% identified an RVEF < 50% with 77% sensitivity and 58% specificity.[78] Isovolumic acceleration of the RV free wall is another measure that has been used for assessment of RV function after the AtrSO.[79]

Three-dimensional echocardiography is a technique that is potentially very useful for the assessment of RV volumes and EF in this population. However, limitations in imaging windows presently limit its feasibility, and there are concerns about the underestimation of RV volumes especially in dilated ventricles.[80,81] Further data are required before this can become a routine clinical technique. RV strain and strain rate imaging may also prove useful in the future. It has been shown that longitudinal systolic strain is significantly reduced in patients after the AtrSO, and the decrease in RV strain correlates with the decrease in RVEF.[82] Moreover, reduced longitudinal RV strain values have been related to adverse clinical outcomes, including worse New York Heart Association classification and higher N-terminal pro–brain natriuretic peptide levels.[83-85] A global longitudinal strain RV value worse than −14% predicted RVEF < 45% with 90% specificity and 83% sensitivity. These data are certainly promising and suggest a growing role for speckle-tracking echocardiography in the routine follow-up of patients after the AtrSO. Because the systemic right ventricle is more hypertrophied,[86] circumferential shortening is increased,[87] which may partially compensate for the reduced longitudinal strain values. Transverse or radial strain has been demonstrated to be predictive of exercise capacity in patients after the AtrSO, suggesting that circumferential and radial shortening might be important parameters to follow serially over time.[88] For patients with decreased RV function as detected on routine echocardiography, CMR may be required for further assessment and follow-up.

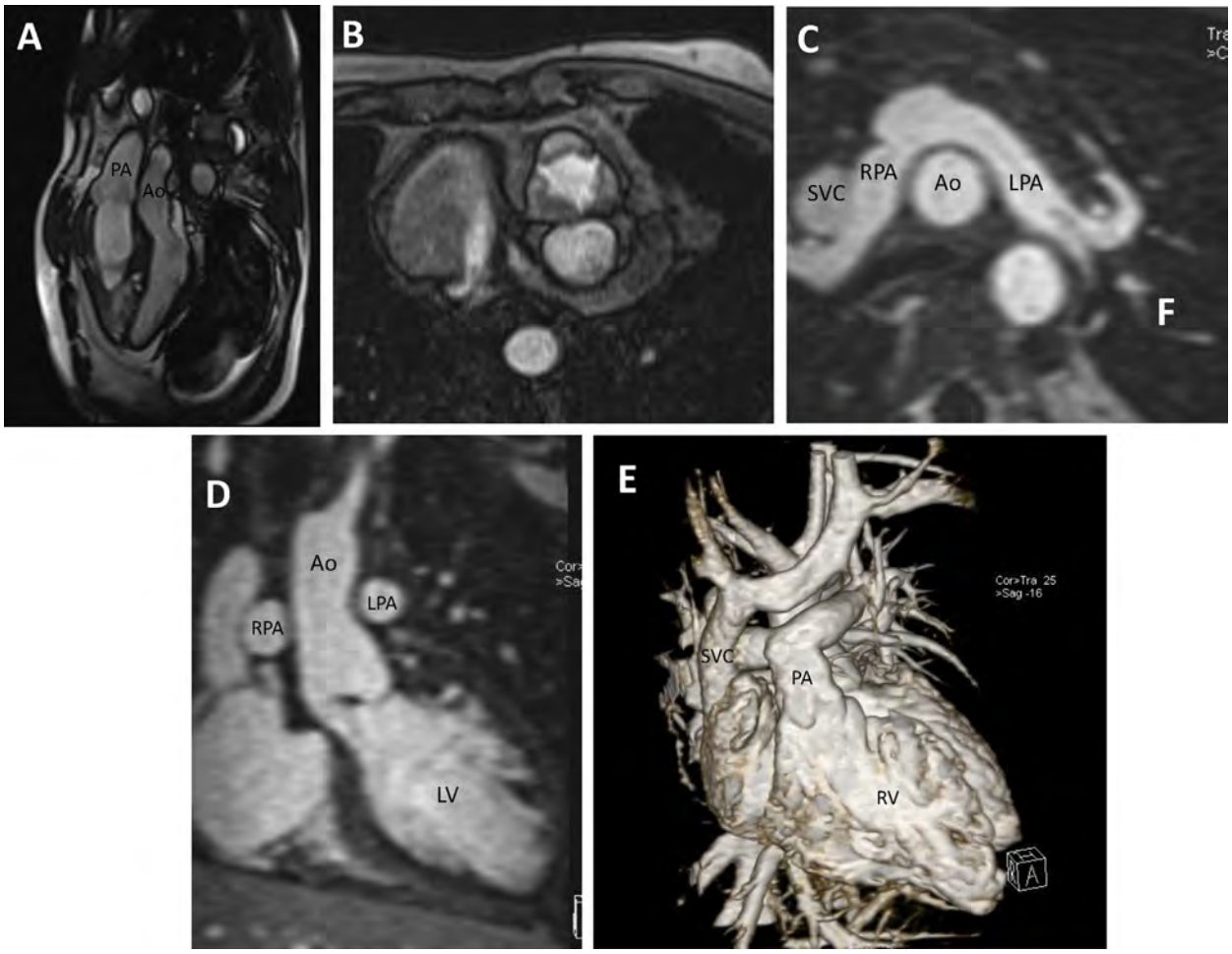

Figure 33 CMR images of TGA following an ASO with a LeCompte maneuver. **(A)** Typical parallel orientation of the great arteries in TGA (cine steady-state free precession [SSFP]). **(B)** Anteriorly positioned trileaflet neopulmonary valve (cine SSFP). The pulmonary artery bifurcation is positioned anterior to the ascending aorta as a result of the LeCompte maneuver. This relationship is illustrated with a contrast 3D angiogram: **(C)** axial view, **(D)** coronal view showing the pulmonary arteries in cross-section on each side of the ascending aorta, and **(E)** 3D volume rendered reconstruction. *Ao*, Aorta; *LPA*, left pulmonary artery; *PA*, pulmonary artery; *RPA*, right pulmonary artery; *RV*, right ventricle.

CMR IMAGING

Overview of Modality

CMR generates information about the heart and blood vessels by using strong magnetic fields and radiofrequency energy. It is able to provide a comprehensive evaluation of cardiac anatomy and function, including ventricular measurements, angiography, blood flow quantification, and assessment myocardial perfusion and fibrosis. Its primary clinical role in TGA is postoperative assessment. The information that can be obtained by CMR for patients with TGA is listed in Table 8.

Strengths and Limitations

Among the advantages of CMR in evaluating patients with TGA is that it consistently and noninvasively provides high-quality images regardless of patient size and without the use of ionizing radiation. Moreover, CMR techniques yield accurate and reproducible data regarding both LV and RV size and function, valvar regurgitation, differential pulmonary blood flow, myocardial perfusion, and myocardial fibrosis. Often the quantitative data can be validated "internally" to ensure accuracy, such as by comparing the main pulmonary artery flow to the sum of the branch pulmonary artery flows. Coronary angiography is also reliable; it is feasible with submillimeter resolution, though image quality is reduced in young infants.[89] Finally, because CMR techniques for measuring flow and ventricular function build images over multiple heartbeats, the resulting data represent an average of all these cardiac cycles and are thus more reflective of the patient's true physiologic state than a single-beat measurement.

One of the drawbacks of CMR is that a comprehensive evaluation typically requires the patient to remain relatively still for 45 to 60 min. Thus, CMR in children younger than 6 to 8 years of age usually necessitates the use of sedation or anesthesia. Newer techniques enable infants <6 months of age to undergo a full study without anesthesia or sedation using the "feed and swaddle" technique.[90-92] Up to 15% of patients who have undergone the AtrSO have cardiac pacemakers; these devices as well as implantable defibrillators have historically been considered a contraindication to CMR.[93] However, research over the past decade has indicated that CMR in some patients with these devices may be reasonable and relatively safe under specific circumstances.[94-96] Furthermore, there are now devices explicitly designed and approved for the magnetic resonance imaging

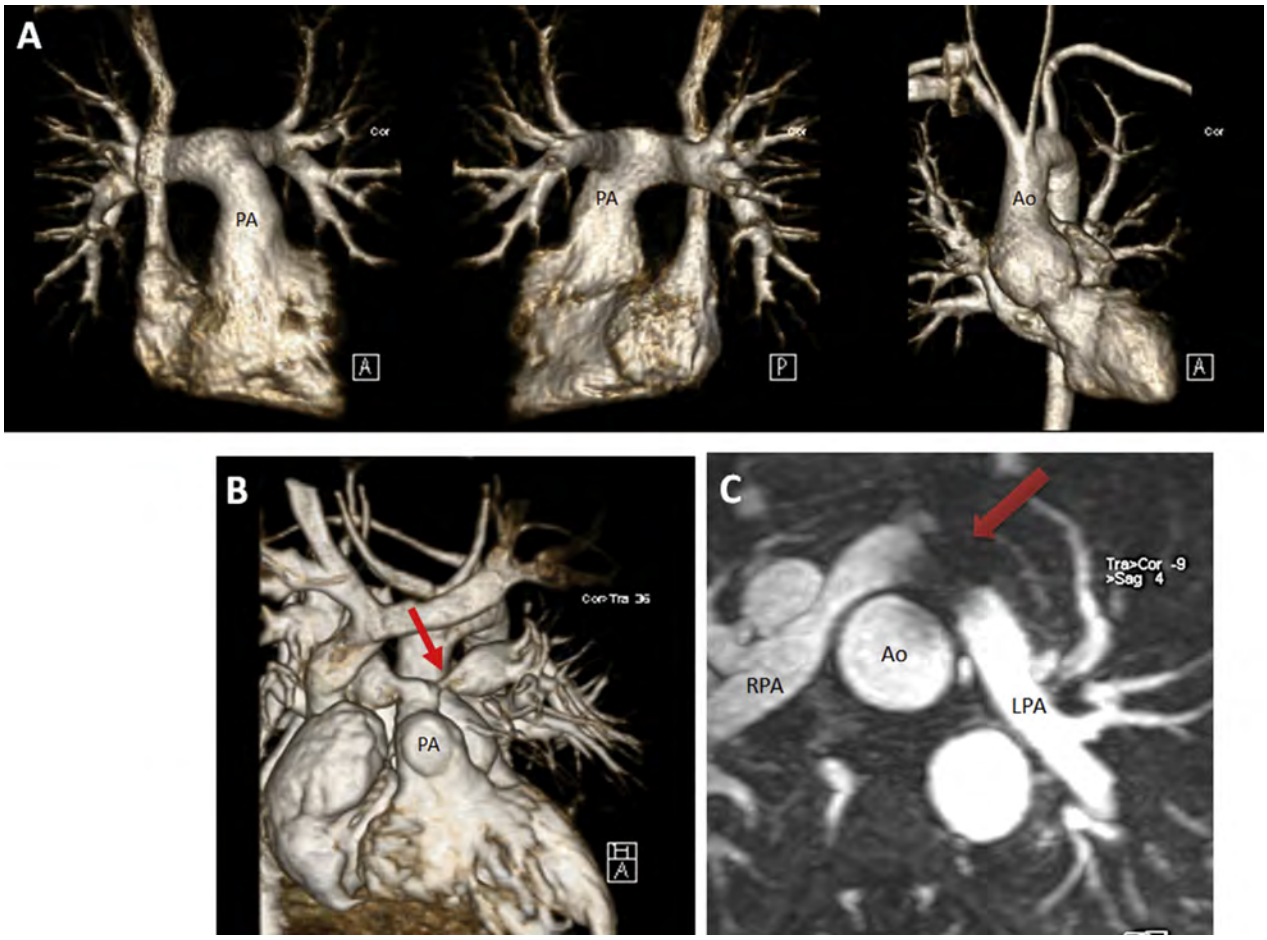

Figure 34 CMR images of TGA following an ASO with a LeCompte maneuver. Using dynamic gadolinium-contrast imaging, 3D reconstructions can be rendered of both the right-sided and left-sided structures separately. **(A)** *Left panel* is anterior and *middle panel* is posterior of the right-sided structures and shows the configuration of the branch pulmonary arteries in the LeCompte maneuver; the *right panel* demonstrates left-sided structures including a dilated neoaortic root. **(B)** Three-dimensional reconstruction demonstrates severe left pulmonary artery stenosis. **(C)** Inversion recovery gradient-echo gadolinium imaging demonstrates the result of stent placement in the left pulmonary artery *(red arrow)* in a different patient. *Ao*, Aorta; *LPA*, left pulmonary artery; *LV*, left ventricle; *PA*, pulmonary artery; *RPA*, right pulmonary artery.

environment.[97] Some patients with TGA may have implanted metallic devices such as septal occluders, vascular occlusion coils, and vascular stents. Although such devices often do not pose a safety risk, they can cause image artifact, which may limit the utility of the CMR examination. If intravenous (IV) contrast in needed for the CMR examination, there is minor risk associated with IV line placement including infiltration and bruising. Finally, unlike echocardiography, CMR is not portable or suitable for bedside evaluation.

Preoperative Assessment of TGA with CMR

CMR is seldom requested for preoperative evaluation of infants with TGA, because echocardiography usually provides all of the necessary diagnostic information for surgical decision making.[41] Details of the intracardiac anatomy such as VSD location or the mechanism of LV outflow tract obstruction are usually better delineated by echocardiography. Moreover, reliable visualization of the CA origins by CMR in newborns with TGA has not yet been demonstrated, because image quality is limited by their small size and rapid motion at high heart rates.[89] CMR can be used to assess the thoracic vessels in the rare cases when echocardiography is inconclusive.[98] Moreover, there is a potential role for CMR in patients who have undergone a pulmonary artery banding procedure to prepare a "deconditioned" left ventricle for an ASO. In particular, it can be used to accurately quantify LV mass, volume, and systolic function, though the criteria to predict adequate preparation have yet to be precisely defined.

Postoperative Assessment of TGA with CMR

Evaluation after ASO. CMR is an important alternative and complementary modality to echocardiography in the noninvasive evaluation of patients who have undergone an ASO. Increasing patient size and postoperative scar tissue often limit visualization of the heart and blood vessels by echocardiography but not by CMR (Figures 33A–33E and 34A–34C, Video 20; available at www.onlinejase.com). Accordingly, studies have shown that detection of branch pulmonary artery stenosis in ASO patients by CMR is accurate and superior to the information obtained by echocardiography.[99-103] Moreover, if the echocardiographic assessment of ventricular parameters or the severity of valve regurgitation is in question, CMR can resolve this uncertainty with reliable

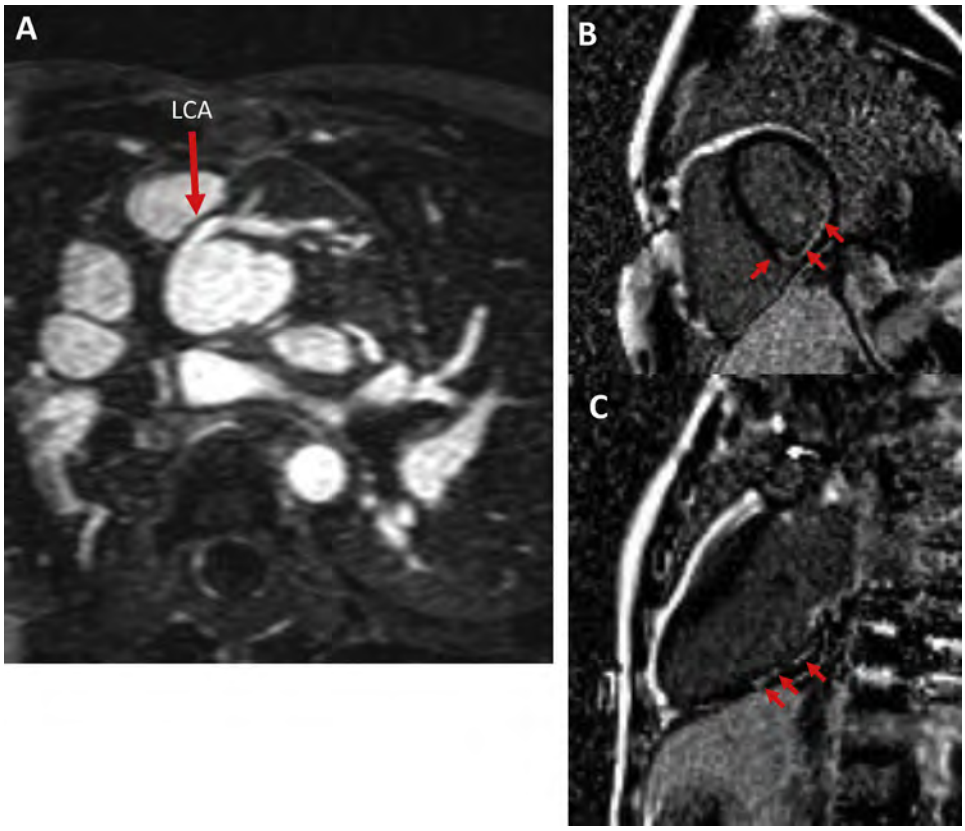

Figure 35 CMR images demonstrating CA imaging and myocardial viability assessment in TGA following an ASO. **(A)** The left main and left anterior descending CAs arise from the anterior coronary cusp with part of the left circumflex also visualized. In this patient, the proximal right CA was occluded, resulting in an inferoseptal and inferior myocardial infarction as seen on viability imaging in short axis **(B)** and long axis **(C)**. Normal viable myocardium is black and fibrotic regions are bright (*red arrows*). *LCA*, Left CA.

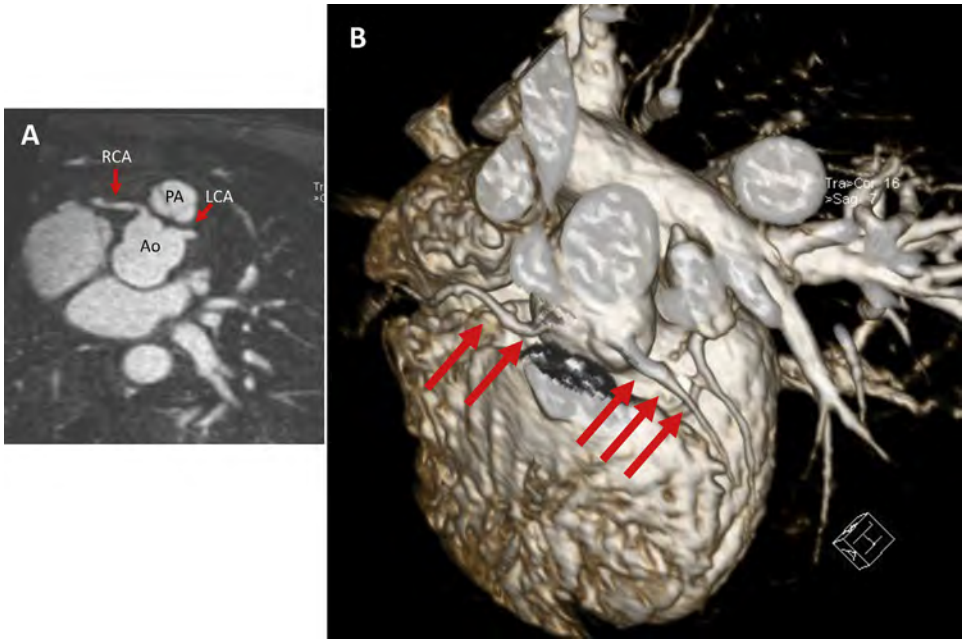

Figure 36 CMR of CA imaging in TGA following an ASO. **(A)** An axial image demonstrates the proximal right CA originating from the right and anterior facing sinus and the proximal left CA originating from the left and anterior facing sinus. **(B)** Three-dimensional reconstruction from the same patient shows the coronary origins and courses *(red arrows)*. *LCA*, Left CA; *RCA*, right CA.

Table 9 Standard CMR protocols for postoperative imaging of TGA

After the ASO
1. Three-plane localizing images
2. ECG gated cine SSFP imaging of the ventricles in two-, three-, and four-chamber planes, RV outflow tract long-axis plane, and a short-axis stack covering both ventricles from base to apex
3. ECG gated cine SSFP imaging stack in short axis to the neoaortic root and long axis to the aortic arch
4. ECG gated cine SSFP imaging stack in an axial plane to image the branch pulmonary arteries
5. Gadolinium contrast-enhanced 3D angiography
6. ECG and respiratory navigator gated 3D CA imaging
7. ECG gated velocity-encoded cine flow measurements in the main, left, and right pulmonary arteries, and ascending aorta; confirmation of ascending aorta flow can be performed by comparing it with the sum of the SVC and descending aorta flows
8. ECG gated LGE imaging in ventricular long- and short-axis planes
9. If there is a concern for inducible CA ischemia, a vasodilator or dobutamine stress protocol should also be considered
After the AtrSO
1. Three-plane localizing images
2. ECG gated cine SSFP imaging stack in an axial plane from the midliver through the top of the aortic arch
3. ECG gated cine SSFP imaging in oblique planes to image the superior and inferior limbs of the systemic venous pathway and the pulmonary venous pathway in long axis
4. ECG gated cine SSFP imaging of the ventricles in two- and four-chamber planes, parallel to the long axis of the outflow tracts, and a short-axis stack covering both ventricles from base to apex
5. Gadolinium contrast-enhanced 3D angiography
6. ECG and respiratory navigator gated 3D CA imaging to cover the heart
7. ECG gated velocity-encoded cine flow measurements in the main pulmonary artery, ascending aorta, tricuspid valve, and mitral valve; in-plane velocity measurements across the outflow tracts if obstruction is suspected
8. ECG gated LGE imaging in ventricular long- and short-axis planes
After the Rastelli or Nikaidoh operation
1. Three-plane localizing images
2. ECG gated cine SSFP imaging of the ventricles in two-, three-, and four-chamber planes, RV outflow tract long-axis plane, and a short-axis stack covering both ventricles from base to apex
3. ECG gated cine SSFP imaging stack in long axis to the conduit from the RV to pulmonary artery
4. ECG gated cine SSFP imaging stack in an axial plane to image the pulmonary arteries
5. Gadolinium contrast-enhanced 3D angiography
6. ECG and respiratory navigator gated 3D CA imaging
7. ECG gated velocity-encoded cine flow measurements in the conduit, left and right pulmonary arteries, and ascending aorta; in-plane velocity measurements across the outflow tracts if obstruction is suspected
8. ECG gated LGE imaging in ventricular long- and short-axis planes

ECG, Electrocardiographically; *LGE*, late gadolinium enhancement; *SSFP*, steady-state free precession.

quantitative data. Serial CMR evaluations can then be compared to assess for disease progression.

CMR can provide high-resolution imaging of the proximal and mid CAs and can help define their relationship to the surrounding structures such as the aorta and main pulmonary artery (Figures 35A–35C and 36A and 36B, Video 21; available at www.onlinejase.com).[73,89,104-109] Nevertheless, the published experience assessing CAs in patients with TGA after ASO is limited to a few reports.[73,108,109] The largest of these reports consisted of 84 CMR examinations and yielded diagnostic image quality of the proximal CAs in 95% and showed stenosis in 11% of the patients.[108]

There are two principal CMR techniques to diagnose inducible CA ischemia: (1) evaluation for perfusion defects using vasodilator stress agents (e.g., adenosine or dipyridamole) and (2) evaluation for regional wall motion abnormalities, most commonly using dobutamine stress. In addition, the CMR late gadolinium enhancement (LGE) technique is highly sensitive for detecting myocardial infarction and focal fibrosis (Figures 35B and 35C). In two reports describing a total of 55 asymptomatic ASO patients who underwent stress perfusion CMR, no defects at stress were detected.[109,110] The LGE technique has identified prior myocardial infarction in only a small proportion of patients after ASO.[73,109,110] Thus, on the basis of these studies, both CMR stress imaging and LGE appear to have a low positive yield in asymptomatic ASO patients. Larger studies that include symptomatic patients and have longer term follow-up are needed to better define the indications and prognostic value of these CMR techniques.

Patient Preparation. Early in the scheduling process, patients should be assessed regarding the need for anesthesia, sedation, and anxiolytic medication, and appropriate preparations made. Similarly, thorough screening for implanted devices or coils that may be contraindications to CMR or cause image artifact must be performed. For those patients who will receive contrast with their CMR examination, renal insufficiency should be excluded. A peripheral IV or central venous catheter is needed for gadolinium administration in all patients, with IV gauge

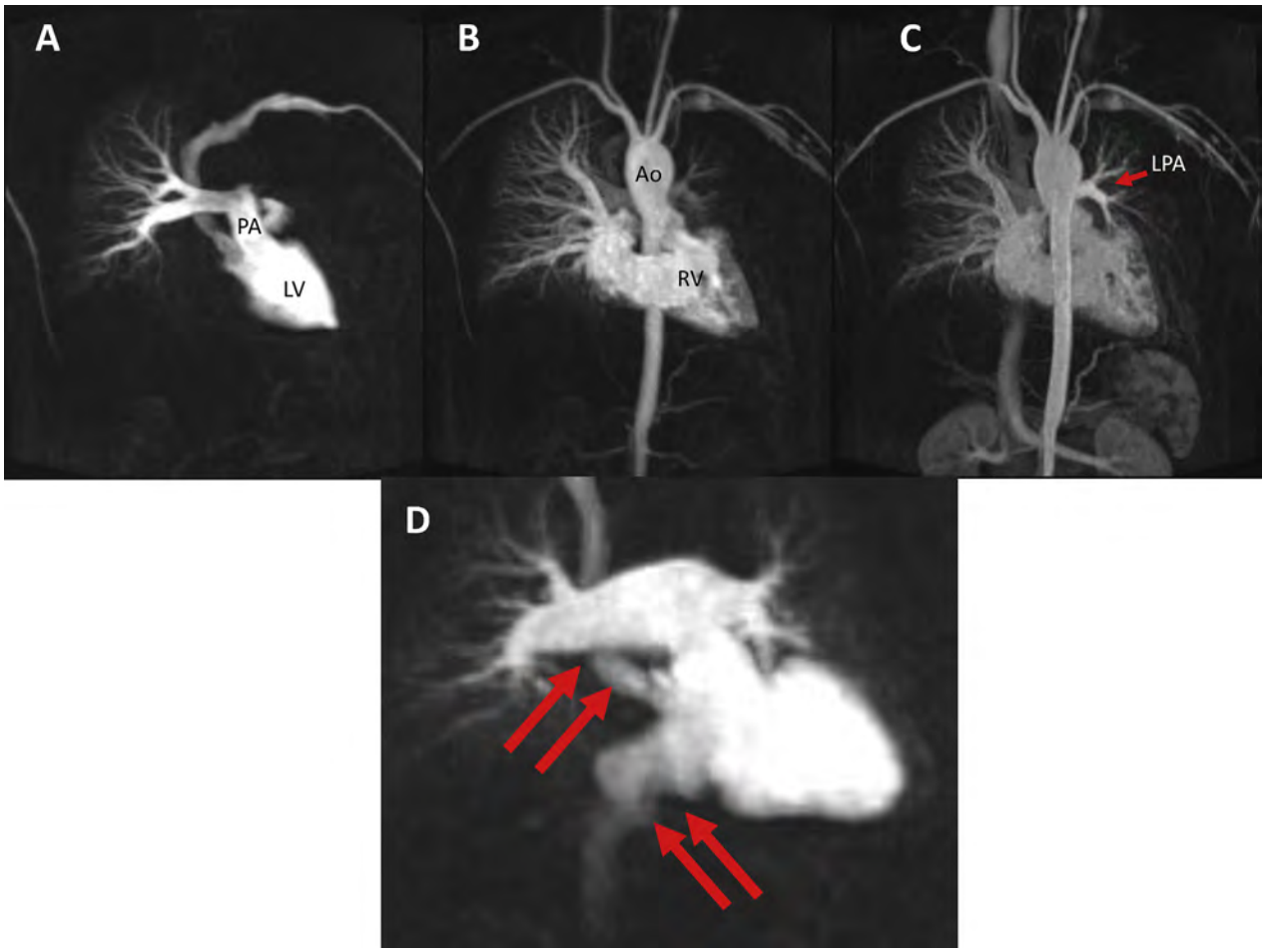

Figure 37 CMR images of an adult patient with TGA after the Senning operation. Dynamic gadolinium contrast imaging with left arm injection demonstrates **(A)** the left ventricle (LV) connected to the pulmonary artery (PA) with increased signal intensity in the right lung due to left PA (LPA) stenosis; **(B)** right ventricle and aorta (Ao) becoming signal intense, and then the left lung begins to become signal intense; **(C)** recirculation phase with signal seen in the pulmonary venous baffle; and **(D)** with reflux into the lower limb of the Senning baffle, both vena caval limbs of the reconstruction can be visualized during initial injection *(red arrows)*.

ranging from 24 to 18 depending on patient size. All institutions should have rigorous pre-CMR screening processes to ensure that patients can safely undergo the procedure.

Scanning Protocol. Table 9 shows a scanning protocol that provides a comprehensive CMR evaluation after the ASO.[111] If there is a concern for inducible CA ischemia, a vasodilator or dobutamine stress protocol should also be considered.

Reporting Elements and Measurements

CMR reports should comprehensively address the most common postoperative sequelae and include the following information:

- LV and RV volume, EF, mass, and regional function
- Presence of myocardial fibrosis and/or infarction
- Extent of LV and RV outflow tract obstruction
- Extent of pulmonary artery obstruction and calculation of the branch pulmonary artery flow distribution
- Neoaortic root size and quantitation of neoaortic valve regurgitation
- Presence of residual atrial septal defects and VSDs, and calculation of the pulmonary-to-systemic flow ratio (Qp/Qs)
- Quantitation of significant AV or neopulmonary valve regurgitation
- Description of the CA origins, course, and degree of obstruction
- Presence and quantitation of aortopulmonary collateral vessels

Evaluation after AtrSO. CMR has a central role in the noninvasive imaging surveillance of patients who have undergone the AtrSO. Assessment of the systemic right ventricle, a key concern in this patient group, can be difficult by echocardiography because of its substernal position and complex shape. CMR can routinely provide complete tomographic imaging of the right ventricle, which allows accurate and reproducible measurements of volume, mass, and EF (Video 22; available at www.onlinejase.com).[112-115] To achieve optimal results, centers should maintain a rigorous and consistent approach to image planning and analysis. Furthermore, to maximize interstudy reproducibility in patients followed longitudinally, the ventricular borders demarcated in the analysis software should be saved so that they can be compared side by side with those from previous studies.

CMR is also indicated to evaluate the systemic and pulmonary venous baffle pathways for obstruction and/or baffle leaks (Figures 37A–37D and 38A–38D). A variety of CMR techniques can be used to demonstrate the baffle anatomy and obstruction, including cine gradient echo, spin echo, velocity-encoded gradient echo, 3D steady-state free precession, and contrast-enhanced 3D magnetic resonance angiography.[64,116-122] The absence of a signal void in

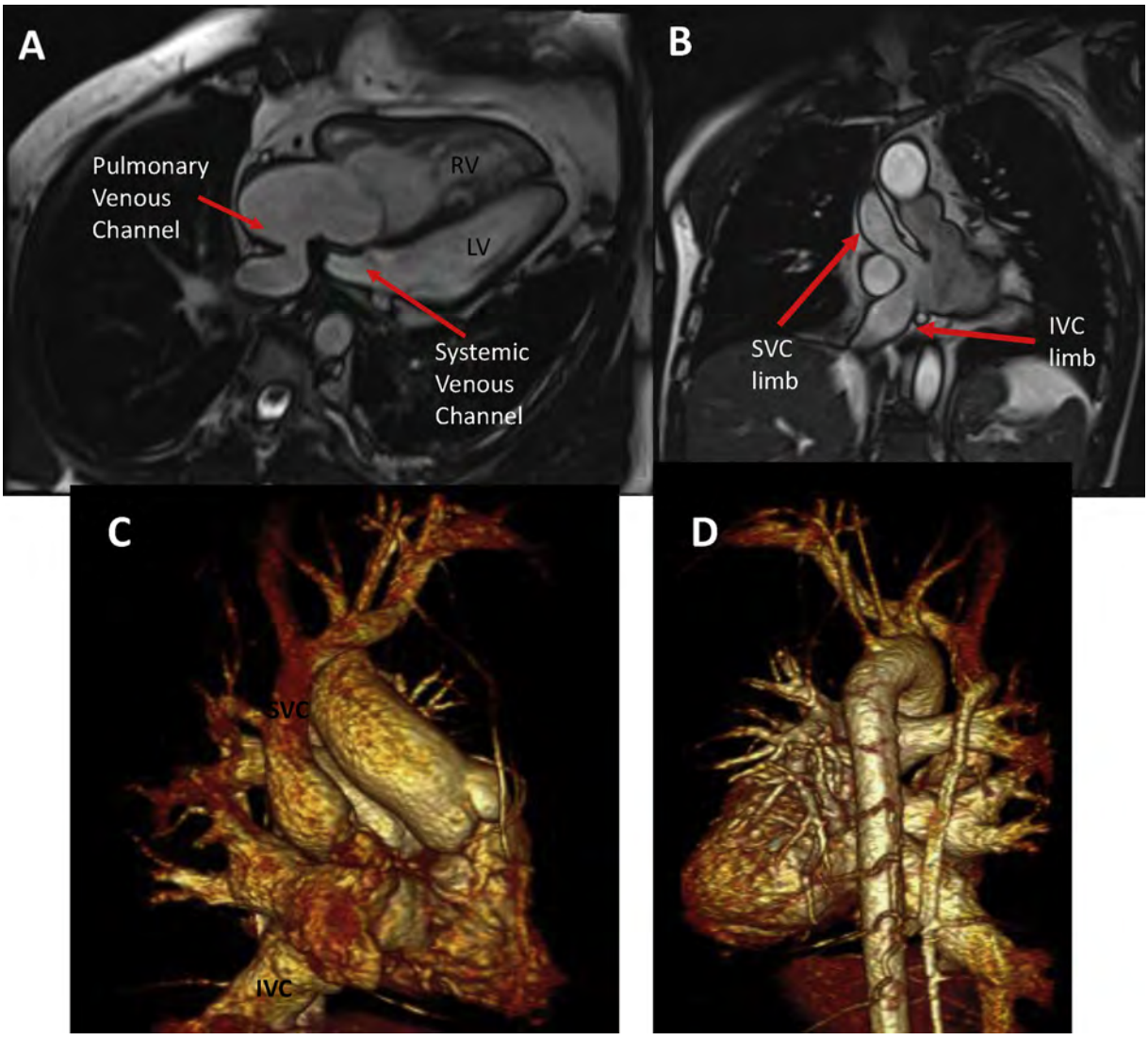

print & web 4C/FPO

Figure 38 CMR images of an adult patient with TGA after the Senning operation. **(A)** Cine four-chamber view shows the distal systemic venous pathway. **(B)** A cine coronal view demonstrates both limbs of the systemic venous pathway. **(C,D)** Three-dimensional reconstructions demonstrating the anterior and posterior portions of the heart, including the Senning baffle.

the cine images, suggest the absence of turbulent flow and therefore implies that there are not significant baffle stenosis or baffle leaks. First-pass perfusion imaging may also help in identifying baffle leaks in these patients. Reversal of flow at the level of the azygous vein by phase contrast imaging may be present with severe obstruction of the superior limb of the systemic venous baffle. The physiologic impact of baffle leaks can be gauged by measuring blood flow in the main pulmonary artery and ascending aorta to calculate the Qp/Qs. Note, however, that a Qp/Qs close to 1 can be seen even in large baffle leaks when there is bidirectional flow; thus, anatomic imaging information and the systemic oxygen saturation must also be considered.

Studies in patients who have undergone the AtrSO have found RV LGE indicative of focal myocardial fibrosis,[123-127] though the reported prevalence of this finding varies. In cross-sectional studies, the presence and extent of LGE have been associated with older age, RV dysfunction, reduced peak oxygen uptake, arrhythmia, and adverse clinical events. The best evidence establishing the prognostic value of LGE comes from a longitudinal study of 55 AtrSO patients showing that RV LGE was independently associated with a composite end point composed primarily of atrial tachyarrhythmia.[126] Finally, the response of the systemic RV to dobutamine stress or to exercise can be tested by CMR,[128-133] but the clinical utility of this information has yet to be firmly established.

Patient Preparation. Patients who have undergone an AtrSO tend to be older than those who have had ASO. Considerations regarding preparation for an AtrSO patient are similar to those mentioned above for an ASO patient. If a pacemaker is present, safety and efficacy of performing CMR in this setting must be considered.

Scanning Protocol. Table 9 shows a scanning protocol that provides a comprehensive CMR evaluation after the AtrSO.[111]

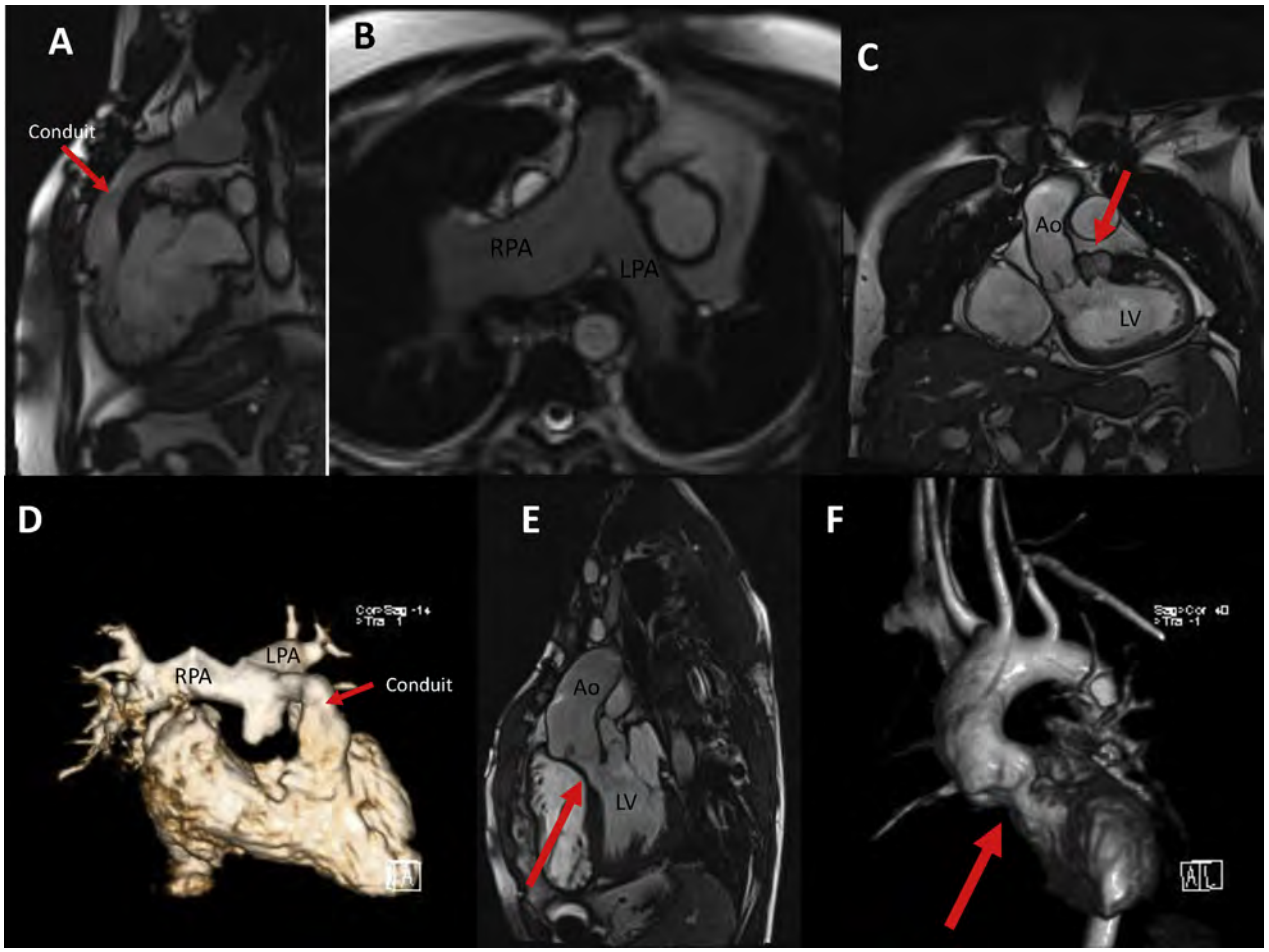

Figure 39 CMR images of a patient after the Rastelli operation. **(A)** Sagittal view of the conduit from right ventricle to pulmonary artery demonstrating moderate diffuse hypoplasia. **(B)** In a bifurcation view, the distal hypoplastic conduit is seen with moderate bilateral branch pulmonary dilation. **(C)** Left ventricular outflow tract view showing the left ventricle (LV)–to–aortic pathway and the residual pulmonary artery stump *(red arrow)*. **(D)** Three-dimensional reconstruction of patient seen in **(C)**. The narrowed LV-to-aortic pathway is demonstrated by cine *(red arrow)* **(E)** and 3D reconstruction **(F)** *(red arrow)*. *Ao*, Aorta; *LPA*, left pulmonary artery; *LV*, left ventricle; *RPA*, right pulmonary artery.

Reporting Elements and Measurements

CMR reports should comprehensively address the most common postoperative sequelae and include the following information:

- LV and RV volume, EF, mass, and regional function
- Extent of systemic and pulmonary venous pathway obstruction, and presence of collateral veins in response to pathway obstruction
- Presence of baffle leaks and Qp/Qs
- Severity of tricuspid valve regurgitation
- Degree of LV and RV outflow tract obstruction
- Presence of residual VSDs and Qp/Qs
- Presence of myocardial fibrosis and infarction
- Extent and quantitation of aortopulmonary collateral vessels

Evaluation after the Rastelli and Nikaidoh Operations. In patients who have undergone the Rastelli or Nikaidoh procedure, CMR can provide high-quality images of the pathway from the left ventricle to the aortic valve, the conduit from the right ventricle to the pulmonary artery, and the branch pulmonary arteries to assess for obstruction (Figures 39A–39F). Velocity-encoded CMR has been used to estimate the pressure gradient across discrete stenoses by measuring the maximum flow velocity and applying the modified Bernoulli equation similar to echocardiography. These data, however, must be interpreted cautiously, as there are a number of factors that may lead to erroneous velocity measurements, including difficulty aligning with complex flow jets, signal loss, and misregistration artifacts. CMR flow measurements can also quantify the degree of conduit valve and aortic valve regurgitation by calculating a regurgitant fraction. The evaluation of the conduit from the right ventricle to the pulmonary artery,[134] along with CA imaging and quantitation of RV size and function,[135] provides important data to determine whether patients are suitable candidates for surgical conduit replacement or catheter-based interventions such as balloon dilation, stent placement, and percutaneous valve implantation.[136] Finally, CMR techniques can localize residual VSDs and assess their impact through measurement of the Qp/Qs and degree of LV dilation (Figure 40).

Patient Preparation. Patients who have undergone the Rastelli or Nikaidoh operation are less likely to have pacemakers than those who have undergone the AtrSO. Considerations regarding patient preparation are similar to those mentioned above for an ASO patient.

Scanning Protocol. Table 9 shows a scanning protocol that provides a comprehensive CMR evaluation after the Rastelli or Nikaidoh procedure.

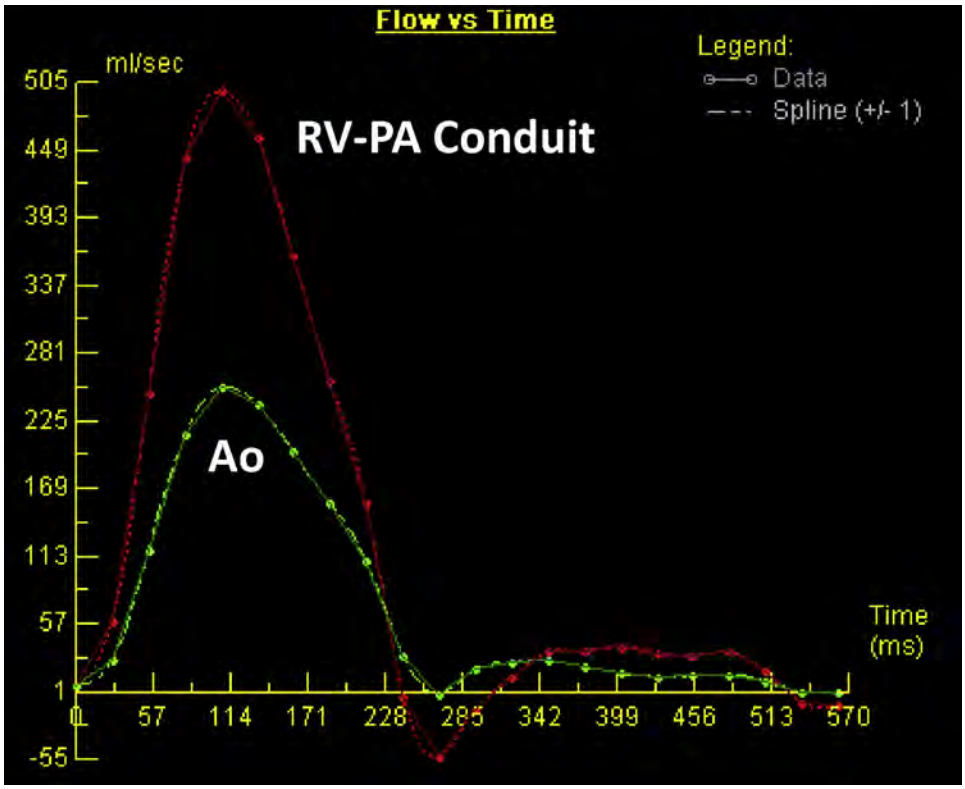

Figure 40 In a patient with TGA after the Rastelli operation who is known to have a residual VSD, the shunt can be measured by CMR. Ascending aorta (Ao) and conduit from right ventricle to pulmonary artery (RV-PA) flow (y axis; cm^3/sec) versus time (x axis; msec). Qp/Qs was calculated at 1.6.

Table 10 When to consider cardiac CT for TGA if imaging is required subsequent to echocardiography*

Patient with pacemaker or defibrillator (CMR generally contraindicated or can cause image artifact)
Patient with pacemaker being considered for biventricular pacing device to determine central venous and coronary venous anatomy before device and lead placement
Artifact (from foreign body) on CMR with nondiagnostic image quality for area of interest
Unable to be imaged in CMR scanner
Critically ill patient, particularly neonate or other patient considered too high risk for anesthesia
Critically ill patient of any age that may not tolerate breath holding or length of CMR scan or for evaluation of ventricular assist device or ECMO cannula position
When CTis indicated to look at noncardiac pathology (i.e., lung parenchyma, airway, skeletal abnormality) and cardiac anatomy can be included without additional risk
Patient with a prosthetic valve for evaluation of valve function and integrity (calcification, stenosis, coaptation defect, leaflet immobility, paravalvular leak, valve vegetation)
Patient with ACHD needing CA evaluation before other cardiac surgical intervention

ACHD, Adult congenital heart disease; *ECMO*, extracorporeal membrane oxygenation.
*Recommendations based on institutions with appropriate technology and trained staff.

Reporting Elements and Measurements

CMR reports should comprehensively address the most common postoperative sequelae and include the following information:

- Extent of obstruction in the pathway from left ventricle to aortic valve, conduit from right ventricle to pulmonary artery, and branch pulmonary arteries
- LV and RV volume, EF, and ventricular mass
- Severity of conduit valve and aortic valve regurgitation
- Presence of residual VSD and Qp/Qs
- Description of the CA origins, course, and degree of obstruction if CA transfer was performed
- Presence of myocardial fibrosis and infarction
- Extent and quantitation of aortopulmonary collateral vessels

Recommendations. CMR should be integrated in the routine evaluation of all postoperative patients with TGA with the frequency dependent on nature of the operation, patient status, and other available clinical data. After ASO, CMR assesses the RV outflow tract and branch pulmonary arteries, quantifies ventricular or valve function, images the proximal CAs, quantifies the Qp/Qs ratio, and assesses for inducible ischemia. After the AtrSO, CMR is recommended to evaluate RV function, tricuspid regurgitation, venous baffle obstruction and leaks, outflow tract obstruction, and myocardial fibrosis. Following the Rastelli and Nikaidoh operations, CMR may be used to assess the pathway from the LV to the aortic valve, the RV outflow tract and branch pulmonary arteries, ventricular and valve function, the proximal CAs, and the Qp/Qs ratio. In some cases, CMR should be considered the primary method for routine noninvasive evaluation with annual or biennial studies.

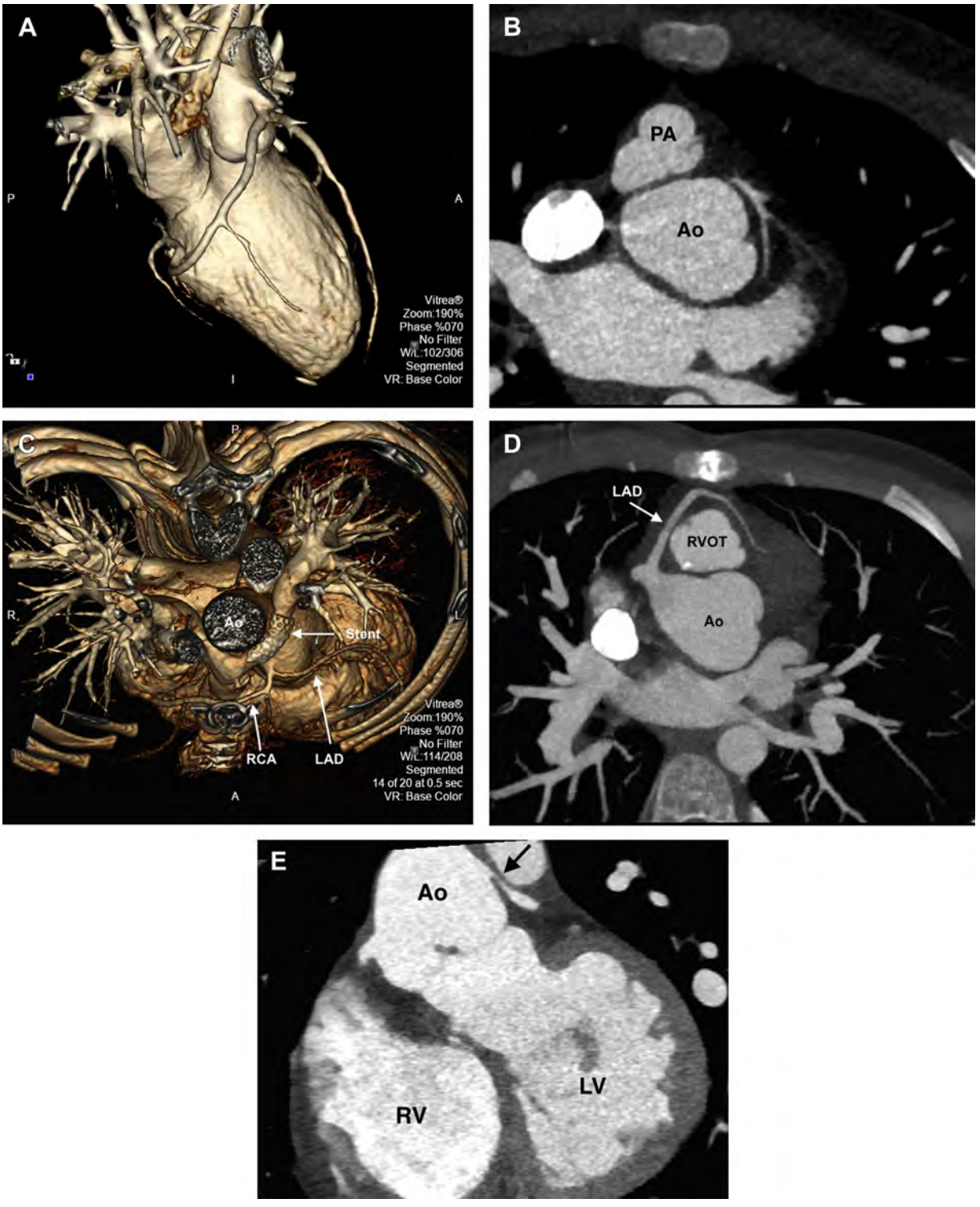

print & web 4C/FPO

Figure 41 Computed tomographic images of the CAs after the ASO. **(A)** A 3D reconstruction demonstrates a single CA arising anteriorly after reimplantation. The pulmonary artery is cut away from the image. **(B)** A 2D image shows severe left main CA stenosis after the ASO. Note the neopulmonary root (PA) anterior to the neoaortic root (Ao). **(C)** A 3D reconstruction after the ASO. Note the stent in the left pulmonary artery, and the substernal right CA (RCA) coursing anterior to the right ventricular outflow tract with a common origin with the left anterior descending CA (LAD). **(D)** Two-dimensional image demonstrates a substernal left anterior descending CA arising from the right coronary cusp of the neoaortic root, coursing directly anterior to the reconstructed right ventricular outflow tract (RVOT). **(E)** Two-dimensional image shows a dilated neoaortic root (Ao) with left main CA narrowing *(black arrow)* directly rightward of the right ventricular outflow tract. *LV*, Left ventricle; *RV*, right ventricle.

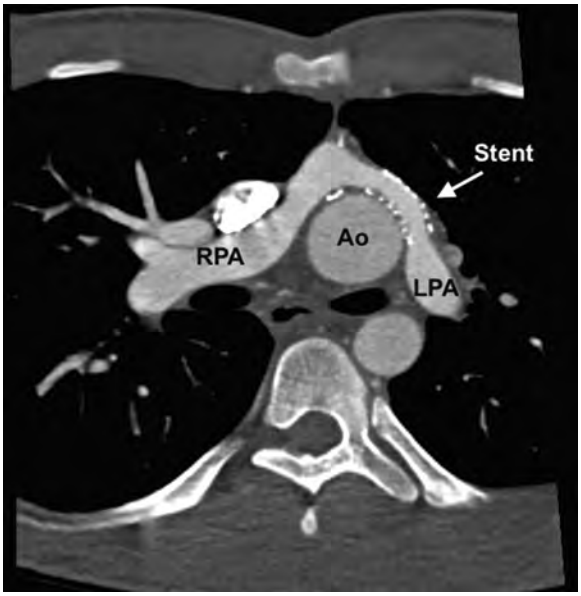

Figure 42 Axial 2D computed tomographic images of a stent in the proximal left pulmonary artery (LPA) after the LeCompte maneuver performed as part of the ASO. *Ao*, Aorta; *RPA*, right pulmonary artery.

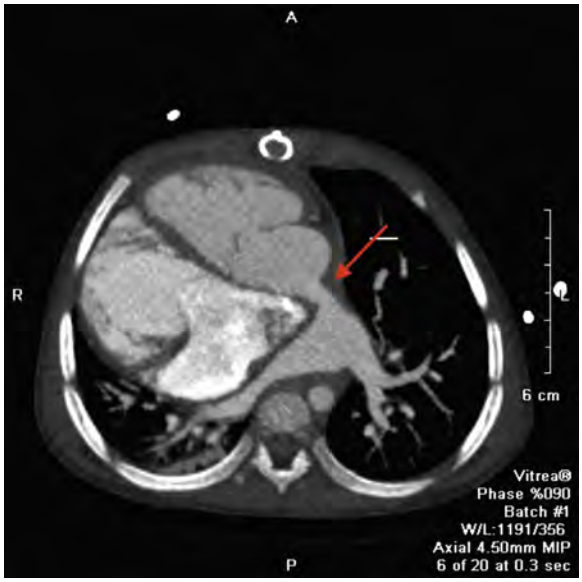

Figure 44 This 2D image shows pulmonary venous baffle obstruction *(red arrow)* in a patient after an atrial switch procedure performed as part of a "double-switch" procedure for left TGA.

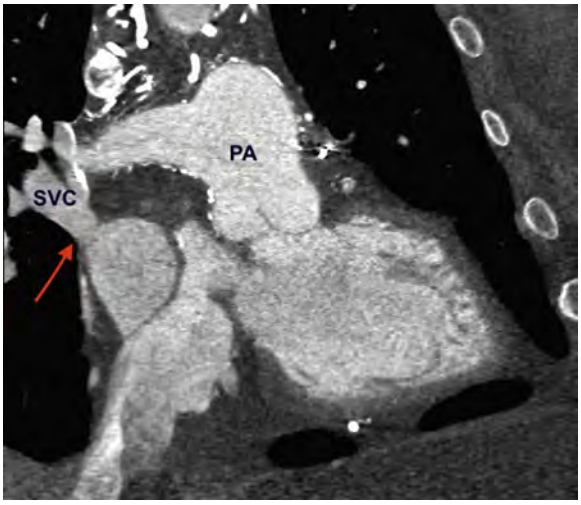

Figure 43 This 2D image from CT performed in a patient after an AtrSO demonstrates complete occlusion of the SVC limb of the systemic venous baffle *(red arrow)*, with opacification via collateral vessels to the IVC from an arm injection. *PA*, Pulmonary artery.

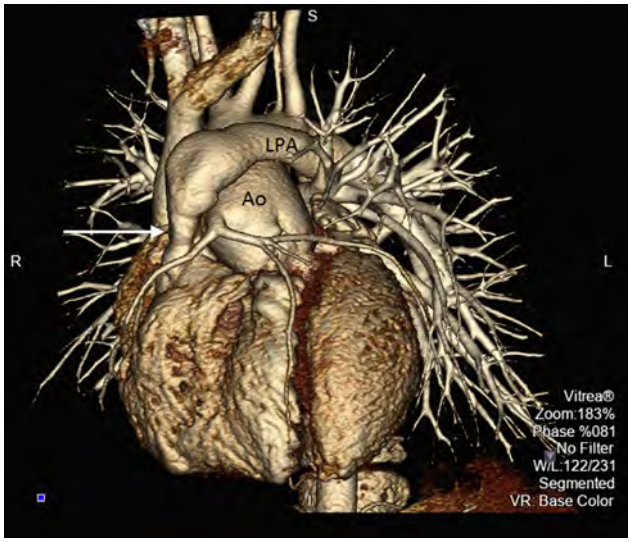

Figure 45 Three-dimensional reconstruction of computed tomographic images from a patient with a conduit from the right ventricle to the pulmonary artery that is significantly obstructed *(white arrow)* after the Rastelli procedure. This image shows both the narrowed proximal conduit and the CA relationship to the conduit. *Ao*, Aorta; *LPA*, left pulmonary artery.

CARDIOVASCULAR CT

Overview of Modality

Cardiovascular CT is a 3D tomographic imaging technique that uses ionizing radiation to create images with exceptional spatial resolution using very short acquisition times. Recent-generation computed tomographic scanners are able to obtain the data for an anatomic scan or detailed CA images at low heart rates (<60 beats/min) in a fraction of a second or a single cardiac cycle. Detailed CA imaging at higher heart rates and functional imaging data sets are acquired over several heartbeats, usually requiring a breath hold. Cardiovascular computed tomographic technology has rapidly advanced in the past several years and has resulted in submillimeter isotropic spatial resolution and temporal resolution as low as 66 msec. These improvements, combined with radiation dose reduction techniques, have decreased the risk and expanded the use of computed tomographic technology in patients of all ages with congenital heart disease.[137-143] Cardiovascular CT provides comprehensive evaluation of cardiac and extracardiac thoracic structures as well as ventricular volumes and functional information when needed. The information that can be obtained by cardiovascular CT is listed in Table 8.

Strengths and Limitations

The strengths of cardiovascular CT are the short acquisition time, the high spatial and temporal resolution of the data set, the ability to safely image patients with pacemakers, defibrillators and retained pacer wires, the ability to image metallic implants with minimal impact on image quality, and the ability to assess the CAs as well as intracardiac and noncardiac structures simultaneously. The short acquisition time makes CT an attractive option for patients who cannot undergo CMR or patients who are hemodynamically unstable.

The rapid data acquisition of the newest computed tomographic scanner technology decreases the sedation and anesthesia needs compared to older scanner platforms. Three hundred twenty–slice volumetric scanners or the second- and third-generation dual-source scanners acquire an anatomic data set in a single heartbeat or a fraction of a second. Studies performed without sedation in children with complex congenital heart disease show no significant movement artifact using these techniques.[144-146] The data needed for functional imaging gated to the electrocardiogram and CA imaging at high heart rates are acquired over several heartbeats, thus usually requiring a single breath hold over several seconds. Proximal CA evaluation in infants using free breathing techniques and without β-blockade shows excellent correlation to surgical findings.[147]

When sedation or anesthesia is needed, no change in equipment is required and the anesthesia period is relatively short, because the data can be acquired in a few breath hold sequences. Up to 15% of patients have pacemakers after the AtrSO because of atrial arrhythmias, sinus node dysfunction, or heart block.[148] Patients with a systemic right ventricle and ventricular dysfunction (EF $<$ 35%) may also have defibrillators in place.[149] Thus, cardiac CT is an extremely useful modality under these conditions.

Cardiovascular CT is an ideal modality for patients needing detailed CA evaluation to assess reimplanted CAs for ostial or distal narrowing or kinking and to assess for atherosclerotic disease. It also can determine the relationship of the CAs to adjacent cardiac and sternal structures before repeat surgical or catheter-directed intervention.[150,151] Both RV and LV volumes and EF can be obtained from an electrocardiographically gated scan.[137,138,152-154] It can also be used in patients who are being evaluated for cardiac resynchronization therapy and upgrade to a biventricular pacing system.[155] Indications for CT in patients with TGA are listed in Table 10.

The main limitations and risks of cardiovascular CT are the use of ionizing radiation and the need for a peripheral IV line and iodinated contrast agents in almost all patients for vascular opacification. An additional limitation is that not all institutions have access to recent-generation scanner platforms or have trained personnel who can adapt protocols specifically for congenital heart disease. Cardiovascular CT in congenital heart disease falls between the traditional disciplines of cardiology and radiology, and almost all practitioners will need additional training or exposure for clinical competence.

Sedation and Anesthesia. For older generation scanners with image acquisition over 5 to 15 sec, sedation may be needed to decrease both respiratory and cardiac motion in patients too young to cooperate. Anesthesia in children with congenital heart disease may have some procedural risk for adverse events.[156-161]

Vascular Access. A peripheral IV line or central venous catheter is needed for contrast administration in all patients, with IV gauge ranging from 24 to 18 depending on patient size. Both power injectors and hand injection are used for contrast administration, with a low rate of adverse events.[162,163]

Iodinated Contrast Exposure. Iodinated contrast is used in almost all patients for vascular opacification. The typical contrast dose is 1 to 2 mL/kg, which is usually well tolerated. Care must be used in patients with a history of renal dysfunction or failure. Allergic reactions are relatively uncommon but increase with age.[164,165]

Medications to Lower Heart Rate. For detailed CA imaging, a heart rate $<$ 60 beats/min maximizes the potential for fully diagnostic images in a single interval and allows the lowest radiation exposure. Higher heart rates often require acquiring the data in end-systole, or widening the acquisition window to include end-systole and early diastole. Heart rate variability also widens the radiated phase of the cardiac cycle (called the acquisition window) and will increase the radiation dose. Preprocedural medication may lower both heart rate and heart rate variability. Beta-blockade protocols have been described for adult and pediatric patients, with a good safety profile.[166,167] Each patient must be screened for contraindications to β-blockers. Patients with pacemakers should have the device interrogated and optimized to achieve AV synchrony during image acquisition.

Radiation Exposure. Radiation exposure is considered to increase the future risk for cancer,[168-171] particularly in young patients with longer life spans.[168] The risk for radiation exposure will vary widely depending on the use and aggressiveness of dose reduction techniques.[172] Radiation doses delivered by cardiac CT have decreased considerably with newer technology, but higher doses may still be delivered if there is not close attention to patient specific dose reduction techniques.[170] A single-institution study showed the median dose for electrocardiographically gated studies in pediatric patients was reduced from 12 to 1.2 mSv between 2005 and 2013.[173] To minimize diagnostic risk, each scan must be tailored to the individual patient and clinical question. Radiation dose for CT angiography has been shown to be 15-fold less than cardiac catheterization in pediatric patients using newer technology and aggressive radiation dose reduction.[174] Physician input and direct supervision is required for patient preparation, scan acquisition, and image interpretation. Estimated radiation doses of approximately 1 mSv are reported for a wide range of congenital cardiac applications, including a cohort of pediatric patients with electrocardiographically triggered coronary scans.[145,147,175-178] Not all centers have achieved this ability as of yet.

Preoperative Assessment of TGA with CT

Cardiac CT is rarely needed before surgical intervention for patients with TGA. The exception is for the definition of complex vascular anatomy in patients with heterotaxy syndrome or patients with extracardiac anomalies. When neonatal anatomic information is needed preoperatively, a prospectively electrocardiographically triggered high-pitch helical or volumetric scan can be obtained without sedation.

Postoperative Assessment of TGA with CT

Refer to the sections above (echocardiography, CMR) for complete description of the anatomic targets of imaging after surgery for TGA. The anatomic targets are identical for all modalities. The CT data set can be oriented in the typical heart-oriented views similar to echocardiography or CMR for illustrating anatomy and facilitating communication with cardiologists and surgeons.

Evaluation after ASO. The anatomic targets after the ASO are similar for all modalities. Cardiovascular CT is typically reserved for

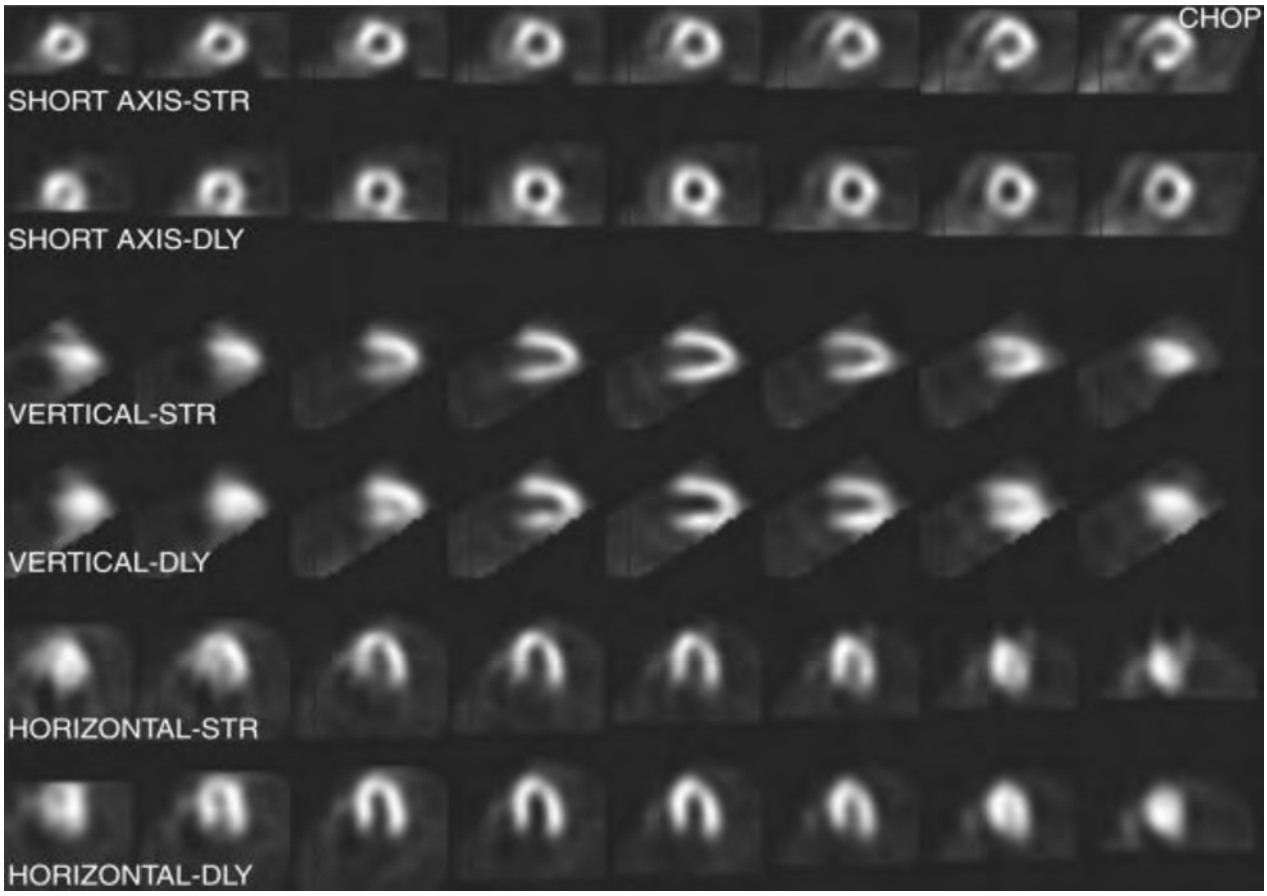

Figure 46 This is a typical display of single-photon emission computed tomographic resting and stress images for myocardial perfusion. Resting and stress images are displayed in the short, vertical, and horizontal axes. This image shows a reversible perfusion defect in the right CA. Note the decreased uptake of isotope in the short-axis stress image compared with the resting images.

patients who have contraindication for CMR, particularly those with implanted devices. Complete 2D and 3D anatomic assessment of the neopulmonary root, branch pulmonary arteries, neoaortic root, and reimplanted CAs can be performed by CT. CA lesions in patients after the ASO may cause myocardial ischemia leading to ventricular dysfunction, arrhythmias, and sudden death.[39] CT can provide high-resolution images of the CAs and can define the relationship of the CAs to adjacent cardiac structures or to the sternum (Figures 41A–41E).[150,151,179,180] Many patients undergo pulmonary arterial intervention to relieve stenosis of the neopulmonary root or branch pulmonary arteries and CT is the ideal method for assessment of the pulmonary arteries in the area of metallic stents in whom CMR is generally nondiagnostic (Figure 42).[181]

Evaluation after AtrSO. The anatomic targets after the AtrSO are similar for all modalities. Cardiovascular CT is typically reserved for patients who have a contraindication for CMR, particularly those with implanted devices (very common in this population). Assessment of the systemic and pulmonary venous pathways for a leak or obstruction is an important part of the postoperative evaluation. The venous pathways have a complex 3D structure that can be difficult to image by echocardiography. The most common site of systemic venous pathway narrowing or obstruction is at the distal superior limb at its entrance into the right atrium (Figure 43). CT is well suited for visualization of this region as well as for evaluation of the pulmonary venous pathway (Figure 44). Decompressing collateral vessels are often visible (Video 23; available at www.onlinejase.com). Systemic venous pathway obstruction is generally treated with stent insertion at the site of obstruction. CT is the method of choice if anatomic restenosis is suspected because of metallic artifact from stents that occurs using CMR.[137] CMR, however, can accurately obtain flow before or after the stent and to a limited extent, visualize the lumen (Figure 34C). Baffle leaks are common and are problematic for CT if a biventricular opacification is used to assess both the right and left heart structures simultaneously. Typically, a baffle leak is best seen by a negative or positive contrast jet, but this is not reliable if both atria are opacified similarly. Pacing and defibrillator leads can be well seen by CT and coronary venous anatomy can be imaged before repeat electrophysiologic intervention such as placement of biventricular pacing leads.

CT can also be used to calculate LV and RV volumes, mass, and EF in patients in whom echocardiography is insufficient and CMR is not possible (Video 24; available at www.onlinejase.com).[181] However, in most cases, CT remains a third-line imaging option.

Evaluation after Rastelli and Nikaidoh Operations. The anatomic targets after the Rastelli and Nikaidoh procedures are similar for all modalities and are described in detail in the echocardiography and CMR sections. The conduit from the right ventricle to the pulmonary artery of patients with Rastelli or Nikaidoh operations almost universally becomes stenotic and requires replacement, typically in the first decade of life. CT can be used to detect this complication and provide

information on the location and extent of conduit calcification and the relationship of the conduit to the CAs and to the sternum in consideration of reoperation (Figure 45). Right CA lesions are more common after the Nikaidoh procedure because of the leftward translocation of the aorta, and this complication is well seen by cardiac CT.

Patient Preparation. A detailed review of the patient history and the pertinent clinical question must be determined for each scan before data acquisition. The scan quality needed (and the resulting radiation dose) will vary considerably on the basis of the indication. Each scan must be tailored to the individual patient. Renal dysfunction needs to be considered with regard to use of contrast agents. Direct physician input is required for patient review, scan planning and acquisition, and interpretation.

In patients with electrophysiologic devices, the underlying heart rhythm and pacing mode should be interrogated and optimized to achieve AV synchrony. If the underlying rate is similar to the paced rate, the paced rate can be reduced or increased to achieve either the underlying rhythm or the paced rhythm but not a competing rhythm.

Scanning Protocol. The following are modifications to standard cardiovascular CT protocols specific to patient with TGA.

Contrast Injection Protocols. For all patients with TGA, there is the potential for both right and left heart pathology. A biventricular injection protocol should be used to opacify the right and left heart simultaneously during a single acquisition. This can be achieved by giving a longer contrast injection at a lower rate, a two-phase contrast injection with a short interval of a standard injection rate followed by a second phase of a slower injection rate, or by keeping the initial injection rate the same and giving the second phase of the injection as a mixture with saline. All injection protocols are followed by a saline flush. This is sometimes called a triphasic injection (two phase contrast and one phase saline).

Scan Initiation. Scan acquisition can be initiated by bolus tracking, a timing bolus, or manual bolus tracking. A timing bolus will increase the contrast dose, and potentially increases the radiation dose. Extending the contrast injection and triggering the scan off the aorta eliminates the need for a timing bolus and allows visualization of both the right and left heart simultaneously. Manually triggering the scan from visualization of opacification on the monitoring sequence is also a reliable method of image acquisition. If there is a high suspicion for superior limb baffle obstruction after the AtrSO, the monitoring sequence and contrast injection should be extended to allow the delayed cardiac opacification of aortopulmonary collateral vessels.

Scan Sequence.

- Retrospectively electrocardiographically gated: This scan mode should be reserved for high resolution CA imaging in a patient with a high and/or irregular heart rate that cannot be normalized by medical management. The scanner will automatically widen the acquisition window if arrhythmia or heart rate variability is detected during the monitoring period or during scan acquisition.
- High-pitch prospectively electrocardiographically triggered or volumetric scan mode: This scan mode can be used for anatomic survey in all patients. It can be used for detailed CA imaging in patients with heart rates < 60 beats/min.
- Prospectively electrocardiographically triggered: This scan mode can be used to image the CAs when there are higher heart rates. The acquisition window should be set for either end-systole or end-diastole depending on heart rate. The width of the acquisition window will depend on the CA detail needed and should be kept to a minimum.
- Prospective triggering via an absolute trigger delay ("millisecond scanning"): This scan mode will acquire data for a specified millisecond time period from the prior QRS, rather than as a percentage of the cardiac cycle. This can be helpful in patients who have arrhythmia or to obtain systolic CA images in patients with higher heart rates.
- Electrocardiographically triggered with pulse modulation for function: In this scan mode, the fully radiated portion of the cardiac cycle is set using the minimal acceptable acquisition window, with approximately 20% of radiation given for the remainder of the cardiac cycle. This provides a high signal diastolic data set in addition to a lower signal systolic data set that is sufficient for estimation of function. Typical data sets are reconstructed in 20 phases per cardiac cycle. Lower doses can be used because the data are typically reconstructed in thicker data sets for evaluation of function (6-8 mm).

Scan Range. The usual scan range for an adult coronary computed tomographic scan is approximately 12 cm. The scan range for all patients with TGA should include the cardiac silhouette and branch pulmonary arteries. The scan range should be extended superiorly for patients with an atrial baffle to assess for baffle patency and collateral vessels.

Recommendations for CA Imaging.

- Consider the use of β-blockade to decrease heart rate and allow use of prospectively electrocardiographically triggered scan modes when possible.
- Use the minimal R-R interval needed on the basis of heart rate (acquisition window), or consider the use of millisecond scanning if there is significant heart rate variability.
- Use the lowest scanner output that will provide a diagnostic image for patient size (tube voltage and tube current–time product).
- Use patient-based automated tube current modulation if available.
- If iterative reconstruction is available, prospectively lower scanner output by 30%.
- Limit the scan range to the area of clinical interest.
- Use a biventricular contrast injection protocol (triphasic) to opacify the right and left sides of the heart simultaneously.

Right and Left Heart Anatomy/Biventricular Function Analysis.

- If fine detail is not needed, consider use of wider collimator and prospectively decrease scanner output (tube voltage and tube current–time product).
- Use a biventricular contrast injection protocol (triphasic) to opacify both the right and left heart simultaneously.
- Increase scan range to include the area of interest (systemic venous and pulmonary venous baffles, aortic root).
- Use electrocardiographic pulse modulation with a narrow acquisition window and low tube voltage to decrease radiation dose for functional imaging. Higher noise levels are tolerated because the data are often reconstructed in thicker data sets for function analysis (6-8 mm)

Reporting Elements and Measurements. All anatomic elements should be reported as described in the complete sections above for echocardiography and CMR. The phase of the cardiac cycle should be noted for thoracic vasculature measurements for accurate comparison to other modalities. Radiation dose reporting and estimates are not yet standardized. Scan dose-length product and/or volume computed tomographic dose index on the basis of a 32-cm phantom, scan length, and scan sequence used should be reported. Scan heart rate should be reported for electrocardiographically triggered examinations.

Recommendations. Cardiovascular CT is an emerging technology that has many applications in TGA. It is usually a third-line modality for patients in whom CMR is contraindicated, but it may be considered a second-line modality for select indications such as detailed CA imaging or evaluation of extracardiac structures. Appropriate technology and well-trained personnel may not be available at all institutions, and aggressive dose reduction techniques should be implemented for every patient to decrease diagnostic risk.

NUCLEAR SCINTIGRAPHY

Overview of Modality

Myocardial perfusion imaging with nuclear scintigraphy has been used for several decades for various types of congenital heart defects. The most common type of imaging is single-photon emission CT (SPECT). Using SPECT, a short half-life isotope, usually ^{99}Tc or ^{201}Tl is injected intravenously and is taken up by the myocardium in proportion to regional myocardial blood flow. Although a resting study may be performed in isolation, SPECT is more typically performed as a combined rest and stress imaging protocol. Rest and stress images are compared for qualitative differences in the regional isotope uptake (Figure 46). Software advances have decreased acquisition time and radiation exposure.[182]

Exercise is the most common stress modality. The advantages of exercise are higher cardiac output and myocardial oxygen consumption compared with pharmacologic stress. Importantly, exercise is also more physiologic and more closely mimics activities of daily living. Pharmacologic stress is usually performed in patients who are either too young to exercise or cannot exercise because of physiologic limitations. The agents most commonly used for pharmacologic stress are adenosine and dobutamine. Adenosine causes maximal dilation of the coronary resistance arterioles. This unmasks proximal stenosis in the larger CAs resulting in decreased regional flow to those areas. As such, it is most useful in those conditions such as TGA where fixed stenotic CA lesions are a concern. Dobutamine infusion raises the heart rate and blood pressure resulting in increased myocardial oxygen consumption. In this sense, it mimics exercise although the effects are more variable. In general, dobutamine usually achieves lower levels of cardiac stress than maximal exercise.[183-185]

Similar to SPECT, positron emission tomography (PET) uses gamma camera technology to measure regional myocardial blood flow. Positron emission tomographic imaging protocols for myocardial blood flow are essentially the same as pharmacologic stress protocols for SPECT. Because of the extremely short life of positron-emitting isotopes (which need to be generated near or onsite and in a very close temporal relation to their use), they are not suitable for use with exercise stress. Like SPECT, PET can be used to assess qualitative differences in regional myocardial blood flow. In addition, with proper software, quantitative flow can be measured for the various regions of the myocardium. This allows the measurement of regional myocardial blood flow reserve when combined with maximal coronary vasodilatation by adenosine.[186,187]

Less commonly, PET is used to assess myocardial metabolism. This is primarily used to distinguish hibernating from infarcted myocardium in the case of an acute CA occlusion. Glucose use will be present in the hibernating ischemic myocardium but not in infarcted myocardium. Positron-emitting fluoride labeled glucose (^{18}F-fluorodeoxyglucose) will be taken up by the hibernating myocardium, indicating viability, and can be used in decisions about possible revascularization procedures.[188]

Strengths and Limitations

The most obvious strength of SPECT over other modalities to evaluate CA status is the ability to combine this imaging modality with maximal exercise. This allows assessment of regional myocardial blood flow with the highest levels of physiologic stress. It also permits an assessment of CA perfusion with exercise-induced symptoms. This is not typically available with other modalities such as CMR that require either pharmacologic stress or submaximal exercise.

Data regarding the sensitivity and specificity of SPECT and PET in identifying significant CA lesions in pediatric acquired and congenital heart disease are very limited. This is due to the small number of pediatric studies, the heterogeneous populations that have been evaluated, and the usually asymptomatic condition of the patients at the time of evaluation.[189,190] The most significant limitation to nuclear scintigraphic imaging is exposure to ionizing radiation. Even with the recent improvements in hardware and software, this remains a major concern especially for pediatric patients. The range of radiation for these procedures is between 7 and 10 mSv.[191]

Postoperative Assessment of TGA with Nuclear Scintigraphy

Because the ASO necessitates CA transfer from the native aortic root to the neoaortic root, morbidity and mortality due to CA ischemia may occur.[192] Possible mechanisms are intimal proliferation around the suture line of the reimplanted ostia, occlusion, compression, or kinking of the CAs. Additionally, a relatively high reimplantation in the ascending aorta, outside the sinuses of Valsalva, may reduce CA flow, particularly during exercise.

There are few reports of the use of nuclear scintigraphy in the assessment of the ASO. Comparison of these reports is limited by the heterogeneity of the subjects studied in each of the series. Studies evaluating the use of SPECT to detect CA blood flow abnormalities in symptomatic patients have reported sensitivity ranging from 50% to 78% and specificity ranging from 69% to 90%.[39,193] The yield of SPECT for asymptomatic subjects has been extremely low, and positive studies have been restricted to those subjects with either a high-risk perioperative course or high-risk CA anatomic variant. In the most recent study, Pizzi *et al.*[194] evaluated 69 patients, of whom 64 were asymptomatic. There were two fixed and six reversible perfusion defects. Of these eight patients, five had either perioperative ischemia and/or an atypical CA variant.

There are also limited data regarding the utility of SPECT in the evaluation of myocardial perfusion following operations for revascularization of patients with significant CA stenosis or occlusion. Raisky *et al.*[195] used SPECT to evaluate 18 of 19 patients following revascularization operations for angiographically diagnosed stenosis or occlusion of CAs after the ASO. SPECT was negative in 16 and minimally positive in two subjects. This was consistent with the CA patency at the time of these studies. These findings would suggest that SPECT may have utility as a follow-up screening tool for revascularization. However, the major weakness of this study is the lack of preoperative SPECT to compare with either the preoperative angiography or the postoperative SPECT.

Patient Preparation. Because of the need for multiple IV line placements and the time required, 2-day protocols should be avoided. A standard 1-day rest/stress protocol is usually optimal. In certain circumstances, a stress only or rest only imaging protocol can be considered.

Scanning Protocol. Following placement of an IV line, resting isotope infusion is performed. Dose should be based on weight for nonobese children. The total dose is typically divided into one quarter given as the first resting injection and three quarters injected during stress. In adolescents, this will result in a dose of approximately 6 to 10 mCi at rest and 20 to 30 mCi with stress.[183,184] Resting images are obtained, and ≥45 min is allowed for isotope decay before beginning the stress study. When exercise is the stressor, injection of the isotope should occur as close as possible to peak exercise,

encouraging the patient to exercise for 1 min after injection.[183,184] Following completion of the stress test, repeat imaging is performed.

Pharmacologic stress should be used when exercise cannot be performed. Because of its very short half-life and vasodilatation properties, adenosine is the agent of choice for evaluating stenotic CA lesions. Resting images are obtained as with the exercise protocol. A second IV line is typically needed for adenosine infusion. After obtaining resting images and suitable decay time, the adenosine infusion is started at 0.14 mg/kg/min. The infusion is continued for 6 min with injection of the isotope at 3 to 4 min into the infusion. The infusion can be stopped for side effects with no other intervention generally needed because of its very short half-life. Poststress images are obtained as with the exercise stress.

PET is currently performed at a very limited number of centers. In general, the protocol for the assessment of regional myocardial blood flow is very similar to SPECT using pharmacological stress. Choice of isotopes is generally center specific.

Recommendations. Given the significant radiation exposure even with state-of-the-art equipment and software, nuclear scintigraphic imaging should not be used for routine screening of asymptomatic low-risk populations. Similar to adults with suspected CA disease, single-photon emission computed tomographic screening to evaluate symptoms is reasonable in high-risk populations. High-risk populations include those patients with atypical CA patterns (especially the presence of an intramural CA course), a history of perioperative ischemia, or a history of documented CA stenosis. In addition, patients in whom ST-segment changes during stress are unreliable markers of myocardial ischemia (such as those with a bundle branch block) also fall into this category. Nuclear scintigraphic imaging should also be considered for screening asymptomatic high-risk patients before participation in vigorous athletics. Finally, SPECT should be considered when looking for evidence of regional myocardial ischemia following revascularization procedures for stenosis or occlusion. Imaging with PET is currently done only rarely and at a relatively small number of institutions. As such it is probably not appropriate to make generalized recommendations for the use of PET at this time.

EXERCISE AND STRESS ECHOCARDIOGRAPHY

Overview of Modality

The exercise or pharmacologic stress test can be a useful adjunct to the postoperative assessment of a patient with TGA. After ASO, a stress evaluation is helpful in detecting problems with myocardial perfusion potentially associated with the translocation and reimplantation of the CAs. Moreover, in the ASO or the AtrSO, stress testing helps determine contractile reserve and exercise capacity.

Stress testing necessitates administering a stressor (e.g., exercise or pharmacologic agent) and evaluating the effects of the stressor on the heart with an appropriate sensor (e.g., electrocardiography, echocardiography, SPECT, CMR). The types of stressors and sensors employed depend on many factors including patient age, indications for testing, and sensitivity and specificity of the sensor.

Strengths and Limitations

Traditional echocardiography is performed with the child in a quiet, resting state, a condition in which children are found for only a minority portion of their typical day. The value of stress echocardiography is that it provides valuable assessment of myocardial perfusion, contractile reserve, and general hemodynamics in a nonresting state. The limitations of stress echocardiography are largely related to image quality. In particular, obtaining adequate images during exercise can be challenging. Various strategies can be used to help overcome these difficulties, such as having the patient hold an exhalation or obtaining images during the immediate recovery phase (rather than at maximal exercise). In addition, for patients without residual shunts, contrast agents can be given to enhance cardiac opacification. Finally, pharmacologic stress can be used as a surrogate for exercise and will avoid motion and respiratory artifact associated with exercise testing.

Evaluation of Myocardial Perfusion

Assessment of myocardial perfusion is discussed in the previous section in detail.

Exercise Capacity and Contractile Reserve

The other major use of stress testing in the TGA population is in the assessment of exercise capacity and contractile reserve.

Evaluation after ASO. Compared with AtrSO patients, the ASO population has much greater exercise capacity, most likely because the operation is more physiologic. Nevertheless, functional capacity in the ASO population is not normal.[196] Many studies have shown that decreased exercise tolerance is due to chronotropic incompetence.[197] Other factors leading to decreased exercise capacity are abnormal CA flow reserve, reduced levels of physical activity (deconditioning), and longer follow-up. This latter finding is particularly concerning given the expected better myocardial performance associated with an ASO over the AtrSO. Giardini *et al.*[198] performed exercise echocardiography on 60 ASO patients at a mean age of nearly 14 years. The maximal V_{O_2}% was 84% of predicted. Correlates of reduced maximal V_{O_2}% were RV outflow tract maximal velocity > 2.5 m/sec.

Evaluation after AtrSO. Impairment of (systemic) RV function and resulting heart failure is a significant problem in patients undergoing prior Mustard or Senning operations. To help predict those patients at risk for systemic ventricular dysfunction, investigators have used stress echocardiography.[199] Li *et al.*[200] performed dobutamine stress echocardiography as well as exercise testing in 27 adult patients after the Mustard procedure. Despite the absence of any symptoms, exercise capacity in these patients was significantly depressed compared with reference values. Decreased exercise capacity correlated with decreased systemic ventricular free wall excursion at rest and during dobutamine stress.

Protocol. Routine Bruce and ramp protocols are used for stress testing in children after surgery for TGA.[201] Stress echocardiography can be used to assess for regional wall motion abnormalities after ASO or after CA reimplantation in patients who have undergone the Nikaidoh operation. ASE guideline recommendations can be used for stress echocardiography.[202] At peak exercise, echocardiography can also be used to assess outflow gradients.

Recommendations. Growth and patency of the CA anastomoses remain significant issues because of reports of myocardial ischemia in the TGA population.[203] Consensus regarding the appropriate monitoring examinations is lacking. Some have recommended serial myocardial perfusion stress testing every 3 years or so during periods of growth and before high school sports participation.[197] Others suggest that stress testing for evaluating myocardial perfusion should be reserved for those patients with symptoms, congenitally abnormal CA pattern, or perioperative ischemic issues.

Monitoring exercise capacity in both ASO and AtrSO patients remains an important diagnostic and predictive test. Chronotropic incompetence during exercise is known to be associated with increased mortality in adults.[197] In these populations, subclinical ventricular dysfunction can be unmasked in patients with normal ventricular function at rest. Long-term follow-up is necessary to determine the significance of these findings.

CARDIAC CATHETERIZATION AND ANGIOGRAPHY

Overview of Modality

The role of cardiac catheterization and angiography has evolved in patients with TGA. In the past, patients required diagnostic catheterization and angiography to determine the relationship of the great arteries to the ventricles (to prove they had TGA) and to evaluate the atrial septal communication. BAS is performed if there was profound cyanosis and the atrial communication is considered inadequate. This can be performed in the cardiac catheterization laboratory under fluoroscopy or at the bedside with echocardiographic guidance. Presently, BAS is completed in anticipation of an ASO, which is usually performed within the first week of life. In the early era of surgery, adequate atrial level mixing by BAS enabled patients to wait for an AtrSO, which was typically performed weeks or months later.[8] After the AtrSO, the systemic and pulmonary venous baffles often require evaluation in the cardiac catheterization laboratory to diagnose and treat stenoses and leaks. The placement of transvenous pacemaker leads makes intervention for these types of problems technically challenging. In the early years of the ASO, catheterization and angiography had a role in defining CA anomalies. In the modern era, improved echocardiographic imaging and surgical techniques have made this less of an issue. Patients with TGA and posterior malalignment VSD who undergo the Rastelli operation are prone to recurrent subaortic stenosis that may require hemodynamic assessment by cardiac catheterization. Moreover, the conduit from the right ventricle to the pulmonary artery has a finite life span, and many of these patients must return to the cardiac catheterization laboratory for percutaneous pulmonary valve or stent placement within the conduit.[204-206]

Strengths and Limitations

Angiography is the oldest imaging modality available in cardiology. It has been used since the 1950's to provide anatomic information in patients with congenital heart disease. It provides excellent detail about CA anatomy. It also delineates the branch pulmonary arteries. In patients with a VSD, angiography allows the detection of additional VSDs (which can be challenging to detect by echocardiography). The major limitation of cardiac catheterization is that is an invasive procedure with potential vascular and cardiac injury. With any invasive procedure, there is a small risk for significant morbidity and even mortality. Fluoroscopy requires radiation exposure. Moreover, sedation or general anesthesia is required in most cases.

Preoperative Assessment of TGA with Cardiac Catheterization and Angiography

In the modern era, the role of cardiac catheterization in patients with TGA is reserved primarily for intervention, specifically, BAS in neonates with insufficient mixing at the atrial level. Transthoracic echocardiographic guidance has enabled bedside BAS in the intensive care unit at some institutions. Other institutions prefer to perform the procedure in the cardiac catheterization laboratory. Bedside intensive care unit procedures are usually performed by umbilical venous access but can also be performed with femoral venous access. The location for BAS is institution specific in a hemodynamically stable patient. In an acidotic unstable patient who is already receiving prostaglandin infusion, emergent BAS should be performed promptly (Figure 47).

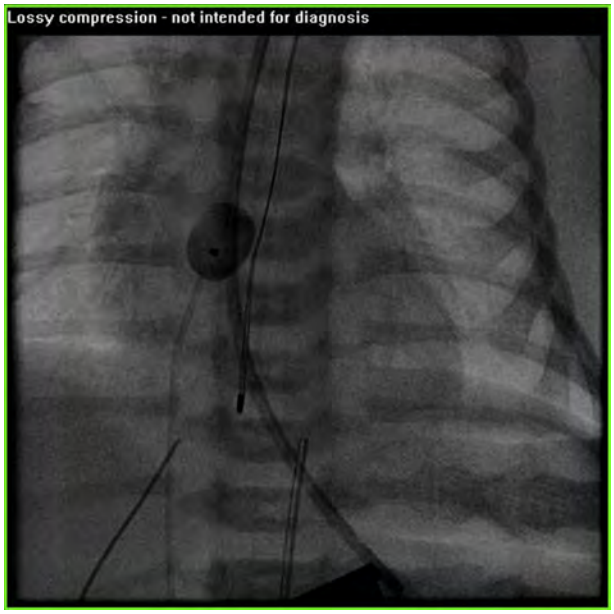

print & web 4C/FPO

Figure 47 Anteroposterior fluoroscopic image during a BAS in a neonate with TGA. The septostomy balloon will be pulled across the atrial septum with a swift, controlled jerk. At the bottom of the image, a surface echo transducer permits simultaneous imaging of the procedure, ensuring that intracardiac structures are not damaged and enabling immediate assessment of the atrial septal flap and adequacy of left-to-right shunt after the maneuver.

If TTE has not adequately delineated the CA anatomy, aortic root angiography may be used to visualize the CA origins. An injection in the ascending aorta, entered prograde from the right ventricle, using a balloon occlusion technique, will usually define the course of the CAs. This is sometimes performed after BAS.

Angiography may be used in TGA to identify multiple VSDs, LV outflow tract obstruction, septal alignment, AV valve regurgitation, or associated aortic arch anomalies. However, the use of angiography for preoperative diagnosis is largely historical.[204] In select patients, there may be a need to directly measure pulmonary artery pressure, calculate pulmonary vascular resistance, or test pulmonary vascular reactivity if there is suspicion of PH.

Assessment of Postoperative TGA with Cardiac Catheterization and Angiography

Evaluation after ASO. Patients after ASO rarely require routine cardiac catheterization. The role for angiography after ASO is currently reserved for select patients in whom incremental information is needed. In the immediate postoperative period after an ASO, if an infant cannot be weaned from cardiopulmonary bypass, there is a role for angiography to determine patency of the proximal CAs.[207] In addition, new onset of ventricular arrhythmia warrants CA imaging to exclude ischemia. If stenosis is diagnosed, there may be a role for CA stenting in this clinical setting.[207]

After ASO, 20% to 30% of patients develop proximal branch pulmonary artery stenoses (Figure 48).[54,55] Some of these patients

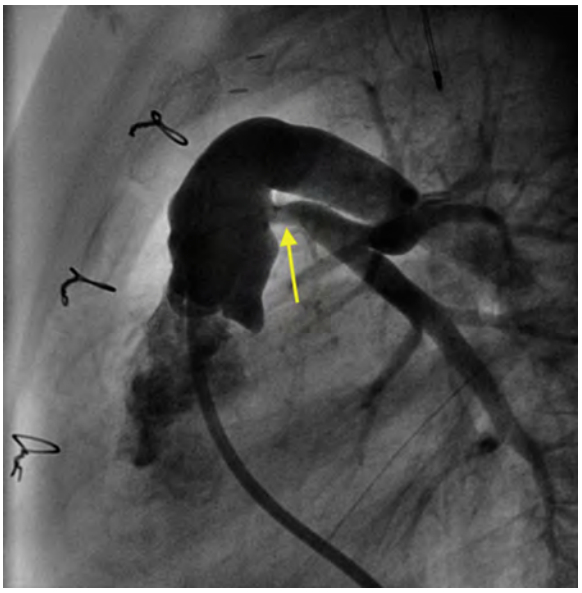

Figure 48 Lateral angiograph demonstrating proximal right pulmonary artery stenosis *(yellow arrow)* in a child after LeCompte maneuver and ASO for TGA.

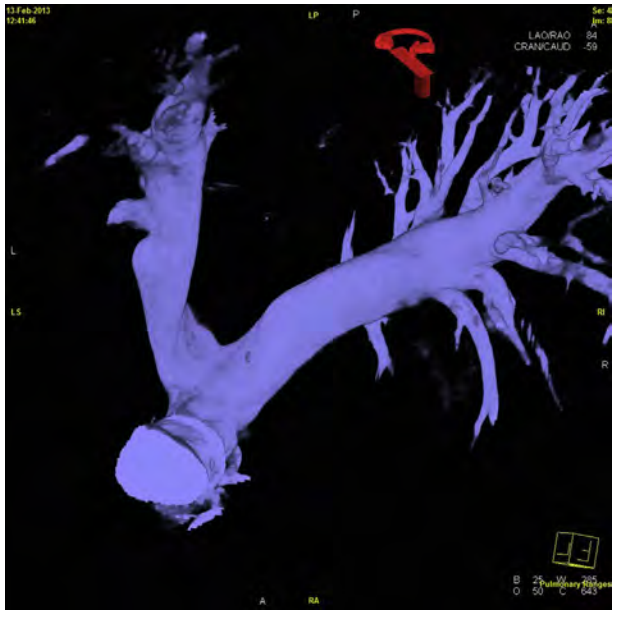

Figure 49 Three-dimensional rotational angiography of the branch pulmonary arteries in a patient after LeCompte maneuver and ASO for TGA.

may require proximal pulmonary artery branch stent placement early in life. These stents may require redilation with future cardiac catheterizations as the child grows. Three-dimensional rotational angiography has shown promise as a tool to assist the interventionalist with balloon angioplasty and stent placement (Figure 49).

Up to 30% of patients with TGA may have aortopulmonary collateral vessels.[53] If large, these vessels can create a hemodynamically important source of excess pulmonary blood flow after the ASO. Descending aorta angiography can delineate these vessels, and transcatheter closure devices or other occluders can be used to ameliorate the shunt.[204]

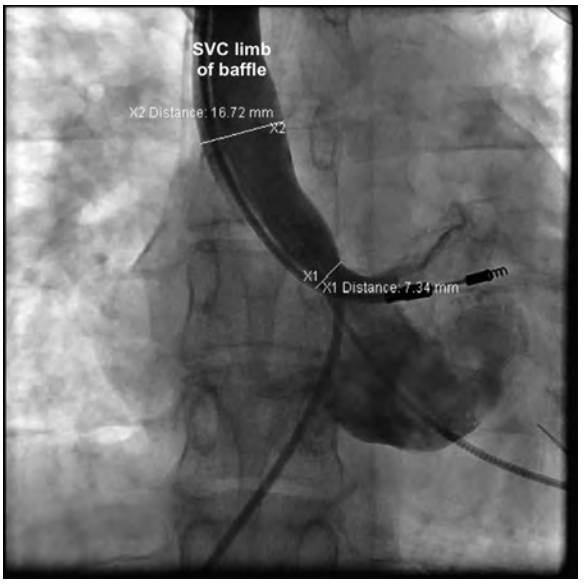

Figure 50 Angiography in a patient after the Mustard operation who has pacing leads. Note that the SVC limb of systemic venous baffle demonstrates stenosis. In this patient, it was elected to jail the leads with stent placement because the atrial lead could not be easily extracted.

Evaluation after AtrSO. *Systemic Venous Baffle Stenoses and Leaks.* Superior limb baffle stenosis occurs in up to 30% of patients after a Mustard operation[62,64]; it may be slightly less frequent in patients after a Senning operation. In addition, approximately 5% of patients who had an AtrSO may develop hemodynamically important inferior limb baffle stenosis.[208] Cardiac catheterization accurately identifies baffle stenosis and baffle leaks. Baffle leaks can be addressed in the cardiac catheterization laboratory with the use of commercially available septal closure devices (Figure 27B). Before transvenous pacemaker lead placement, a thorough evaluation for interatrial shunting should be performed. If a baffle leak is detected, it should be addressed before pacemaker placement because of the concern that paradoxical emboli may result from debris accumulation on the lead.[15,77]

Angiography of the superior and inferior limbs of the systemic venous baffle is performed via standard femoral venous access. Baffle narrowing tends to be intracardiac near where the baffle crosses toward the morphologic left atrium (Figure 50). Systemic venous baffle stenosis may be underestimated by noninvasive imaging, especially in adults with suboptimal acoustic windows. In a recent study, unrecognized baffle stenoses (gradient $\geq$ 4 mm Hg) were identified and treated in the catheterization laboratory.[209] Flow into the azygos vein can confound assessment of baffle stenosis because it decompresses the SVC and thereby decreases the measurable gradient. Systemic venous baffle stenosis has been treated with open cell, bare-metal stents originally designed for biliary use. Covered stents may also be used in this manner.

The placement of transvenous dual-chamber pacing systems is fairly common after AtrSO. The pacing leads course posteriorly and appear in unique locations (left ventricle) compared with the usual position in an anatomically normal heart (Figures 51A and 51B). Pacemaker leads coursing through the superior limb of the systemic venous baffle provide unique issues if stenosis develops and stent placement is required. Although it is never optimal to "jail" a pacing lead against the wall of the baffle with a stent, sometimes this is

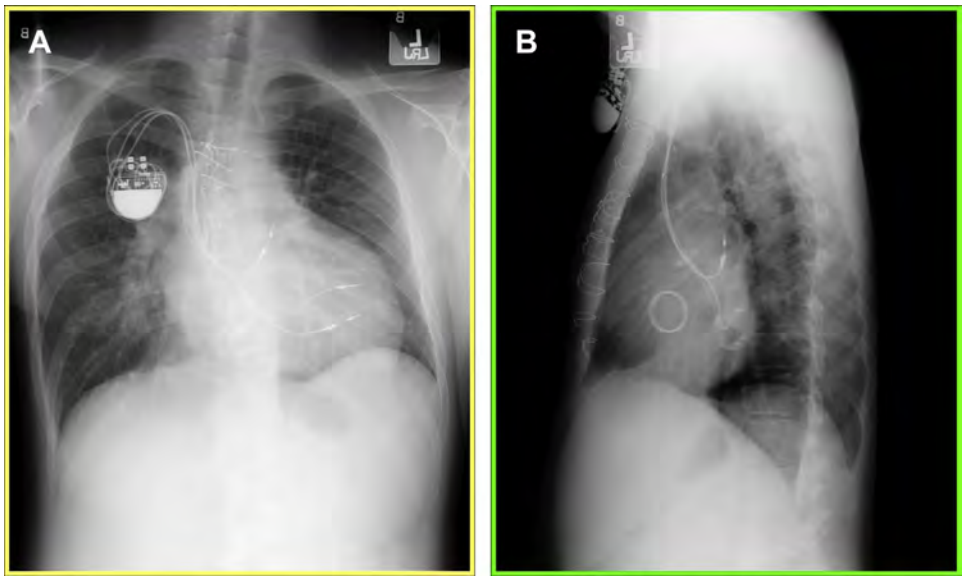

Figure 51 **(A)** Anteroposterior and **(B)** lateral chest radiographs demonstrate the posterior positioning of atrial and ventricular pacemaker leads in the systemic venous baffle in an adult after a Senning operation.

unavoidable. Patients with jailed pacing leads need meticulous follow-up to ensure that the lead function remains normal.

Approach to Pulmonary Venous Baffle Obstruction. Pulmonary venous baffle obstruction is more common after the Senning operation compared with the Mustard operation because of the manner in which native atrial tissue needs to be tailored to form the systemic venous baffle.[210] It has been estimated that 8% of patients after Senning operation develop hemodynamically important pulmonary venous baffle obstruction.[210] It is a potentially repairable cause of PH in patients with TGA. Transbaffle approach through an existing defect or use of a transseptal puncture can be used to address this issue. The area of pulmonary venous baffle obstruction can also be approached in a retrograde manner from the systemic right ventricle. The retrograde approach has inherent issues related to tricuspid valve trauma, which may be deleterious to the patient's overall condition. Often, reoperation is required.

Evaluation after Rastelli or Nikaidoh Operation. Inherent to the long-term follow-up of patients with TGA after the Rastelli or Nikaidoh operation is the finite life span of the conduit from the right ventricle to the pulmonary artery. Freedom from reoperation or death after conduit placement has been reported at 54% at 10-year follow-up.[211] In addition, freedom from major homograft dysfunction (primarily regurgitation) at 10-year follow-up has been reported to be only 22%. Patients after the Rastelli or Nikaidoh procedure are destined to require multiple sternotomies for conduit replacement. In the current era, the role of percutaneous pulmonary valve placement has resurrected the need for cardiac catheterization and angiography. The Melody (Medtronic, Minneapolis, MN) and the SAPIEN (Edwards Lifesciences, Irvine, CA) valves are used worldwide for treatment of conduit or pulmonary bioprosthetic valve dysfunction.[212,213]

Patients with TGA after a Rastelli or Nikaidoh operation have benefited from use of these percutaneous valves. In the US Melody valve clinical trial, patients with TGA and conduits from the right ventricle to the pulmonary artery constituted approximately 15% of those implanted with a percutaneous pulmonary valve.[214] Before Melody valve implantation, preparing the conduit from the right ventricle to the pulmonary artery with a bare-metal stent has become a standard procedure.[215] The bare-metal stent provides a stable circular landing zone for the Melody valve and decreases the incidence of stent fracture. The conduits in these patients have been inserted in an extra-anatomic location. Therefore, CA angiography during conduit balloon dilation ensures that CA occlusion does not occur when the Melody valve is expanded. Short-term follow-up data from patients who underwent percutaneous pulmonary valve replacement are good. Freedom from significant valve regurgitation has been excellent (>90% at 4 years).[214] In the initial US trial, recurrent valve stenosis afflicted nearly 20% of patients where conduit prestenting was prohibited.[216] Fracture rate was reduced to <5% in the postapproval study cohort in which homografts were prestented and valve-in-valve cases were included.[217] The evolution of percutaneous pulmonary valve replacement technology offers the hope for patients after Rastelli operation to have fewer reoperations.

Cardiac Catheterization and the "Late Switch". Despite improved prenatal diagnosis, the presentation of infants with TGA beyond the neonatal period still occurs. The management of these patients can be challenging, especially if the left ventricle is "deconditioned" and is at pulmonary artery pressure. The longer a patient waits before the ASO, the higher the risk that the surgery will fail because of LV dysfunction. Various strategies have been used to manage these patients. Some centers have proposed the use of a pulmonary artery band with insertion of a systemic to pulmonary shunt to "train" the left ventricle. These patients tend to be quite ill, and many have biventricular dysfunction due to the combined acute changes in pressure and volume loads. However, in small babies, the "training phase" for the left ventricle may take only a few days.

After 8 weeks of age, morbidity and the need for mechanical support after ASO increases and hospitalization is prolonged.[218] In countries where mechanical support is not readily available, some have proposed the use of a Mustard or Senning procedure for older patients with TGA. Cardiac catheterization may be helpful if hemodynamic assessment of pulmonary artery pressure and resistance is required.

Patient Preparation. Before cardiac catheterization, patients should have a comprehensive echocardiographic assessment to determine if invasive angiography is indicated. The patient's medical record is reviewed for information related to surgical intervention as well as previous cardiac catheterization procedures. Sedation is selected based on patient age and the procedure being performed. Neonates usually have general anesthesia during cardiac catheterization. Older children may undergo diagnostic catheterization using conscious sedation barring any airway or respiratory issues. Percutaneous access is obtained for catheter insertion using sterile technique. Biplane angiography is typically performed from various standard and nonstandard angles.

Scanning Protocol. The protocol for cardiac catheterization and angiography is out of the scope of this guideline. Standard views for angiography are used, depending on the region of interest as presented above.

Recommendations. The role for cardiac catheterization and angiography for patients with TGA has undergone an evolution over the years. Decades ago, cardiac catheterization provided basic anatomic information regarding the orientation of the great arteries. Many years later, effective palliation with BAS is still used to manage these infants. Patients after ASO may require long-term CA surveillance. After AtrSO, intervention may be required to address baffle stenosis or leaks. For patients after the Rastelli operation, cardiac catheterization has now evolved into a treatment modality with the use of percutaneous pulmonary valve replacement for conduit dysfunction. Advances in echocardiography over the decades have largely supplanted the diagnostic role of cardiac catheterization for patients with TGA. However, the modern era has brought a new and exciting role for cardiac catheterization that may obviate the need for repetitive surgeries.

MULTIMODALITY APPROACH

Echocardiography alone can define all aspects of anatomy in a majority of patients with TGA preoperatively, including unusual findings such as juxtaposition of the atrial appendages. CA anatomy can usually be identified by echocardiography in infants and small children, and additional modalities are rarely required before intervention because the surgeon is able to visualize the CA origins during the procedure. In some cases of suspected intramural course of the CA, CT or x-ray angiography may be used to confirm this diagnosis. Although intramural CAs can still be "switched," the risk for CA kinking or stenosis is much higher in this population.[38] Echocardiography can also be used primarily to guide BAS, particularly if the procedure is performed in the intensive care unit. The advantage of echocardiography (either TTE or TEE depending on the clinical situation) is that the atrial septum can be seen so that the balloon can be directed up against the septum accurately. With angiography, the atrial septum cannot be directly visualized.

A larger subset of patients will require advanced imaging to define anatomic detail after surgical intervention. TGA is one of the most common congenital diagnoses referred for both CMR and cardiovascular CT.[141] Both modalities offer excellent visualization of complex anatomy and postoperative complications as well as accurate quantification of ventricular function.

After the AtrSO, evaluation of systemic and pulmonary venous baffles, systemic RV systolic function, or AV valve regurgitation is commonly required. Although echocardiography can act as a first-line imaging modality to perform surveillance for these findings, it can miss potentially important complications. There is a relatively high rate of unsuspected atrial baffle occlusion and baffle leaks in patients screened by echocardiography.[64,209] Advanced imaging (CMR or CT) is reasonable before repeat intervention as it may change the catheterization or surgical approach.

CMR as an initial screening tool to assess for CA issues in older children and adolescents is accepted as standard of care.[106-109,219,220] CA imaging in pediatric patients <2 years of age can be more challenging. CMR imaging of the CAs in patients with slow, regular breathing, and without arrhythmia is optimal, although CMR can be performed to assess CAs in patients with fast breathing as well. Newer 3D CMR imaging techniques have improved the quality of CA imaging and may expand the usefulness of this technique in the future.

Computed tomographic angiography has been shown to have diagnostic visualization of CAs in unrepaired congenital heart disease in a wide range of patients from infants to adolescents using computed tomographic angiography at a radiation dose < 1 mSv.[221] CT has been shown to be accurate compared with invasive angiography for CA lesions after the ASO.[150,179,222] There is a wide range of radiation doses delivered to larger patients and to those with higher heart rates or arrhythmia, particularly if attempts to use the lowest possible radiation dose are not implemented.[223]

Both CMR and CT allow calculation of EF from tracing the endocardial borders in end-systole and end-diastole from a short-axis data set. CMR has the advantage that it does not require contrast agents or radiation to assess ventricular function and is considered the gold standard.[224,225] Acceptable correlation between the two modalities for this indication has been shown.[138,226] These modalities should be considered if accurate assessment of EF, particularly of the right ventricle, is needed. CMR can also provide accurate information on severity of valve regurgitation using velocity-encoded phase contrast and cine imaging to determine regurgitant fraction.

Stress imaging can be used in the outpatient setting as a screening tool to determine if there is suspicion of CA ischemia. Exercise testing can be done in association with outpatient visits; pharmacologic stress requires a day procedure in the hospital setting. Exercise stress testing can be performed every few years to assess whether patients can safely exercise and/or participate in sports. If ischemia is suspected on exercise or stress testing, further evaluation is warranted by nuclear scintigraphy, CMR or CT. These options are available before deciding to perform cardiac catheterization, which is an invasive procedure that carries sedation or anesthesia risk, radiation risk and risk for vascular injury.

It is recommended that all patients with reimplanted CAs undergo angiography at least once in adulthood to ensure vessel patency.[227] CA occlusion or narrowing can be asymptomatic in children and young adults. CA angiography is also recommended before RV outflow tract reintervention, including transcatheter pulmonary valve replacement and in adult patients who undergoing any cardiac procedure.[227] In addition, cardiac catheterization is indicated if an interventional procedure is being considered.

The choice of imaging modality should be made by determining the best test with the least risk to the patient given a specific clinical question. In some cases, it should be determined by the age of the patient. The best test for an individual patient will vary on the basis of the availability of both advanced imaging technology and skilled personnel available at each institution.

REVIEWERS

This document was reviewed by members of the 2015-2016 ASE Guidelines and Standards Committee, the 2015-2016 ASE Board of Directors, and external reviewers.

ASE reviewers included Deborah A. Agler, RCT, RDCS, FASE, Federico M. Asch, MD, FASE, Merri L. Bremer, EdD, RN, EDCS, ACS, FASE, Benjamin Byrd, MD, FASE, Hollie D. Carron, RDCS, FASE, Frederick C. Cobey, MD, FASE, Patrick Collier, MD, PhD, FASE, Patrick D. Coon, RCCS, RDCS, FASE, Adam Dorfman, MD, FASE, Fadia Makarem Ezzeddine, RT, RCS, FASE, Craig Fleishman, MD, FASE, Yvonne E. Gilliland, MD, FASE, Aasha S. Gopal, MD, FASE, Lanqi Hua, RDCS, FASE, Soo Kim, MD, MPH, FASE, Allan L. Klein, MD, FASE, Joe R. Kreeger, ACS, RCCS, RDCS, FASE, Stephen H. Little, MD, FASE, Sunil Mankad, MD, FASE, Tasneem Naqvi, MD, FASE, Maryellen H. Orsinelli, RN, RDCS, FASE, Andy Pellett, PhD, RCS, RDCS, FASE, Patricia A. Pellikka, MD, FASE, Sue D. Phillip, RCS, FASE, Juan Carlos Plana, MD, FASE, Michael Quartermain, MD, FASE, Vera H. Rigolin, MD, FASE, Brad J. Roberts, ACS, RCS, FASE, Lawrence Rudski, MD, FASE, Vandana Sachdev, MD, FASE, Anita Sadeghpour, MD, FASE, Fadi Shamoun, MD, FASE, Elaine Shea, ACS, RCS, RCCS, FASE, Roman M. Sniecinski, MD, FASE, Vincent L. Sorrell, MD, FASE, Cynthia Taub, MD, FASE, Neil J. Weissman, MD, FASE, Susan E. Wiegers, MD, FASE. External reviewers included Brian Ghoshhajra, MD, MBA, Shaine A. Morris, MD, and Olga Toro-Salazar, MD.

NOTICE AND DISCLAIMER

This report is made available by the ASE as a courtesy reference source for members. This report contains recommendations only and should not be used as the sole basis to make medical practice decisions or for disciplinary action against any employee. The statements and recommendations contained in this report are based primarily on the opinions of experts, rather than on scientifically verified data. The ASE makes no express or implied warranties regarding the completeness or accuracy of the information in this report, including the warranty of merchantability or fitness for a particular purpose. In no event shall the ASE be liable to you, your patients, or any other third parties for any decision made or action taken by you or such other parties in reliance on this information. Nor does your use of this information constitute the offering of medical advice by the ASE or create any physician-patient relationship between the ASE and your patients or anyone else.

SUPPLEMENTARY DATA

Supplementary data related to this article can be found at http://dx.doi.org/10.1016/j.echo.2016.04.002.

REFERENCES

1. Hoffman JI, Kaplan S. The incidence of congenital heart disease. J Am Coll Cardiol 2002;39:1890-900.
2. Fulton DR, Fyler DC. D-transposition of the great arteries. In: Keane JF, Lock JE, Fyler DC, editors. Nadas' Pediatric Cardiology. 2nd ed. Philadelphia: Saunders Elsevier; 2006. pp. 645-61.
3. De Luca A, Sarkozy A, Consoli F, Ferese R, Guida V, Dentici ML, et al. Familial transposition of the great arteries caused by multiple mutations in laterality genes. Heart 2010;96:673-7.
4. Lisowski LA, Verheijen PM, Copel JA, Kleinman CS, Wassink S, Visser GH, et al. Congenital heart disease in pregnancies complicated by maternal diabetes mellitus. An international clinical collaboration, literature review, and meta-analysis. Herz 2010;35:19-26.
5. Costell M, Carmona R, Gustafsson E, Gonzalez-Iriarte M, Fassler R, Munoz-Chapuli R. Hyperplastic conotruncal endocardial cushions and transposition of great arteries in perlecan-null mice. Circ Res 2002;91:158-64.
6. Miyake T, Yokoyama T, Shirotani H. Transposition of the great arteries with posterior aorta: detection by two-dimensional echocardiography. Pediatr Cardiol 1990;11:102-4.
7. Mertens LL, Vogt MO, Marek J, Cohen MS. Transposition of the great arteries. In: Lai WW, Mertens LL, Cohen MS, Geva T, editors. Echocardiography in Pediatric and Congenital Heart Disease: From Fetus to Adult. Wiley-Blackwell; 2009. pp. 398-416.
8. Rashkind WJ, Miller WW. Creation of an atrial septal defect without thoracotomy. A palliative approach to complete transposition of the great arteries. JAMA 1966;196:991-2.
9. Liebman J, Cullum L, Belloc NB. Natural history of transpositon of the great arteries. Anatomy and birth and death characteristics. Circulation 1969;40:237-62.
10. Mustard WT, Chute AL, Keith JD, Sirek A, Rowe RD, Vlad P. A surgical approach to transposition of the great vessels with extracorporeal circuit. Surgery 1954;36:31-51.
11. Senning A. Surgical correction of transposition of the great vessels. Surgery 1959;45:966-80.
12. Mustard WT. Successful Two-Stage Correction of Transposition of the Great Vessels. Surgery 1964;55:469-72.
13. Mustard WT, Keith JD, Trusler GA, Fowler R, Kidd L. The Surgical Management of Transposition of the Great Vessels. J Thorac Cardiovasc Surg 1964;48:953-8.
14. Wilson NJ, Clarkson PM, Barratt-Boyes BG, Calder AL, Whitlock RM, Easthope RN, et al. Long-term outcome after the mustard repair for simple transposition of the great arteries. 28-year follow-up. J Am Coll Cardiol 1998;32:758-65.
15. Dos L, Teruel L, Ferreira IJ, Rodriguez-Larrea J, Miro L, Girona J, et al. Late outcome of Senning and Mustard procedures for correction of transposition of the great arteries. Heart 2005;91:652-6.
16. Wells WJ, Blackstone E. Intermediate outcome after Mustard and Senning procedures: A study by the Congenital Heart Surgeons Society. Semin Thorac Cardiovasc Surg Pediatr Card Surg Annu 2000;3:186-97.
17. Konstantinov IE, Alexi-Meskishvili VV, Williams WG, Freedom RM, Van Praagh R. Atrial switch operation: past, present, and future. Ann Thorac Surg 2004;77:2250-8.
18. Jatene AD, Fontes VF, Paulista PP, de Souza LC, Neger F, Galantier M, et al. Successful anatomic correction of transposition of the great vessels. A preliminary report. Arq Bras Cardiol 1975;28:461-4.
19. Lecompte Y, Zannini L, Hazan E, Jarreau MM, Bex JP, Tu TV, et al. Anatomic correction of transposition of the great arteries. J Thorac Cardiovasc Surg 1981;82:629-31.
20. Rastelli GC, Wallace RB, Ongley PA. Complete repair of transposition of the great arteries with pulmonary stenosis. A review and report of a case corrected by using a new surgical technique. Circulation 1969;39:83-95.
21. Nikaidoh H. Aortic translocation and biventricular outflow tract reconstruction. A new surgical repair for transposition of the great arteries associated with ventricular septal defect and pulmonary stenosis. J Thorac Cardiovasc Surg 1984;88:365-72.
22. Valente AM, Cook S, Festa P, Ko HH, Krishnamurthy R, Taylor AM, et al. Multimodality imaging guidelines for patients with repaired tetralogy of fallot: a report from the American Society of Echocardiography: developed in collaboration with the Society for Cardiovascular Magnetic Resonance and the Society for Pediatric Radiology. J Am Soc Echocardiogr 2014;27:111-41.

23. Lai WW, Geva T, Shirali GS, Frommelt PC, Humes RA, Brook MM, et al. Guidelines and standards for performance of a pediatric echocardiogram: a report from the Task Force of the Pediatric Council of the American Society of Echocardiography. J Am Soc Echocardiogr 2006;19:1413-30.
24. Ayres NA, Miller-Hance W, Fyfe DA, Stevenson JG, Sahn DJ, Young LT, et al. Indications and guidelines for performance of transesophageal echocardiography in the patient with pediatric acquired or congenital heart disease: report from the task force of the Pediatric Council of the American Society of Echocardiography. J Am Soc Echocardiogr 2005;18:91-8.
25. Rudolph AM. Transposition of the great arteries (aortopulmonary transposition). Congenital Diseases of the Heart: Clinical-Physiological Considerations, Fully Revised and Updated 2nd Edition. Armonk, NY: Futura Publishing Company; 2001. pp. 675-736.
26. Van Praagh S, O'Sullivan J, Brili S, Van Praagh R. Juxtaposition of the morphologically right atrial appendage in solitus and inversus atria: a study of 35 postmortem cases. Am Heart J 1996;132:382-90.
27. Ueda Y, Miki S, Okita Y, Tahata T, Sakai T, Matsuyama K, et al. Transposition of the great arteries associated with total anomalous pulmonary venous return. Ann Thorac Surg 1994;57:470-2.
28. Lai WW, Ravishankar C, Gross RP, Kamenir SA, Lopez L, Nguyen KH, et al. Juxtaposition of the atrial appendages: a clinical series of 22 patients. Pediatr Cardiol 2001;22:121-7.
29. Deal BJ, Chin AJ, Sanders SP, Norwood WI, Castaneda AR. Subxiphoid two-dimensional echocardiographic identification of tricuspid valve abnormalities in transposition of the great arteries with ventricular septal defect. Am J Cardiol 1985;55:1146-51.
30. Moene RJ, Oppenheimer-Dekker A. Congenital mitral valve anomalies in transposition of the great arteries. Am J Cardiol 1982;49:1972-8.
31. Van Praagh R, Weinberg PM, Calder L, Buckley LFP, Van Praagh S. The transposition complexes: how many are there? In: Davila JC, editor. Second Henry Ford Hospital International Symposium of Cardiac Surgery. New York: Appleton-Century-Crofts; 1977. pp. 207-13.
32. Van Praagh R. Anatomic variations in transposition of the great arteries. In: Takahashi M, Wells WJ, Lindesmith GG, editors. Challenges in the Treatment of Congenital Cardiac Anomalies. Mount Kisco, NY: Futura; 1986. pp. 107-35.
33. Serraf A, Nakamura T, Lacour-Gayet F, Piot D, Bruniaux J, Touchot A, et al. Surgical approaches for double-outlet right ventricle or transposition of the great arteries associated with straddling atrioventricular valves. J Thorac Cardiovasc Surg 1996;111:527-35.
34. Van Praagh R, Layton WM, Van Praagh S. The morphogenesis of normal and abnormal relationships between the great arteries and the ventricles: pathologic and experimental data. In: Van Praagh R, Takao A, editors. Etiology and Morphogenesis of Congenital Heart Disease. Mount Kisco, NY: Futura; 1980. pp. 271-316.
35. Pasquini L, Sanders SP, Parness IA, Colan SD, Van Praagh S, Mayer JE Jr, et al. Conal anatomy in 119 patients with d-loop transposition of the great arteries and ventricular septal defect: an echocardiographic and pathologic study. J Am Coll Cardiol 1993;21:1712-21.
36. Anderson RH, Weinberg PM. The clinical anatomy of transposition. Cardiol Young 2005;15 Suppl 1:76-87.
37. Day RW, Laks H, Drinkwater DC. The influence of coronary anatomy on the arterial switch operation in neonates. J Thorac Cardiovasc Surg 1992;104:706-12.
38. Pasquali SK, Hasselblad V, Li JS, Kong DF, Sanders SP. Coronary artery pattern and outcome of arterial switch operation for transposition of the great arteries: a meta-analysis. Circulation 2002;106:2575-80.
39. Legendre A, Losay J, Touchot-Kone A, Serraf A, Belli E, Piot JD, et al. Coronary events after arterial switch operation for transposition of the great arteries. Circulation 2003;108 Suppl 1:II186-90.
40. Asou T, Karl TR, Pawade A, Mee RB. Arterial switch: translocation of the intramural coronary artery. Ann Thorac Surg 1994;57:461-5.
41. Blume ED, Altmann K, Mayer JE, Colan SD, Gauvreau K, Geva T. Evolution of risk factors influencing early mortality of the arterial switch operation. J Am Coll Cardiol 1999;33:1702-9.
42. Brown JW, Park HJ, Turrentine MW. Arterial switch operation: factors impacting survival in the current era. Ann Thorac Surg 2001;71:1978-84.
43. Pretre R, Tamisier D, Bonhoeffer P, Mauriat P, Pouard P, Sidi D, et al. Results of the arterial switch operation in neonates with transposed great arteries. Lancet 2001;357:1826-30.
44. Garcia Hernandez JA, Montero Valladares C, Martinez Lopez AI, Romero Parreno A, Grueso Montero J, Gil-Fournier Carazo M, et al. Risk factors associated with arterial switch operation for transposition of the great arteries. Rev Esp Cardiol 2005;58:815-21.
45. Qamar ZA, Goldberg CS, Devaney EJ, Bove EL, Ohye RG. Current risk factors and outcomes for the arterial switch operation. Ann Thorac Surg 2007;84:871-8. discussion 8–9.
46. Wong SH, Finucane K, Kerr AR, O'Donnell C, West T, Gentles TL. Cardiac outcome up to 15 years after the arterial switch operation. Heart Lung Circ 2008;17:48-53.
47. Daebritz SH, Nollert G, Sachweh JS, Engelhardt W, von Bernuth G, Messmer BJ. Anatomical risk factors for mortality and cardiac morbidity after arterial switch operation. Ann Thorac Surg 2000;69:1880-6.
48. Wong D, Golding F, Hess L, Caldarone CA, Van Arsdell G, Manlhiot C, et al. Intraoperative coronary artery pulse Doppler patterns in patients with complete transposition of the great arteries undergoing the arterial switch operation. Am Heart J 2008;156:466-72.
49. Sallaam S, Natarajan G, Aggarwal S. Persistent Pulmonary Hypertension of the Newborn with D-transposition of the Great Arteries: Management and Prognosis. Congenit Heart Dis 2015 [Epub ahead of print].
50. Newfeld EA, Paul MM, Muster AJ, Idriss FS. Pulmonary vascular disease in complete transposition of the great arteries: a study of 200 patients. Am J Cardiol 1974;34:75-82.
51. Sreeram N, Petros A, Peart I, Arnold R. Progressive pulmonary hypertension after the arterial switch procedure. Am J Cardiol 1994;73:620-1.
52. Rivenes SM, Grifka RG, Feltes TF. Development of advanced pulmonary vascular disease in D-transposition of the great arteries after the neonatal arterial switch operation. Tex Heart Inst J 1998;25:201-5.
53. Wernovsky G, Bridges ND, Mandell VS, Castaneda AR, Perry SB. Enlarged bronchial arteries after early repair of transposition of the great arteries. J Am Coll Cardiol 1993;21:465-70.
54. Haas F, Wottke M, Poppert H, Meisner H. Long-term survival and functional follow-up in patients after the arterial switch operation. Ann Thorac Surg 1999;68:1692-7.
55. Losay J, Touchot A, Serraf A, Litvinova A, Lambert V, Piot JD, et al. Late outcome after arterial switch operation for transposition of the great arteries. Circulation 2001;104:I121-6.
56. Marino BS, Wernovsky G, McElhinney DB, Jawad A, Kreb DL, Mantel SF, et al. Neo-aortic valvar function after the arterial switch. Cardiol Young 2006;16:481-9.
57. Losay J, Touchot A, Capderou A, Piot JD, Belli E, Planche C, et al. Aortic valve regurgitation after arterial switch operation for transposition of the great arteries: incidence, risk factors, and outcome. J Am Coll Cardiol 2006;47:2057-62.
58. Angeli E, Raisky O, Bonnet D, Sidi D, Vouhe PR. Late reoperations after neonatal arterial switch operation for transposition of the great arteries. Eur J Cardiothorac Surg 2008;34:32-6.
59. Schwartz ML, Gauvreau K, del Nido P, Mayer JE, Colan SD. Long-term predictors of aortic root dilation and aortic regurgitation after arterial switch operation. Circulation 2004;110:II128-32.
60. McMahon CJ, Ravekes WJ, Smith EO, Denfield SW, Pignatelli RH, Altman CA, et al. Risk factors for neo-aortic root enlargement and aortic regurgitation following arterial switch operation. Pediatr Cardiol 2004;25:329-35.
61. Tsuda T, Bhat AM, Robinson BW, Baffa JM, Radtke W. Coronary artery problems late after arterial switch operation for transposition of the great arteries. Circ J 2015;79:2372-9.
62. Mohsen AE, Rosenthal E, Qureshi SA, Tynan M. Stent implantation for superior vena cava occlusion after the Mustard operation. Catheter Cardiovasc Interv 2001;52:351-4.

63. Moons P, Gewillig M, Sluysmans T, Verhaaren H, Viart P, Massin M, et al. Long term outcome up to 30 years after the Mustard or Senning operation: a nationwide multicentre study in Belgium. Heart 2004;90:307-13.
64. Bottega NA, Silversides CK, Oechslin EN, Dissanayake K, Harrison JL, Provost Y, et al. Stenosis of the superior limb of the systemic venous baffle following a Mustard procedure: an under-recognized problem. Int J Cardiol 2012;154:32-7.
65. Rastelli GC, McGoon DC, Wallace RB. Anatomic correction of transposition of the great arteries with ventricular septal defect and subpulmonary stenosis. J Thorac Cardiovasc Surg 1969;58:545-52.
66. Preminger TJ, Sanders SP, van der Velde ME, Castaneda AR, Lock JE. "Intramural" residual interventricular defects after repair of conotruncal malformations. Circulation 1994;89:236-42.
67. Patel JK, Glatz AC, Ghosh RM, Jones SM, Natarajan S, Ravishankar C, et al. Intramural Ventricular Septal Defect Is a Distinct Clinical Entity Associated With Postoperative Morbidity in Children After Repair of Conotruncal Anomalies. Circulation 2015;132:1387-94.
68. Lang RM, Badano LP, Mor-Avi V, Afilalo J, Armstrong A, Ernande L, et al. Recommendations for cardiac chamber quantification by echocardiography in adults: an update from the American Society of Echocardiography and the European Association of Cardiovascular Imaging. J Am Soc Echocardiogr 2015;28:1-39.
69. Lopez L, Colan SD, Frommelt PC, Ensing GJ, Kendall K, Younoszai AK, et al. Recommendations for quantification methods during the performance of a pediatric echocardiogram: a report from the Pediatric Measurements Writing Group of the American Society of Echocardiography Pediatric and Congenital Heart Disease Council. J Am Soc Echocardiogr 2010;23:465-95. quiz 576–7.
70. Colan SD, Boutin C, Castaneda AR, Wernovsky G. Status of the left ventricle after arterial switch operation for transposition of the great arteries. Hemodynamic and echocardiographic evaluation. J Thorac Cardiovasc Surg 1995;109:311-21.
71. Vandekerckhove KD, Blom NA, Lalezari S, Koolbergen DR, Rijlaarsdam ME, Hazekamp MG. Long-term follow-up of arterial switch operation with an emphasis on function and dimensions of left ventricle and aorta. Eur J Cardiothorac Surg 2009;35:582-7. discussion 7–8.
72. Mor-Avi V, Lang RM, Badano LP, Belohlavek M, Cardim NM, Derumeaux G, et al. Current and evolving echocardiographic techniques for the quantitative evaluation of cardiac mechanics: ASE/EAE consensus statement on methodology and indications endorsed by the Japanese Society of Echocardiography. J Am Soc Echocardiogr 2011;24:277-313.
73. Taylor AM, Dymarkowski S, Hamaekers P, Razavi R, Gewillig M, Mertens L, et al. MR coronary angiography and late-enhancement myocardial MR in children who underwent arterial switch surgery for transposition of great arteries. Radiology 2005;234:542-7.
74. Nagueh SF, Appleton CP, Gillebert TC, Marino PN, Oh JK, Smiseth OA, et al. Recommendations for the evaluation of left ventricular diastolic function by echocardiography. J Am Soc Echocardiogr 2009;22:107-33.
75. Klitsie LM, Roest AA, Kuipers IM, Hazekamp MG, Blom NA, Ten Harkel AD. Left and right ventricular performance after arterial switch operation. J Thorac Cardiovasc Surg 2014;147:1561-7.
76. Rudski LG, Lai WW, Afilalo J, Hua L, Handschumacher MD, Chandrasekaran K, et al. Guidelines for the echocardiographic assessment of the right heart in adults: a report from the American Society of Echocardiography endorsed by the European Association of Echocardiography, a registered branch of the European Society of Cardiology, and the Canadian Society of Echocardiography. J Am Soc Echocardiogr 2010;23:685-713. quiz 86–8.
77. Agnetti A, Carano N, Cavalli C, Tchana B, Bini M, Squarcia U, et al. Long-term outcome after senning operation for transposition of the great arteries. Clin Cardiol 2004;27:611-4.
78. Khattab K, Schmidheiny P, Wustmann K, Wahl A, Seiler C, Schwerzmann M. Echocardiogram versus cardiac magnetic resonance imaging for assessing systolic function of subaortic right ventricle in adults with complete transposition of great arteries and previous atrial switch operation. Am J Cardiol 2013;111:908-13.
79. Vogel M, Derrick G, White PA, Cullen S, Aichner H, Deanfield J, et al. Systemic ventricular function in patients with transposition of the great arteries after atrial repair: a tissue Doppler and conductance catheter study. J Am Coll Cardiol 2004;43:100-6.
80. Grewal J, Majdalany D, Syed I, Pellikka P, Warnes CA. Three-dimensional echocardiographic assessment of right ventricular volume and function in adult patients with congenital heart disease: comparison with magnetic resonance imaging. J Am Soc Echocardiogr 2010;23:127-33.
81. Khoo NS, Young A, Occleshaw C, Cowan B, Zeng IS, Gentles TL. Assessments of right ventricular volume and function using three-dimensional echocardiography in older children and adults with congenital heart disease: comparison with cardiac magnetic resonance imaging. J Am Soc Echocardiogr 2009;22:1279-88.
82. Eyskens B, Weidemann F, Kowalski M, Bogaert J, Dymarkowski S, Bijnens B, et al. Regional right and left ventricular function after the Senning operation: an ultrasonic study of strain rate and strain. Cardiol Young 2004;14:255-64.
83. Diller GP, Radojevic J, Kempny A, Alonso-Gonzalez R, Emmanouil L, Orwat S, et al. Systemic right ventricular longitudinal strain is reduced in adults with transposition of the great arteries, relates to subpulmonary ventricular function, and predicts adverse clinical outcome. Am Heart J 2012;163:859-66.
84. Kalogeropoulos AP, Deka A, Border W, Pernetz MA, Georgiopoulou VV, Kiani J, et al. Right ventricular function with standard and speckle-tracking echocardiography and clinical events in adults with D-transposition of the great arteries post atrial switch. J Am Soc Echocardiogr 2012;25:304-12.
85. Eindhoven JA, Menting ME, van den Bosch AE, McGhie JS, Witsenburg M, Cuypers JA, et al. Quantitative assessment of systolic right ventricular function using myocardial deformation in patients with a systemic right ventricle. Eur Heart J Cardiovasc Imaging 2015;16:380-8.
86. Lipczynska M, Szymanski P, Kumor M, Klisiewicz A, Mazurkiewicz L, Hoffman P. Global longitudinal strain may identify preserved systolic function of the systemic right ventricle. Can J Cardiol 2015;31:760-6.
87. Pettersen E, Helle-Valle T, Edvardsen T, Lindberg H, Smith HJ, Smevik B, et al. Contraction pattern of the systemic right ventricle shift from longitudinal to circumferential shortening and absent global ventricular torsion. J Am Coll Cardiol 2007;49:2450-6.
88. Di Salvo G, Pacileo G, Rea A, Limongelli G, Baldini L, D'Andrea A, et al. Transverse strain predicts exercise capacity in systemic right ventricle patients. Int J Cardiol 2010;145:193-6.
89. Tangcharoen T, Bell A, Hegde S, Hussain T, Beerbaum P, Schaeffter T, et al. Detection of coronary artery anomalies in infants and young children with congenital heart disease by using MR imaging. Radiology 2011;259:240-7.
90. Fogel MA, Pawlowski TW, Harris MA, Whitehead KK, Keller MS, Wilson J, et al. Comparison and usefulness of cardiac magnetic resonance versus computed tomography in infants six months of age or younger with aortic arch anomalies without deep sedation or anesthesia. Am J Cardiol 2011;108:120-5.
91. Windram J, Grosse-Wortmann L, Shariat M, Greer ML, Crawford MW, Yoo SJ. Cardiovascular MRI without sedation or general anesthesia using a feed-and-sleep technique in neonates and infants. Pediatr Radiol 2012;42:183-7.
92. Shariat M, Mertens L, Seed M, Grosse-Wortmann L, Golding F, Mercer-Rosa L, et al. Utility of feed-and-sleep cardiovascular magnetic resonance in young infants with complex cardiovascular disease. Pediatr Cardiol 2015;36:809-12.
93. Shellock FG, Spinazzi A. MRI safety update 2008: part 2, screening patients for MRI. AJR Am J Roentgenol 2008;191:1140-9.
94. Martin ET, Coman JA, Shellock FG, Pulling CC, Fair R, Jenkins K. Magnetic resonance imaging and cardiac pacemaker safety at 1.5-Tesla. J Am Coll Cardiol 2004;43:1315-24.
95. Pulver AF, Puchalski MD, Bradley DJ, Minich LL, Su JT, Saarel EV, et al. Safety and imaging quality of MRI in pediatric and adult congenital heart disease patients with pacemakers. Pacing Clin Electrophysiol 2009;32:450-6.

96. Nordbeck P, Ertl G, Ritter O. Magnetic resonance imaging safety in pacemaker and implantable cardioverter defibrillator patients: how far have we come? Eur Heart J 2015;36:1505-11.
97. Al-Wakeel N, O H-Ici D, Schmitt KR, Messroghli DR, Riesenkampff E, Berger F, et al. Cardiac MRI in patients with complex CHD following primary or secondary implantation of MRI-conditional pacemaker system. Cardiol Young 2016;26:306-14.
98. Tsai-Goodman B, Geva T, Odegard KC, Sena LM, Powell AJ. Clinical role, accuracy, and technical aspects of cardiovascular magnetic resonance imaging in infants. Am J Cardiol 2004;94:69-74.
99. Beek FJ, Beekman RP, Dillon EH, Mali WP, Meiners LC, Kramer PP, et al. MRI of the pulmonary artery after arterial switch operation for transposition of the great arteries. Pediatr Radiol 1993;23:335-40.
100. Hardy CE, Helton GJ, Kondo C, Higgins SS, Young NJ, Higgins CB. Usefulness of magnetic resonance imaging for evaluating great-vessel anatomy after arterial switch operation for D-transposition of the great arteries. Am Heart J 1994;128:326-32.
101. Blakenberg F, Rhee J, Hardy C, Helton G, Higgins SS, Higgins CB. MRI vs echocardiography in the evaluation of the Jatene procedure. J Comput Assist Tomogr 1994;18:749-54.
102. Weiss F, Habermann CR, Lilje C, Nimz M, Rasek V, Dallmeyer J, et al. [MRI of pulmonary arteries in follow-up after arterial-switch-operation (ASO) for transposition of great arteries (d-TGA)]. Rofo 2005;177:849-55.
103. Gutberlet M, Boeckel T, Hosten N, Vogel M, Kuhne T, Oellinger H, et al. Arterial switch procedure for D-transposition of the great arteries: quantitative midterm evaluation of hemodynamic changes with cine MR imaging and phase-shift velocity mapping-initial experience. Radiology 2000;214:467-75.
104. McConnell MV, Ganz P, Selwyn AP, Li W, Edelman RR, Manning WJ. Identification of anomalous coronary arteries and their anatomic course by magnetic resonance coronary angiography. Circulation 1995;92:3158-62.
105. Kim WY, Danias PG, Stuber M, Flamm SD, Plein S, Nagel E, et al. Coronary magnetic resonance angiography for the detection of coronary stenoses. N Engl J Med 2001;345:1863-9.
106. Taylor AM, Thorne SA, Rubens MB, Jhooti P, Keegan J, Gatehouse PD, et al. Coronary artery imaging in grown up congenital heart disease: complementary role of magnetic resonance and x-ray coronary angiography. Circulation 2000;101:1670-8.
107. Su JT, Chung T, Muthupillai R, Pignatelli RH, Kung GC, Diaz LK, et al. Usefulness of real-time navigator magnetic resonance imaging for evaluating coronary artery origins in pediatric patients. Am J Cardiol 2005;95:679-82.
108. Marin Rodriguez C, Lancharro Zapata A, Rodriguez Ogando A, Carrasco Munoz S, Ruiz Martin Y, Sanchez Alegre ML, et al. Quality of 3D magnetic resonance imaging of coronary arteries in patients with D-transposition of the great arteries after the Jatene switch procedure. Radiologia 2015;57:326-32.
109. Tobler D, Motwani M, Wald RM, Roche SL, Verocai F, Iwanochko RM, et al. Evaluation of a comprehensive cardiovascular magnetic resonance protocol in young adults late after the arterial switch operation for d-transposition of the great arteries. J Cardiovasc Magn Reson 2014;16:98.
110. Manso B, Castellote A, Dos L, Casaldaliga J. Myocardial perfusion magnetic resonance imaging for detecting coronary function anomalies in asymptomatic paediatric patients with a previous arterial switch operation for the transposition of great arteries. Cardiol Young 2010;20:410-7.
111. Fratz S, Chung T, Greil GF, Samyn MM, Taylor AM, Valsangiacomo Buechel ER, et al. Guidelines and protocols for cardiovascular magnetic resonance in children and adults with congenital heart disease: SCMR expert consensus group on congenital heart disease. J Cardiovasc Magn Reson 2013;15:51.
112. Luijnenburg SE, Robbers-Visser D, Moelker A, Vliegen HW, Mulder BJ, Helbing WA. Intra-observer and interobserver variability of biventricular function, volumes and mass in patients with congenital heart disease measured by CMR imaging. Int J Cardiovasc Imaging 2010;26:57-64.
113. Helbing WA, Rebergen SA, Maliepaard C, Hansen B, Ottenkamp J, Reiber JH, et al. Quantification of right ventricular function with magnetic resonance imaging in children with normal hearts and with congenital heart disease. Am Heart J 1995;130:828-37.
114. Lorenz CH, Walker ES, Graham TP Jr., Powers TA. Right ventricular performance and mass by use of cine MRI late after atrial repair of transposition of the great arteries. Circulation 1995;92:II233-9.
115. Mooij CF, de Wit CJ, Graham DA, Powell AJ, Geva T. Reproducibility of MRI measurements of right ventricular size and function in patients with normal and dilated ventricles. J Magn Reson Imaging 2008;28:67-73.
116. Chung KJ, Simpson IA, Glass RF, Sahn DJ, Hesselink JR. Cine magnetic resonance imaging after surgical repair in patients with transposition of the great arteries. Circulation 1988;77:104-9.
117. Groenink M, Mulder BJ, van der Wall EE. Value of magnetic resonance imaging in functional assessment of baffle obstruction after the Mustard procedure. J Cardiovasc Magn Reson 1999;1:49-51.
118. Johansson B, Babu-Narayan SV, Kilner PJ, Cannell TM, Mohiaddin RH. 3-dimensional time-resolved contrast-enhanced magnetic resonance angiography for evaluation late after the mustard operation for transposition. Cardiol Young 2010;20:1-7.
119. Sampson C, Kilner PJ, Hirsch R, Rees RS, Somerville J, Underwood SR. Venoatrial pathways after the Mustard operation for transposition of the great arteries: anatomic and functional MR imaging. Radiology 1994;193:211-7.
120. Theissen P, Kaemmerer H, Sechtem U, Luhmer I, Smolarz K, Kallfelz HC, et al. Magnetic resonance imaging of cardiac function and morphology in patients with transposition of the great arteries following Mustard procedure. Thorac Cardiovasc Surg 1991;39 Suppl 3:221-4.
121. Campbell RM, Moreau GA, Johns JA, Burger JD, Mazer M, Graham TP Jr, et al. Detection of caval obstruction by magnetic resonance imaging after intraatrial repair of transposition of the great arteries. Am J Cardiol 1987;60:688-91.
122. Muzzarelli S, Ordovas KG, Higgins CB, Meadows AK. Collateral flow measurement by phase-contrast magnetic resonance imaging for the assessment of systemic venous baffle patency after atrial switch repair for transposition of the great arteries. J Thorac Imaging 2012;27:175-8.
123. Babu-Narayan SV, Goktekin O, Moon JC, Broberg CS, Pantely GA, Pennell DJ, et al. Late gadolinium enhancement cardiovascular magnetic resonance of the systemic right ventricle in adults with previous atrial redirection surgery for transposition of the great arteries. Circulation 2005;111:2091-8.
124. Fratz S, Hauser M, Bengel FM, Hager A, Kaemmerer H, Schwaiger M, et al. Myocardial scars determined by delayed-enhancement magnetic resonance imaging and positron emission tomography are not common in right ventricles with systemic function in long-term follow up. Heart 2006;92:1673-7.
125. Giardini A, Lovato L, Donti A, Formigari R, Oppido G, Gargiulo G, et al. Relation between right ventricular structural alterations and markers of adverse clinical outcome in adults with systemic right ventricle and either congenital complete (after Senning operation) or congenitally corrected transposition of the great arteries. Am J Cardiol 2006;98:1277-82.
126. Rydman R, Gatzoulis MA, Ho SY, Ernst S, Swan L, Li W, et al. Systemic right ventricular fibrosis detected by cardiovascular magnetic resonance is associated with clinical outcome, mainly new-onset atrial arrhythmia, in patients after atrial redirection surgery for transposition of the great arteries. Circ Cardiovasc Imaging 2015;8.
127. Preim U, Hoffmann J, Lehmkuhl L, Kehrmann J, Riese F, Daehnert I, et al. Systemic right ventricles rarely show myocardial scars in cardiac magnetic resonance delayed-enhancement imaging. Clin Res Cardiol 2013;102:337-44.
128. Fratz S, Hager A, Busch R, Kaemmerer H, Schwaiger M, Lange R, et al. Patients after atrial switch operation for transposition of the great arteries can not increase stroke volume under dobutamine stress as opposed to patients with congenitally corrected transposition. Circ J 2008;72:1130-5.
129. Oosterhof T, Tulevski II, Roest AA, Steendijk P, Vliegen HW, van der Wall EE, et al. Disparity between dobutamine stress and physical exercise magnetic resonance imaging in patients with an intra-atrial correction for

transposition of the great arteries. J Cardiovasc Magn Reson 2005;7:383-9.
130. Roest AA, Lamb HJ, van der Wall EE, Vliegen HW, van den Aardweg JG, Kunz P, et al. Cardiovascular response to physical exercise in adult patients after atrial correction for transposition of the great arteries assessed with magnetic resonance imaging. Heart 2004;90:678-84.
131. Tops LF, Roest AA, Lamb HJ, Vliegen HW, Helbing WA, van der Wall EE, et al. Intraatrial repair of transposition of the great arteries: use of MR imaging after exercise to evaluate regional systemic right ventricular function. Radiology 2005;237:861-7.
132. Tulevski II, Lee PL, Groenink M, van der Wall EE, Stoker J, Pieper PG, et al. Dobutamine-induced increase of right ventricular contractility without increased stroke volume in adolescent patients with transposition of the great arteries: evaluation with magnetic resonance imaging. Int J Card Imaging 2000;16:471-8.
133. Tulevski II, van der Wall EE, Groenink M, Dodge-Khatami A, Hirsch A, Stoker J, et al. Usefulness of magnetic resonance imaging dobutamine stress in asymptomatic and minimally symptomatic patients with decreased cardiac reserve from congenital heart disease (complete and corrected transposition of the great arteries and subpulmonic obstruction). Am J Cardiol 2002;89:1077-81.
134. Holmqvist C, Oskarsson G, Stahlberg F, Thilen U, Bjorkhem G, Laurin S. Functional evaluation of extracardiac ventriculopulmonary conduits and of the right ventricle with magnetic resonance imaging and velocity mapping. Am J Cardiol 1999;83:926-32.
135. Samyn MM, Powell AJ, Garg R, Sena L, Geva T. Range of ventricular dimensions and function by steady-state free precession cine MRI in repaired tetralogy of Fallot: right ventricular outflow tract patch vs. conduit repair. J Magn Reson Imaging 2007;26:934-40.
136. Schievano S, Migliavacca F, Coats L, Khambadkone S, Carminati M, Wilson N, et al. Percutaneous pulmonary valve implantation based on rapid prototyping of right ventricular outflow tract and pulmonary trunk from MR data. Radiology 2007;242:490-7.
137. Cook SC, McCarthy M, Daniels CJ, Cheatham JP, Raman SV. Usefulness of multislice computed tomography angiography to evaluate intravascular stents and transcatheter occlusion devices in patients with d-transposition of the great arteries after mustard repair. Am J Cardiol 2004;94:967-9.
138. Raman SV, Cook SC, McCarthy B, Ferketich AK. Usefulness of multidetector row computed tomography to quantify right ventricular size and function in adults with either tetralogy of Fallot or transposition of the great arteries. Am J Cardiol 2005;95:683-6.
139. Al-Mousily F, Shifrin RY, Fricker FJ, Feranec N, Quinn NS, Chandran A. Use of 320-detector computed tomographic angiography for infants and young children with congenital heart disease. Pediatr Cardiol 2011;32:426-32.
140. Han BK, Lindberg J, Grant K, Schwartz RS, Lesser JR. Accuracy and safety of high pitch computed tomography imaging in young children with complex congenital heart disease. Am J Cardiol 2011;107:1541-6.
141. Han BK, Lesser JR. CT imaging in congenital heart disease: an approach to imaging and interpreting complex lesions after surgical intervention for tetralogy of Fallot, transposition of the great arteries, and single ventricle heart disease. J Cardiovasc Comput Tomogr 2013;7:338-53.
142. Dillman JR, Hernandez RJ. Role of CT in the evaluation of congenital cardiovascular disease in children. AJR Am J Roentgenol 2009;192:1219-31.
143. Hlavacek AM. Imaging of congenital cardiovascular disease: the case for computed tomography. J Thorac Imaging 2010;25:247-55.
144. Lell MM, May M, Deak P, Alibek S, Kuefner M, Kuettner A, et al. High-pitch spiral computed tomography: effect on image quality and radiation dose in pediatric chest computed tomography. Invest Radiol 2011;46:116-23.
145. Jadhav SP, Golriz F, Atweh LA, Zhang W, Krishnamurthy R. CT angiography of neonates and infants: comparison of radiation dose and image quality of target mode prospectively ECG-gated 320-MDCT and ungated helical 64-MDCT. AJR Am J Roentgenol 2015;204:W184-91.
146. Han BK, Overman DM, Grant K, Rosenthal K, Rutten-Ramos S, Cook D, et al. Non-sedated, free breathing cardiac CT for evaluation of complex congenital heart disease in neonates. J Cardiovasc Comput Tomogr 2013;7:354-60.
147. Vastel-Amzallag C, Le Bret E, Paul JF, Lambert V, Rohnean A, El Fassy E, et al. Diagnostic accuracy of dual-source multislice computed tomographic analysis for the preoperative detection of coronary artery anomalies in 100 patients with tetralogy of Fallot. J Thorac Cardiovasc Surg 2011;142:120-6.
148. Warnes CA. Transposition of the great arteries. Circulation 2006;114:2699-709.
149. Khairy P, Van Hare GF, Balaji S, Berul CI, Cecchin F, Cohen MI, et al. PACES/HRS Expert Consensus Statement on the Recognition and Management of Arrhythmias in Adult Congenital Heart Disease: developed in partnership between the Pediatric and Congenital Electrophysiology Society (PACES) and the Heart Rhythm Society (HRS). Endorsed by the governing bodies of PACES, HRS, the American College of Cardiology (ACC), the American Heart Association (AHA), the European Heart Rhythm Association (EHRA), the Canadian Heart Rhythm Society (CHRS), and the International Society for Adult Congenital Heart Disease (ISACHD). Heart Rhythm 2014;11:e102-65.
150. Ou P, Celermajer DS, Marini D, Agnoletti G, Vouhe P, Brunelle F, et al. Safety and accuracy of 64-slice computed tomography coronary angiography in children after the arterial switch operation for transposition of the great arteries. JACC Cardiovasc Imaging 2008;1:331-9.
151. Marcora S, Di Renzi P, Giannico S, Pierleoni M, Bellelli A, Sanders SP. A CT Study of Coronary Arteries in Adult Mustard Patients. JACC Cardiovasc Imaging 2011;4:89-93.
152. Sharma A, Einstein AJ, Vallakati A, Arbab-Zadeh A, Mukherjee D, Lichstein E. Meta-analysis of global left ventricular function comparing multidetector computed tomography with cardiac magnetic resonance imaging. Am J Cardiol 2014;113:731-8.
153. Rizvi A, Deano RC, Bachman DP, Xiong G, Min JK, Truong QA. Analysis of ventricular function by CT. J Cardiovasc Comput Tomogr 2015;9:1-12.
154. Zhang XC, Yang ZG, Guo YK, Zhang RM, Wang J, Zhou DQ, et al. Assessment of right ventricular function for patients with rheumatic mitral stenosis by 64-slice multi-detector row computed tomography: comparison with magnetic resonance imaging. Chin Med J 2012;125:1469-74.
155. Ruckdeschel ES, Quaife R, Lewkowiez L, Kay J, Sauer WH, Collins KK, et al. Preprocedural imaging in patients with transposition of the great arteries facilitates placement of cardiac resynchronization therapy leads. Pacing Clin Electrophysiol 2014;37:546-53.
156. Greenberg SB. Rebalancing the risks of Computed Tomography and Magnetic Resonance imaging. Pediatr Radiol 2011;41:951-2.
157. Ramamoorthy C, Haberkern CM, Bhananker SM, Domino KB, Posner KL, Campos JS, et al. Anesthesia-related cardiac arrest in children with heart disease: data from the Pediatric Perioperative Cardiac Arrest (POCA) registry. Anesth Analg 2010;110:1376-82.
158. Girshin M, Shapiro V, Rhee A, Ginsberg S, Inchiosa MA Jr. Increased risk of general anesthesia for high-risk patients undergoing magnetic resonance imaging. J Comput Assist Tomogr 2009;33:312-5.
159. Flick RP, Katusic SK, Colligan RC, Wilder RT, Voigt RG, Olson MD, et al. Cognitive and behavioral outcomes after early exposure to anesthesia and surgery. Pediatrics 2011;128:e1053-61.
160. Ing C, DiMaggio C, Whitehouse A, Hegarty MK, Brady J, von Ungern-Sternberg BS, et al. Long-term differences in language and cognitive function after childhood exposure to anesthesia. Pediatrics 2012;130:e476-85.
161. Rappaport B, Mellon RD, Simone A, Woodcock J. Defining safe use of anesthesia in children. N Engl J Med 2011;364:1387-90.
162. Kaste SC, Young CW. Safe use of power injectors with central and peripheral venous access devices for pediatric CT. Pediatr Radiol 1996;26:499-501.
163. Amaral JG, Traubici J, BenDavid G, Reintamm G, Daneman A. Safety of power injector use in children as measured by incidence of extravasation. AJR Am J Roentgenol 2006;187:580-3.

164. Dillman JR, Strouse PJ, Ellis JH, Cohan RH, Jan SC. Incidence and severity of acute allergic-like reactions to i.v. nonionic iodinated contrast material in children. AJR Am J Roentgenol 2007;188:1643-7.
165. Callahan MJ, Poznauskis L, Zurakowski D, Taylor GA. Nonionic iodinated intravenous contrast material-related reactions: incidence in large urban children's hospital–retrospective analysis of data in 12,494 patients. Radiology 2009;250:674-81.
166. Mahabadi AA, Achenbach S, Burgstahler C, Dill T, Fischbach R, Knez A, et al. Safety, efficacy, and indications of beta-adrenergic receptor blockade to reduce heart rate prior to coronary CT angiography. Radiology 2010;257:614-23.
167. Rigsby CK, deFreitas RA, Nicholas AC, Leidecker C, Johanek AJ, Anley P, et al. Safety and efficacy of a drug regimen to control heart rate during 64-slice ECG-gated coronary CTA in children. Pediatr Radiol 2010;40:1880-9.
168. Brenner D, Elliston C, Hall E, Berdon W. Estimated risks of radiation-induced fatal cancer from pediatric CT. AJR Am J Roentgenol 2001;176:289-96.
169. Einstein AJ, Moser KW, Thompson RC, Cerqueira MD, Henzlova MJ. Radiation dose to patients from cardiac diagnostic imaging. Circulation 2007;116:1290-305.
170. Johnson JN, Hornik CP, Li JS, Benjamin DK Jr., Yoshizumi TT, Reiman RE, et al. Cumulative radiation exposure and cancer risk estimation in children with heart disease. Circulation 2014;130:161-7.
171. Hoffmann A, Engelfriet P, Mulder B. Radiation exposure during follow-up of adults with congenital heart disease. Int J Cardiol 2007;118:151-3.
172. Halliburton SS, Abbara S, Chen MY, Gentry R, Mahesh M, Raff GL, et al. SCCT guidelines on radiation dose and dose-optimization strategies in cardiovascular CT. J Cardiovasc Comput Tomogr 2011;5:198-224.
173. Meinel FG, Henzler T, Schoepf UJ, Park PW, Huda W, Spearman JV, et al. ECG-synchronized CT angiography in 324 consecutive pediatric patients: spectrum of indications and trends in radiation dose. Pediatr Cardiol 2015;36:569-78.
174. Watson TG, Mah E, Joseph Schoepf U, King L, Huda W, Hlavacek AM. Effective radiation dose in computed tomographic angiography of the chest and diagnostic cardiac catheterization in pediatric patients. Pediatr Cardiol 2013;34:518-24.
175. Han BK, Lindberg J, Overman D, Schwartz RS, Grant K, Lesser JR. Safety and accuracy of dual-source coronary computed tomography angiography in the pediatric population. J Cardiovasc Comput Tomogr 2012;6:252-9.
176. Stehli J, Fuchs TA, Bull S, Clerc OF, Possner M, Buechel RR, et al. Accuracy of coronary CT angiography using a submillisievert fraction of radiation exposure: comparison with invasive coronary angiography. J Am Coll Cardiol 2014;64:772-80.
177. Achenbach S, Marwan M, Ropers D, Schepis T, Pflederer T, Anders K, et al. Coronary computed tomography angiography with a consistent dose below 1 mSv using prospectively electrocardiogram-triggered high-pitch spiral acquisition. Eur Heart J 2010;31:340-6.
178. Ghoshhajra BB, Lee AM, Engel LC, Celeng C, Kalra MK, Brady TJ, et al. Radiation dose reduction in pediatric cardiac computed tomography: experience from a tertiary medical center. Pediatr Cardiol 2014;35:171-9.
179. Ou P, Mousseaux E, Azarine A, Dupont P, Agnoletti G, Vouhe P, et al. Detection of coronary complications after the arterial switch operation for transposition of the great arteries: first experience with multislice computed tomography in children. J Thorac Cardiovasc Surg 2006;131:639-43.
180. Oztunc F, Baris S, Adaletli I, Onol NO, Olgun DC, Guzeltas A, et al. Coronary events and anatomy after arterial switch operation for transposition of the great arteries: detection by 16-row multislice computed tomography angiography in pediatric patients. Cardiovasc Intervent Radiol 2009;32:206-12.
181. Puranik R, Muthurangu V, Celermajer DS, Taylor AM. Congenital heart disease and multi-modality imaging. Heart Lung Circ 2010;19:133-44.
182. Smith MF. Recent advances in cardiac SPECT instrumentation and system design. Curr Cardiol Rep 2013;15:387.
183. Klocke FJ, Baird MG, Lorell BH, Bateman TM, Messer JV, Berman DS, et al. ACC/AHA/ASNC guidelines for the clinical use of cardiac radionuclide imaging–executive summary: a report of the American College of Cardiology/American Heart Association Task Force on Practice Guidelines (ACC/AHA/ASNC Committee to Revise the 1995 Guidelines for the Clinical Use of Cardiac Radionuclide Imaging). Circulation 2003;108:1404-18.
184. Hesse B, Tagil K, Cuocolo A, Anagnostopoulos C, Bardies M, Bax J, et al. EANM/ESC procedural guidelines for myocardial perfusion imaging in nuclear cardiology. Eur J Nucl Med Mol Imaging 2005;32:855-97.
185. Dey D, Slomka PJ, Berman DS. Achieving very-low-dose radiation exposure in cardiac computed tomography, single-photon emission computed tomography, and positron emission tomography. Circ Cardiovasc Imaging 2014;7:723-34.
186. Bengel FM, Hauser M, Duvernoy CS, Kuehn A, Ziegler SI, Stollfuss JC, et al. Myocardial blood flow and coronary flow reserve late after anatomical correction of transposition of the great arteries. J Am Coll Cardiol 1998;32:1955-61.
187. Turner DR, Muzik O, Forbes TJ, Sullivan NM, Singh TP. Coronary diameter and vasodilator function in children following arterial switch operation for complete transposition of the great arteries. Am J Cardiol 2010;106:421-5.
188. Rickers C, Sasse K, Buchert R, Stern H, van den Hoff J, Lubeck M, et al. Myocardial viability assessed by positron emission tomography in infants and children after the arterial switch operation and suspected infarction. J Am Coll Cardiol 2000;36:1676-83.
189. Neglia D, Rovai D, Caselli C, Pietila M, Teresinska A, Aguade-Bruix S, et al. Detection of significant coronary artery disease by noninvasive anatomical and functional imaging. Circ Cardiovasc Imaging 2015;8.
190. Duvall WL, Savino JA, Levine EJ, Baber U, Lin JT, Einstein AJ, et al. A comparison of coronary CTA and stress testing using high-efficiency SPECT MPI for the evaluation of chest pain in the emergency department. J Nucl Cardiol 2014;21:305-18.
191. Lindner O, Bengel FM, Hacker M, Schafer W, Burchert W, Working Group Cardiovascular Nuclear Medicine of German Society of Nuclear M. Use of myocardial perfusion imaging and estimation of associated radiation doses in Germany from 2005 to 2012. Eur J Nucl Med Mol Imaging 2014;41:963-71.
192. Hutter PA, Bennink GB, Ay L, Raes IB, Hitchcock JF, Meijboom EJ. Influence of coronary anatomy and reimplantation on the long-term outcome of the arterial switch. Eur J Cardiothorac Surg 2000;18:207-13.
193. Acar P, Maunoury C, Bonnet D, Sebahoun S, Bonhoeffer P, Saliba Z, et al. Comparison of myocardial perfusion single-photon emission computed tomography with coronary artery angiography after arterial switch operation. Am J Cardiol 2001;87:1425-7.
194. Pizzi MN, Franquet E, Aguade-Bruix S, Manso B, Casaldaliga J, Cuberas-Borros G, et al. Long-term follow-up assessment after the arterial switch operation for correction of dextro-transposition of the great arteries by means of exercise myocardial perfusion-gated SPECT. Pediatr Cardiol 2014;35:197-207.
195. Raisky O, Bergoend E, Agnoletti G, Ou P, Bonnet D, Sidi D, et al. Late coronary artery lesions after neonatal arterial switch operation: results of surgical coronary revascularization. Eur J Cardiothorac Surg 2007;31:894-8.
196. Mahle WT, McBride MG, Paridon SM. Exercise performance after the arterial switch operation for D-transposition of the great arteries. Am J Cardiol 2001;87:753-8.
197. Sterrett LE, Schamberger MS, Ebenroth ES, Siddiqui AR, Hurwitz RA. Myocardial perfusion and exercise capacity 12 years after arterial switch surgery for D-transposition of the great arteries. Pediatr Cardiol 2011;32:785-91.
198. Giardini A, Khambadkone S, Rizzo N, Riley G, Pace Napoleone C, Muthialu N, et al. Determinants of exercise capacity after arterial switch operation for transposition of the great arteries. Am J Cardiol 2009;104:1007-12.

199. Vogt M, Kuhn A, Wiese J, Eicken A, Hess J, Vogel M. Reduced contractile reserve of the systemic right ventricle under Dobutamine stress is associated with increased brain natriuretic peptide levels in patients with complete transposition after atrial repair. Eur J Echocardiogr 2009;10:691-4.
200. Li W, Hornung TS, Francis DP, O'Sullivan C, Duncan A, Gatzoulis M, et al. Relation of biventricular function quantified by stress echocardiography to cardiopulmonary exercise capacity in adults with Mustard (atrial switch) procedure for transposition of the great arteries. Circulation 2004;110:1380-6.
201. Pianosi PT, Driscoll DJ. Exercise testing. In: Allen HD, Driscoll DJ, Shaddy RE, Feltes TF, editors. Moss and Adams' Heart Disease in Infants, Children, and Adolescents Including the Fetus and Young Adult. 8th ed. Phildalephia, PA: Lippincott Williams & Wilkins; 2013. pp. 118-33.
202. Pellikka PA, Nagueh SF, Elhendy AA, Kuehl CA, Sawada SG, American Society of E. American Society of Echocardiography recommendations for performance, interpretation, and application of stress echocardiography. J Am Soc Echocardiogr 2007;20:1021-41.
203. Lalezari S, Bruggemans EF, Blom NA, Hazekamp MG. Thirty-year experience with the arterial switch operation. Ann Thorac Surg 2011;92:973-9.
204. Wernovsky G. Transposition of the great arteries. In: Allen HD, Driscoll DJ, Shaddy RE, Feltes TF, editors. Moss and Adams' Heart Disease in Infants, Children, and Adolescents 7th Edition. 7th ed. West Sussex, UK: Lippincott Williams & Wilkins; 2008. pp. 1038-87.
205. Schultz AH, Lewin MB. d-Transposition of the great arteries. In: Eidem BW, Cetta F, O'Leary PW, editors. Echocardiography in Pediatric and Adult Congenital Heart Disease 1st Edition. 1st ed. West Sussex, UK: Lippincott Williams & Wilkins; 2010. pp. 249-68.
206. Cetta F, Driscoll DJ, Eidem BW. Evaluation of the adult with transposition after atrial switch operation. In: Eidem BW, Cetta F, O'Leary PW, editors. Echocardiography in Pediatric and Adult Congenital Heart Disease 1st Edition. 1st ed. West Sussex, UK: Lippincott Williams & Wilkins; 2010. pp. 442-9.
207. Sinelnikov YS, Kornilov IA, Redkin DA, Strelnikova MS, Ivantsov SM, Kalinin RA, et al. Left main coronary artery stenting in a neonate after arterial switch operation for transposition of the great arteries. World J Pediatr Congenit Heart Surg 2014;5:105-9.
208. Horer J, Karl E, Theodoratou G, Schreiber C, Cleuziou J, Prodan Z, et al. Incidence and results of reoperations following the Senning operation: 27 years of follow-up in 314 patients at a single center. Eur J Cardiothorac Surg 2008;33:1061-7. discussion 7-8.
209. Patel S, Shah D, Chintala K, Karpawich PP. Atrial baffle problems following the Mustard operation in children and young adults with dextro-transposition of the great arteries: the need for improved clinical detection in the current era. Congenit Heart Dis 2011;6:466-74.
210. Khairy P, Landzberg MJ, Lambert J, O'Donnell CP. Long-term outcomes after the atrial switch for surgical correction of transposition: a meta-analysis comparing the Mustard and Senning procedures. Cardiol Young 2004;14:284-92.
211. Tweddell JS, Pelech AN, Frommelt PC, Mussatto KA, Wyman JD, Fedderly RT, et al. Factors affecting longevity of homograft valves used in right ventricular outflow tract reconstruction for congenital heart disease. Circulation 2000;102:III130-5.
212. Bonhoeffer P, Boudjemline Y, Qureshi SA, Le Bidois J, Iserin L, Acar P, et al. Percutaneous insertion of the pulmonary valve. J Am Coll Cardiol 2002;39:1664-9.
213. Holzer RJ, Hijazi ZM. Transcatheter pulmonary valve replacement: State of the art. Catheter Cardiovasc Interv 2015.
214. McElhinney DB, Hellenbrand WE, Zahn EM, Jones TK, Cheatham JP, Lock JE, et al. Short- and medium-term outcomes after transcatheter pulmonary valve placement in the expanded multicenter US melody valve trial. Circulation 2010;122:507-16.
215. Carr M, Bergersen L, Marshall AC, Keane JF, Lock JE, Emani SM, et al. Bare metal stenting for obstructed small diameter homograft conduits in the right ventricular outflow tract. Catheter Cardiovasc Interv 2013;81:E44-52.
216. McElhinney DB, Cheatham JP, Jones TK, Lock JE, Vincent JA, Zahn EM, et al. Stent fracture, valve dysfunction, and right ventricular outflow tract reintervention after transcatheter pulmonary valve implantation: patient-related and procedural risk factors in the US Melody Valve Trial. Circ Cardiovasc Interv 2011;4:602-14.
217. Armstrong AK, Balzer DT, Cabalka AK, Gray RG, Javois AJ, Moore JW, et al. One-year follow-up of the Melody transcatheter pulmonary valve multicenter post-approval study. JACC Cardiovasc Interv 2014;7:1254-62.
218. Edwin F, Mamorare H, Brink J, Kinsley R. Primary arterial switch operation for transposition of the great arteries with intact ventricular septum–is it safe after three weeks of age? Interact Cardiovasc Thorac Surg 2010;11:641-4.
219. Rajiah P, Setser RM, Desai MY, Flamm SD, Arruda JL. Utility of free-breathing, whole-heart, three-dimensional magnetic resonance imaging in the assessment of coronary anatomy for congenital heart disease. Pediatr Cardiol 2011;32:418-25.
220. Beerbaum P, Sarikouch S, Laser KT, Greil G, Burchert W, Korperich H. Coronary anomalies assessed by whole-heart isotropic 3D magnetic resonance imaging for cardiac morphology in congenital heart disease. J Magn Reson Imaging 2009;29:320-7.
221. Paul JF, Rohnean A, Elfassy E, Sigal-Cinqualbre A. Radiation dose for thoracic and coronary step-and-shoot CT using a 128-slice dual-source machine in infants and small children with congenital heart disease. Pediatr Radiol 2011;41:244-9.
222. Ou P, Khraiche D, Celermajer DS, Agnoletti G, Le Quan Sang KH, Thalabard JC, et al. Mechanisms of coronary complications after the arterial switch for transposition of the great arteries. J Thorac Cardiovasc Surg 2013;145:1263-9.
223. Hausleiter J, Meyer T, Hermann F, Hadamitzky M, Krebs M, Gerber TC, et al. Estimated radiation dose associated with cardiac CT angiography. JAMA 2009;301:500-7.
224. Mor-Avi V, Sugeng L, Weinert L, MacEneaney P, Caiani EG, Koch R, et al. Fast measurement of left ventricular mass with real-time three-dimensional echocardiography: comparison with magnetic resonance imaging. Circulation 2004;110:1814-8.
225. Kuhl HP, Schreckenberg M, Rulands D, Katoh M, Schafer W, Schummers G, et al. High-resolution transthoracic real-time three-dimensional echocardiography: quantitation of cardiac volumes and function using semi-automatic border detection and comparison with cardiac magnetic resonance imaging. J Am Coll Cardiol 2004;43:2083-90.
226. Lembcke A, Dohmen PM, Dewey M, Klessen C, Elgeti T, Hermann KG, et al. Multislice computed tomography for preoperative evaluation of right ventricular volumes and function: comparison with magnetic resonance imaging. Ann Thorac Surg 2005;79:1344-51.
227. Warnes CA, Williams RG, Bashore TM, Child JS, Connolly HM, Dearani JA, et al. ACC/AHA 2008 Guidelines for the Management of Adults with Congenital Heart Disease: a report of the American College of Cardiology/American Heart Association Task Force on Practice Guidelines (writing committee to develop guidelines on the management of adults with congenital heart disease). Circulation 2008;118:e714-833.